

University of Montana

ScholarWorks at University of Montana

Graduate Student Theses, Dissertations, &
Professional Papers

Graduate School

2009

Mass Spectrometric Characterization and Fluorophore-Assisted Light Inactivation of Human Excitatory Amino Acid Transporter

Ran Ye

The University of Montana

Follow this and additional works at: <https://scholarworks.umt.edu/etd>

Let us know how access to this document benefits you.

Recommended Citation

Ye, Ran, "Mass Spectrometric Characterization and Fluorophore-Assisted Light Inactivation of Human Excitatory Amino Acid Transporter" (2009). *Graduate Student Theses, Dissertations, & Professional Papers*. 649.

<https://scholarworks.umt.edu/etd/649>

This Dissertation is brought to you for free and open access by the Graduate School at ScholarWorks at University of Montana. It has been accepted for inclusion in Graduate Student Theses, Dissertations, & Professional Papers by an authorized administrator of ScholarWorks at University of Montana. For more information, please contact scholarworks@mso.umt.edu.

MASS SPECTROMETRIC CHARACTERIZATION AND FLUOROPHORE-
ASSISTED LIGHT INACTIVATION OF HUMAN EXCITATORY AMINO ACID
TRANSPORTER 2

By

RAN YE

B.S., University of Science and Technology of China, Hefei, China, 1998

Dissertation

presented in partial fulfillment of the requirements
for the degree of

Doctor of Philosophy
in Chemistry

The University of Montana
Missoula, MT
March 2009

Approved by:

Dr. Perry J. Brown,
Associate Provost for Graduate Education

Dr. Richard J. Bridges, Chair
Department of Biomedical and Pharmaceutical Sciences

Dr. Edward Rosenberg,
Department of Chemistry and Biochemistry

Dr. Charles M. Thompson,
Department of Biomedical and Pharmaceutical Sciences

Dr. John M. Gerdes,
Department of Biomedical and Pharmaceutical Sciences

Dr. Kent Sugden,
Department of Chemistry and Biochemistry

Dr. J. B. Alexander Ross,
Department of Chemistry and Biochemistry

Mass spectrometric characterization and fluorophore-assisted light inactivation of human excitatory amino acid transporter 2.

Chairperson: Richard J. Bridges

Glia-expressing excitatory amino acid transporter 2 (EAAT2) mediates the bulk of glutamate re-uptake in the human central nervous system (CNS) and is associated with a variety of neurological disorders. Our understanding of the structure and mechanism of this integral membrane protein is limited. The goal of this study was to use pharmacological, mass spectrometric (MS) and photochemical approaches to probe EAAT2. For MS characterization, a hexahis epitope was incorporated into the N-terminus of human EAAT2. The recombinant protein was functionally expressed in HEK 293T cells and purified through a single-step nickel column. In-gel and in-solution trypsin digestions were conducted on the isolated protein. Overall, eighty-nine percent sequence coverage of the protein was achieved. An 88-amino acid tryptic peptide covering the proposed substrate binding site was revealed after *N*-deglycosylation. This study provided an efficient and simple method to purify, digest and characterize integral membrane proteins by MS. In addition, the EAAT2 peptide fingerprint obtained by digestion offered a template for later protein modification studies. In an effort to design photoaffinity labels for hEAAT2, a series of aryl diaminopropionic acids and aryl aspartylamide compounds were synthesized and characterized as potent EAAT inhibitors. Compounds containing 9-fluorenone groups were found to be able to irreversibly inactivate EAATs under UV-A illumination. The mechanism underlying the photo-inactivation was shown to be singlet oxygen mediated protein oxidation. The specificity of the photo-inactivation was illustrated by the protection effects of inhibitors, as well as the proximity between the transporter and ligands. Trypsin digestion and MS analyses revealed a mass change of a peptide from hEAAT2 binding pocket in the photo-inactivated protein. Molecular docking results supported our speculation that a tryptophan residue was oxidized during the photo-inactivation. The identification of possible EAAT2 photo-inactivation site provided additional information for the location of the EAAT2 lipophilic interaction domain.

ACKNOWLEDGEMENTS

First and foremost I would to express my deep and sincere gratitude to my advisor, mentor, and friend, Dr. Richard Bridges. I have been privileged to have Rich guiding me through the ups and downs of my graduate research. The completion of this dissertation would not have been possible without his scientific insight, leadership and endless support. I would like to thank my committee members: Dr. Charles Thompson, Dr. Ed Rosenberg, Dr. Sandy Ross, Dr. Kent Sugden and Dr. John Gerdes, for their times and advices. Especially, I acknowledge Dr. Thompson and Dr. Rosenberg for allowing me to use the Mass Spectrometry facility and the UV photolysis equipments. I thank Dr. Bill Laws for guiding my first project. I thank both the Department of Chemistry and the Department of Biomedical and Pharmaceutical Sciences for giving me such a wonderful time to do science under the Big Sky. I give thanks to all the current and former members of the Bridges lab, Sarj Patel, Fred Rhoderick, Todd Seib, Melissa Pathmajeyan, Shailesh Agarwal, Brady Warren, Wes Smith and Erin O'Brien. It has been a memorable experience to work in the Bridges lab and I am very grateful for the help, friendship and support they provided. I would also like to thank Brent Lyda of Dr. Sean Esslinger's lab, David Holley and Greg Leary of Dr. Michael Kavanaugh's lab, CK Chao and Beverley Parker of Dr. Chuck Thompson's lab, for the helpful discussions. I acknowledge the help of all faculty members, staff and students of the Center for Structural and Functional Neuroscience. A special thank to my beloved girlfriend Lilu whose love and encouragement mean the world to me. Lastly, I thank my dad and mom for their love and support.

TABLE OF CONTENTS

CHAPTER 1	1
STRUCTURE, FUNCTION AND PHARMACOLOGY OF EXCITATORY AMINO ACID TRANSPORTERS (EAATS)	1
1.1 L-Glutamate as a Neurotransmitter	1
1.2 Glutamate Neurotransmission (Figure 1.1)	2
<i>1.2.1 Glutamate Receptors</i>	4
<i>1.2.2 Excitotoxicity</i>	5
<i>1.2.3 Glutamate Transporters</i>	6
1.3 EAAT Subtypes	8
1.4 Regulation of EAATs	8
1.5 EAAT Mechanism	9
1.6 EAAT Pharmacology	10
1.7 EAAT Structures	17
1.8 Conclusions	22
CHAPTER 2	24
EXPRESSION, PURIFICATION, DIGESTION AND MASS SPECTROMETRIC ANALYSIS OF HUMAN EXCITATORY AMINO ACID TRANSPORTER 2 (EAAT2)	24
2.1 Introduction	24
2.2 Materials and Methods	27
<i>2.2.1 Materials</i>	27

2.2.2 Construction of Hexahistidine-tagged hEAAT2.....	27
2.2.3 Cell Culture and Transfection	28
2.2.4 Transporter Activity	28
2.2.5 Membrane Preparation and Immobilized Metal Affinity Chromatography (IMAC)	29
2.2.6 Western Blotting.....	30
2.2.7 SDS-PAGE for In-gel Digestion	30
2.2.8 Intact Protein MALDI-TOF Analysis	31
2.2.9 Protein Deglycosylation	31
2.2.10 In-Solution Digestion.....	32
2.2.11 In-Gel Digestion.....	32
2.2.12 MALDI-TOF MS Analysis	33
2.3.1 Expression and Transporter Activity.....	34
2.3.3 Intact 6XHIS hEAAT2 Protein Analysis by MALDI-TOF	41
2.3.4 In-gel Trypsin Digestion and MALDI-MS.....	43
CHAPTER 3	54
FLUOROPHORE-ASSISTED LIGHT INACTIVATION OF HUMAN EXCITATORY AMINO ACID TRANSPORTER 2 (EAAT2)	54
3.1 Introduction	54
3.1.1 Photochemical Tools in Studying Protein Structures	54
3.1.2 Chromophore-Assisted Laser Inactivation (CALI) and Fluorophore- Assisted Light Inactivation (FALI)	60
3.2 Materials and Methods.....	64

3.2.1 Synthesis of Aryl Diaminopropionic Acidss	64
3.2.2 Cell Culture and Transfection	66
3.3 Results	70
3.3.1 Synthesis of Aryl Diaminopropionic acidss	70
3.3.2 Pharmacological Characterization of β -2-CFoDA at EAATs.....	70
3.3.3 Photo-Inactivation of EAATs by β -2-CFoDA	76
3.3.4 Photosensitizer-Induced EAAT Photo-Inactivation is via Singlet Oxygen Mechanism.....	80
3.3.5 EAAT2 Inhibitors Protect Against β -2-CFoDA-Induced Photo- Inactivation.....	88
3.4 Discussion	93
3.4.1 9-Fluorenone-Mediated EAAT Inactivation is via Singlet Oxygen Mechanism.....	94
3.4.2 Photosensitizer-Induced EAAT2 Inactivation Exhibited Different Specificity	96
3.4.3 Trp472 is the Site of Photo-Oxidation in b-2-CFoDA-Induced EAAT2 Inactivation.....	98
REFERENCES	105

LIST OF FIGURES, SCHEMES AND TABLES

Figure 1.1. L-glutamate-mediated neurotransmission in a typical glutamatergic synapse.	3
Figure 1.2. Substrates and substrate inhibitors of EAATs.	11
Figure 1.3. EAAT inhibitors from simple substitutions on the glutamate or aspartate backbones.	13
Figure 1.4. Conformationally-constrained glutamate or aspartate analogues are inhibitors that can be used to delineate binding pocket structure and create pharmacophores.	15
Figure 1.5. Aspartate analogues containing large lipophilic groups can be potent EAAT inhibitors.	16
Figure 1.6. Aryl aspartylamides are the most potent group of EAAT inhibitors identified to date with low nanomolar IC ₅₀ values.	18
Figure 1.7. Secondary structure illustration of <i>Glt_{Ph}</i> .	20
Figure 1.8. Tertiary structure of human EAATs based on the sequence alignment against <i>Glt_{Ph}</i> .	21
Figure 2.1. Transport activities of 6XHIS hEAAT2 and non-tagged hEAAT2 expressed in HEK 293T cells.	35
Figure 2.2. Western blot analysis of hEAAT2 immunoreactivity in HEK 293T cell membrane preparation.	37
Figure 2.3. IMAC purification of 6XHIS hEAAT2.	39
Figure 2.4. MALDI-TOF mass analysis of native and in-gel trypsin-digested, purified 6XHIS hEAAT2.	41

Figure 2.5. Amino acid sequence of the N-terminal 6XHIS-tagged human EAAT2.	44
Figure 2.6. MALDI-TOF mass analysis of in-solution trypsin digestion of purified 6XHIS hEAAT2.	48
Figure 2.7. Trypsin 6XHIS hEAAT2 coverage map of MALDI-TOF analysis.	49
Table 2.1. MALDI-TOF Fingerprinting of 6XHIS hEAAT2 Digested with Trypsin.	50
Figure 3.1. Commonly-used photoaffinity labeling groups.	55
Scheme 3.1. UV photo-activation of benzophenone group.	56
Figure 3.2. Competing pathways and reactions of triplet state photosensitizer 3P .	58
Scheme 3.2. Synthesis of aryl diaminopropionic acids.	70
Table 3.1. Pharmacological screening of aryl diaminopropionic acids and aryl aspartylamides on EAAT1-3.	72
Figure 3.3. Dose-response curves showing competitive inhibitory activity of β -2-carboxy-fluorenyl diaminopropionic acids on EAAT1-3.	73
Figure 3.4. EAAT2 activity is irreversibly inhibited by UV-A illumination in the presence of 9-fluorenone-containing compounds.	77
Figure 3.5. Time-dependent photo-inactivation of EAAT2 by β -2-CFoDA.	78
Figure 3.6. Compounds containing 9-fluorenone groups inactivate EAAT activity under 350 nm UV illumination.	80
Figure 3.7. Photosensitizer-induced EAAT2 photo-inactivation is blocked by singlet oxygen quencher NaN_3 , but not by ROS scavengers D-mannitol or GSH.	82
Figure 3.8. Photosensitizer-induced EAAT2 photo-inactivation is via singlet oxygen ($^1\text{O}_2$) mechanism.	84
Figure 3.9. Methylene blue (MB) does not photo-inactivate either EAAT subtype.	86

- Figure 3.10.** β -2-CFoDA- and 9F2C- induced EAAT2 photo-inactivation has different levels of specificity suggested by protective effects of EAAT2 inhibitors. 88
- Figure 3.11.** MALDI MS analysis reveals an oxidized peptide in β -2-CFoDA-induced EAAT2 photo-inactivation. 91
- Figure 3.12.** Molecular docking of β -2-CFoDA into the binding domain of an EAAT2 model showed the proximity from β -2-CFoDA to W472. 99

CHAPTER 1

STRUCTURE, FUNCTION AND PHARMACOLOGY OF EXCITATORY AMINO ACID TRANSPORTERS (EAATS)

1.1 L-Glutamate as a Neurotransmitter

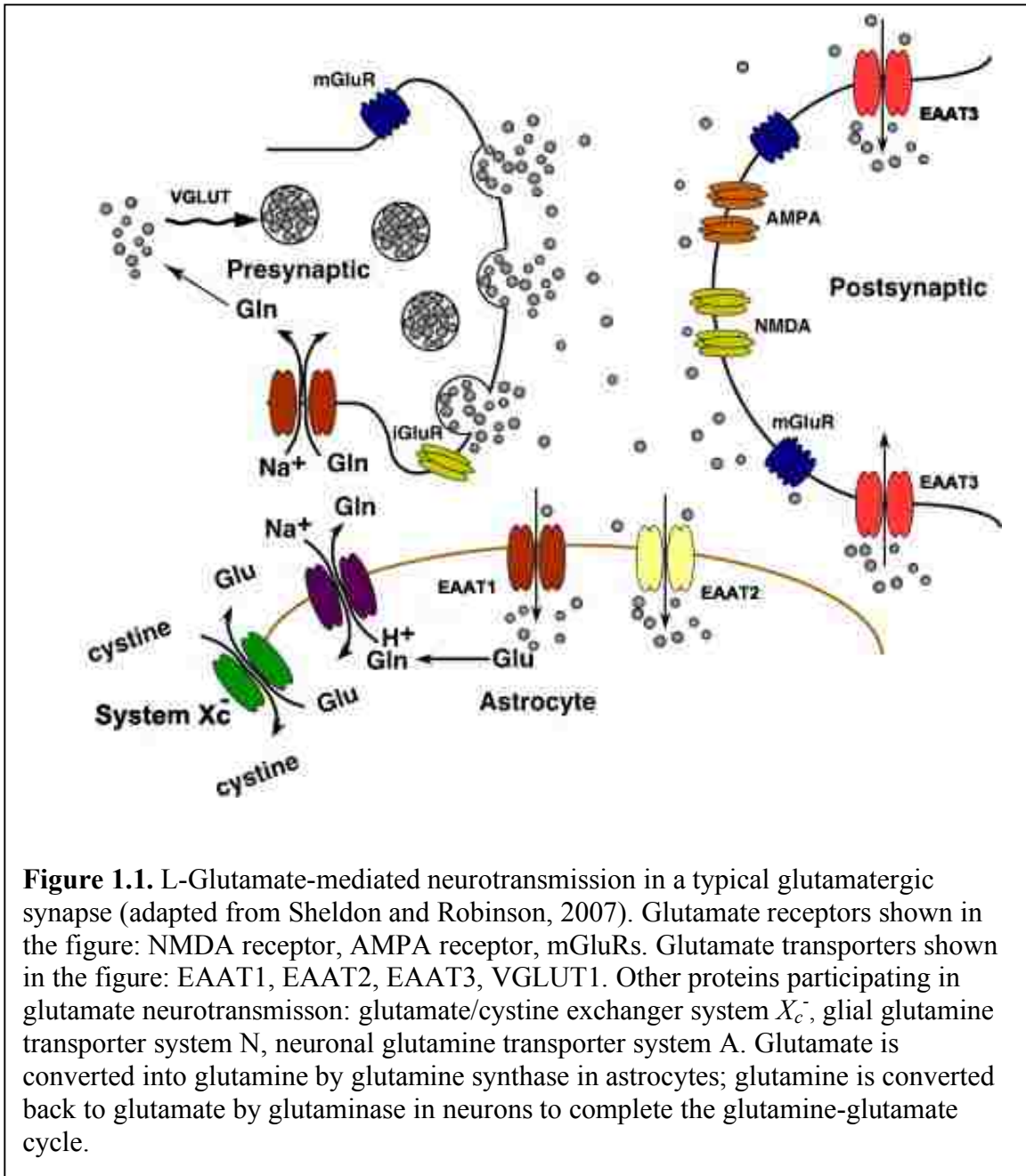
In addition to its role in protein synthesis, L-glutamate is an essential amino acid in mammalian cellular metabolism. The deamination of L-glutamate yields α -ketoglutarate, an important intermediate in the TCA cycle. In amino acid metabolism, the degradation of L-glutamate represents an amino group source for transamination reactions. Glutamate dehydrogenase catalyses the glutamate deamination reaction that is also involved in nitrogen metabolism. In addition, L-glutamate also serves as a precursor for other small molecules, including glutathione.

It has been known for a long time that glutamate exists in high levels in the brain. The average concentration of glutamate in the human brain is estimated to be around 10 mM. The first series of observations on the excitatory action of L-glutamate on neurons were made by Curtis and colleagues (Curtis et al., 1960; Curtis et al., 1961). However, the role of L-glutamate as an excitatory amino acid (EAA) in the neurotransmission was not fully established until the 1980s, when NMDA and non-NMDA receptors were identified as the synaptic receptors that are responsible for glutamate-mediated excitation in cat spinal Renshaw cells (reviewed in Watkins and Jane, 2006). With a better

understanding of the components, function and distribution of the EAA system, L-glutamate is now clearly recognized as the major excitatory neurotransmitter in the mammalian central nervous system (CNS). Current estimates suggest that about 30-40% of the synapses in the mammalian CNS are glutamatergic (Nieoullon et al., 2006). Glutamatergic neurons are localized in nearly all regions of the brain, with particularly high densities in the areas involved in learning and memory, such as cerebral cortex and hippocampus.

1.2 Glutamate Neurotransmission (Figure 1.1)

In the brain, glutamate is synthesized via two routes: the transamination of α -oxoglutarate and the metabolism of glutamine. Glutamine is synthesized in glial cells, transported into presynaptic neurons, and converted to glutamate by the neuro-specific enzyme glutaminase. In presynaptic glutamatergic neurons, L-glutamate is packaged into synaptic vesicles by the vesicular glutamate transporter (VGLUT1, 2 and 3). The uptake of L-glutamate into the vesicles is driven by a proton electrochemical gradient generated by the vacuolar type ATPase. It was estimated that each synaptic vesicle contains anywhere from 400 - 5,000 glutamate molecules (Clements et al., 1992; Barbour and Hausser, 1997). Glutamate is released from synaptic vesicles via exocytosis in response to the action potential-induced presynaptic membrane depolarization and increased Ca^{2+} concentrations in active zones. During release, the glutamate concentration in the synaptic cleft quickly rises to the millimolar range (Diamond and Jahr, 1997). The released glutamate



in the synaptic acts on postsynaptic neurons through the activation of a wide variety of postsynaptic excitatory amino acid (EAA) receptors.

1.2.1 Glutamate Receptors

Based on pharmacology, structures, and functional properties, EAA receptors can be categorized into two major classes: ionotropic glutamate receptors (iGluRs) and metabotropic glutamate receptors (mGluRs). The classification of postsynaptic glutamate receptors has been based primarily on the agonist sensitivity. Ionotropic glutamate receptors are ligand-gated ion channels that are responsible for the depolarizing actions of L-glutamate action. Three main subtypes of iGluRs are NMDA (NR1, NR2A-D, NR3), AMPA (GluR1-4) and kainate receptors (GluR5-7, KA1-2). Functionally, AMPA and kainate receptors (or non-NMDA receptors) are voltage-independent ion channels that mediate fast excitatory synaptic transmission. Activation of these receptors induces postsynapse depolarization, primarily through the gating of Na^+ currents. NMDA receptors, on the other hand, are ligand-gated and voltage-dependent ion channels that mediate slower synaptic signaling. Membrane depolarization and glutamate binding induce the release of Mg^{2+} from the NMDA receptor channel that then allows the influx of Ca^{2+} and activation of a variety of cellular pathways. In addition to the glutamate site, there are multiple sites through which the activity of the NMDA receptor can be regulated, including a co-agonist glycine site, a polyamine site, and a phencyclidine (PCP) site where noncompetitive inhibitors such as MK-801 bind. The combination of its voltage dependency and Ca^{2+} permeation provide a mechanism through which NMDA receptors contribute to higher order processes such as long-term potentiation (LTP), long-

term depression (LTD) and synaptic plasticity (Bliss and Collingridge, 1993). Not surprisingly, the NMDA receptor has also become a potentially important therapeutic target.

The other major family of glutamate receptors are mGluRs, which are linked to G-proteins and second-messenger systems. Structurally they exhibit many of the features common to all G-protein coupled receptors (GPCRs). Functionally, mGluRs exert their actions through the regulation of protein phosphorylation and second-messenger cascades. The mGluRs are subdivided into 3 groups based upon pharmacological differences and downstream effectors: group I (mGluR1, mGluR5) and II (mGluR2, mGluR3) are activated by trans-ACPD, while group III receptors (mGluR4, mGluR6, mGluR7, mGluR8) are activated by L-AP4. Group I metabotropic glutamate receptors are coupled to phospholipase C while groups II and III receptors are coupled to adenylate cyclase (Schoepp et al., 1999).

1.2.2 Excitotoxicity

In addition to its role in excitatory signaling, the activation of iGluRs can also induce neuronal pathology. This process is referred to as excitotoxicity and involves several pathological pathways. Most importantly, rapid increases in intracellular Ca^{2+} that follow the excessive activation of NMDA receptors, can trigger both necrotic and apoptotic pathways and ultimately result in cell death. Energy consumption and increased rates of reactive oxygen species (ROS) generation are also associated with the over activation of glutamate receptors and mitochondria damage. Excitotoxicity is now well-recognized as a primary or secondary mechanism underlying the pathology observed

in growing number of acute insults to the CNS (e.g., ischemia, hypoglycemia, spinal cord injury, traumatic brain injury), as well as chronic neurological and neuropsychological disorders (e.g., amyotrophic lateral sclerosis, epilepsy, schizophrenia, Huntington's disease, Alzheimer's disease) (Natale et al., 2006; Foster and Kemp, 2006; Waxman and Dijk-Hajj, 2005; Hynd et al., 2004; Olney, 2003; Rao and Bredesen, 2004; Coyle, 2004).

1.2.3 Glutamate Transporters

The rapid and efficient clearance of extracellular L-glutamate into neurons and glia by the EAATs is believed to contribute to the termination of its excitatory signal, the recycling of the neurotransmitter, and the prevention of excitotoxicity. The role of EAATs in controlling excitatory neurotransmission is achieved by the high expression level of the transporters near the synapse, as well as the high binding affinities for L-glutamate. The combination of both factors allows the transporters to overcome their slow operation time (10-75 ms) and efficiently clear the extracellular L-glutamate (Wadiche et al., 1995; Bergles and Jahr, 1997). Another aspect of the EAATs' function in terminating excitatory signal lies in the regulation of glutamate spillover. Controlled extrasynaptic signaling may have significant roles in processes associated with learning and memory, such as LTP (Vizi and Mike, 2006). Transporter expression patterns and functional studies using inhibitors suggested that the majority of released L-glutamate is recycled into glial cells via EAAT1 and EAAT2-mediated mechanism. These neurotransmitters are subsequently converted into glutamine which serves as the precursor to glutamate in the glutamate-glutamine cycle. The transport of L-glutamate into neurons by EAAT3, although only accounts for a small percentage of the total

glutamate uptake, has functional importance in supplying a precursor for GABA synthesis (Mathews and Diamond, 2003) and glutathione synthesis (Aoyama et al., 2006). The role of EAATs in preventing excitotoxicity was first demonstrated by the high neuronal death observed in isolated neuronal culture but not in neuronal-glia co-culture when high concentrations of L-glutamate were included in the buffers (Rosenberg et al., 1992). Several *in vitro* studies also showed blocking EAATs with inhibitors potentiated excitotoxicity (Robinson et al., 1993; Dugan et al., 1995) and induced necrotic neurodegeneration (Guiramand et al., 2005; Bonde et al., 2005). In addition, GLT-1 (EAAT2) knockout mice display lethal spontaneous seizures and exacerbation of cortical injury that can be attributed to elevated L-glutamate levels (Tanaka et al., 1997).

Alterations in glutamate transporter activities and expressions have been found in a variety of neurological disorders. Amyotrophic lateral sclerosis (ALS) is probably the most extensively studied disease that has the connection with EAATs. It was observed that expression levels of EAAT2 were significantly reduced in ALS patients (Rothstein et al., 1995). Recent evidence suggested that the loss of EAAT2 is due to the selective cleavage of the EAAT2 via activation of caspase 3 by superoxide dismutase 1 (SOD1) mutants in ALS patients (Boston-Howes et al., 2006). Instead of having a primary link between transporters' pathology, as in ALS, excitotoxicity plays a role in many other neurodegenerative diseases, including Alzheimer's disease (AD), Parkinson's disease (PD), Huntington's disease (HD) and stroke. In both AD and HD, reduced surface expression of EAAT2 was observed (Masliah et al., 2000; Brustovetsky et al., 2004). The associations between PD and glutamate toxicity were based on the neuroprotective effects offered by NMDA receptor antagonists (Klockgether and Turski, 1990) but the

direct connection with EAATs is still unknown. During a cerebral stroke, the glutamate concentration in the cerebrospinal fluid (CSF) is significantly elevated. An EAAT2 promoter polymorphism was recently found to downregulate the EAAT2 expression after stroke, which may have increased the likelihood of excitotoxic damage (Mallolas et al., 2006).

1.3 EAAT Subtypes

Molecular cloning studies in the 1990s successfully identified five membrane protein subtypes, termed EAAT1-5 (in humans) that are responsible for glutamate reuptake (Storck et al., 1992; Tanaka, 1993; Pines et al., 1992; Kanai and Hediger, 1992; Fairman et al., 1995; Arriza et al., 1997). The five subtypes share 50%-60% sequence homology and they belong to solute carrier 1 (SLC1) family, along with neutral amino acid transporters ASCT1 and ASCT2. The localization of EAATs differs among subtypes; with EAAT1 and EAAT2 are primarily localized in glia cells, EAAT3 and EAAT4 are generally considered to be neuronal, and EAAT5 is highly restricted to the retina. In most brain areas, EAAT2 is responsible for the majority of glutamate uptake (Haugeto et al., 1996).

1.4 Regulation of EAATs

When compared to the monoamine family of neurotransmitter transporters, the regulation of glutamate transporters is just beginning to be understood. There is evidence showing that the EAATs are associated with cholesterol-rich lipid raft microdomains

(Butchbach et al., 2004; Raunser et al., 2006). The targeting of transporters into such domains requires interacting scaffolding proteins. Rothstein and colleagues have identified a few interacting scaffolding proteins of EAAT3 and EAAT4 such as GTRAPs (Jackson et al., 2001; Lin et al., 2001) and RTN2B (Liu et al., 2008). While the GTRAPs all interact with the C-termini of the transporters, a LIM protein Ajuba, was found to interact with N-terminus of EAAT2 and suggested to be part of a protein complex that stabilizes the transporter at the plasma membrane (Marie et al., 2002). Protein kinases and phosphatases such as PKC and PP2A have been shown to regulate the activities of glutamate transporters (Gonzalez and Robinson, 2004). Protein phosphorylation and dephosphorylation seem to have different effects on different EAAT subtypes (Gonzalez et al., 2002, 2003) and the exact mechanisms are still unclear. The interacting proteins involved in regulating EAAT trafficking and internalization have yet to be identified.

1.5 EAAT Mechanism

The process of transporting glutamate into the cell against its concentration gradient by EAATs is driven by the coupled-influx of Na^+ and efflux of K^+ down their respective concentrations gradients. The current kinetic model suggests that the translocation of one glutamate molecule into the cell is coupled with the inward co-transport of three Na^+ and one H^+ . After the release of glutamate, one K^+ binds to the empty carrier before being exported to the extracellular space (Zerangue and Kavanaugh, 1996). The electrogenic nature of glutamate transporters has also allowed their actions to be studied electrophysiologically. Substrates induce currents, while non-substrate

inhibitors themselves do not, but can block substrate-induced currents. This transport cycle has to be completed before glutamate can be concentrated in the cells. A rat GLT-1 mutant E404D that lacks K⁺-binding ability has been shown to only operate in the exchange mode, i.e. glutamate re-binds empty carrier intracellularly and is exported. This “alternate access model” would require the transporter protein to have an external gate and an internal gate. The exact location of both gates and the conformational changes associated with the translocation process has yet to be elucidated, although recent crystallographic data (see below) have begun to provide some insight.

1.6 EAAT Pharmacology

The cloning of each subtypes of glutamate transporters allowed researchers to develop heterogeneous expression models, such as *Xenopus* oocytes, C17.2 and HEK 293 cell lines, to study the subtype-selectivity of the drugs. These systems provide an advantage over native brain preparations, such as synaptosomes where cross-reactivity among subtypes and with various receptors can not be easily separated. The endogenous substrates of EAATs, L-glutamate and L-aspartate, are efficiently transported into cells by all five subtype, along with several closely related analogues including D-aspartate (Figure 1.2). Many of the inhibitors identified do not possess the ability to be translocated into the cells and are thus referred to as non-substrate inhibitors. Recognizing the structural differences between substrates and non-substrate inhibitors will greatly advance our understanding of the protein binding domain structure, transport mechanism and the development of therapeutic drugs targeting these transporters.

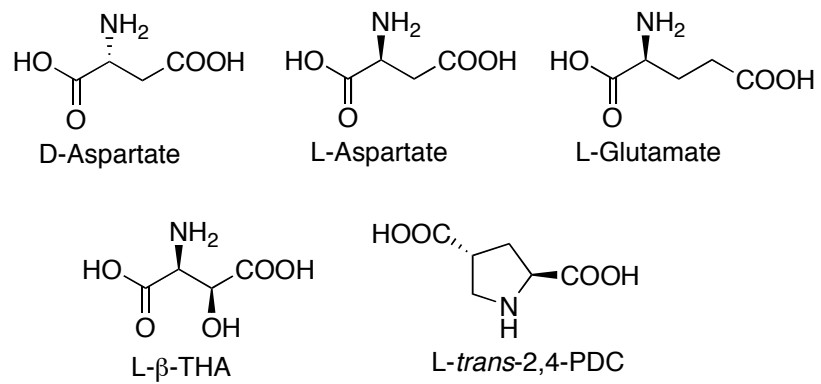


Figure 1.2. Substrates and substrate inhibitors of EAATs.

The search for potent, subtype-selective glutamate transporter inhibitors in the past 20 years has yielded a large collection of compounds that differ greatly in structure, potency and subtype-specificity. The developments in EAAT pharmacology have been covered in several excellent reviews (Bridges et al., 1999; Shigeri et al., 2004; Bridges and Esslinger, 2005; Dunlop and Butera, 2006). Rather than revisiting the history of EAAT pharmacology, the major classes of EAAT inhibitors and their representative compounds are described.

Early attempts in designing EAAT inhibitors took the approach of simple substitutions on the glutamate or aspartate backbones (Figure 1.3). Methylation on C3 and C4 positions of L-glutamate produced two inhibitors with different EAAT inhibitory profiles. *Threo*-3-methylglutamate (T3MG) preferentially inhibits EAAT2 over EAAT1 and EAAT3, while being a substrate of EAAT4 (Vandenberg et al., 1997; Eliasof et al., 2001). The 4-methylated glutamate, (2*S*,4*R*)-4-methylglutamate, is a non-substrate inhibitor of EAAT2 and a less potent, but transportable substrate of EAAT1 (Aprico et al., 2001, 2004). Isosteric replacements of the γ -carboxyl group into sulphonic acid and hydroxamic acid groups generated a substrate of EAAT1, L-serine-O-sulfate (L-SOS), and a nonspecific inhibitor in L-aspartate- β -hydroxamic acid.

The free rotation of the sigma bonds in linear glutamate analogues made it difficult to probe the ligand-protein interaction sites. Bridges and colleagues developed a series of conformationally constrained glutamate/aspartate analogues (Figure 1.4) and were able to generate EAAT pharmacophores based on these compounds (Esslinger et al., 2005). One of the first of this group is dihydrokainate (DHK) (Sonnenberg et al., 1996), and still remains one of the best EAAT2-selective inhibitors. The selectivity of DHK

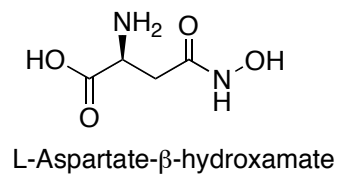
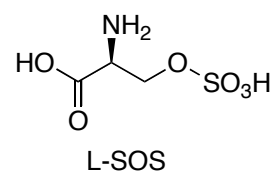
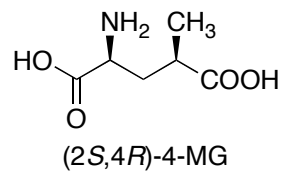
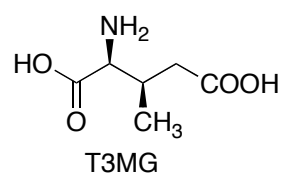


Figure 1.3. EAAT inhibitors from simple substitutions on the glutamate or aspartate backbones.

displayed on EAAT2 is more than 100 fold over EAAT1 and EAAT3 in various expression systems (Arriza et al., 1994). Other categories of conformationally constrained analogues include 2-(carboxycyclopropyl)glycines (CCGs), aminocyclobutane dicarboxylates (ACBDs) and pyrrolidine dicarboxylates (PDCs). Most of these compounds showed comparable inhibition potencies across the EAAT subtypes.

Hydroxyl- substitution on the C3 of L-aspartate affords *L-threo*- β -hydroxy-aspartate (*L*- β -THA), a substrate inhibitor of EAAT1-3 (Arriza et al., 1994). While *L*- β -THA did not receive a lot of attention, further substitutions on the β - hydroxyl group yielded a series of breakthrough inhibitors that were a major advance in EAAT pharmacology (Figure 1.5). The pharmacological characterization of *DL-threo*- β -benzyloxyaspartate (*DL*-TBOA) (Shimamoto et al., 1998) and its derivatives (Shimamoto et al., 2000) demonstrated that compounds bearing large lipophilic groups have the potential to be very potent EAAT inhibitors. Both TBOAs and *threo*- β -naphthhyloxyaspartates (TNOAs) have IC₅₀ values in low micromolar range on all subtypes. One of the most potent EAAT inhibitors reported to date is (2*S*,3*S*)-3-{3-[4-(trifluoromethyl)benzoylamino]benzyloxy} aspartate (TFB-TBOA), with IC₅₀ values of 22 nM, 17 nM and 300 nM on EAAT1-3, respectively (Shimamoto et al., 2004). Removal of the ether linkage in TBOA resulted in a subtype specific inhibitor, *L*- β -*threo*-benzylaspartate (TBA), which showed a 10-fold preference for the EAAT3 (Esslinger et al., 2005). Additional TBA derivatives have also been recently characterized (Mavencamp et al., 2008).

The reports of a new family of very potent EAAT inhibitors bearing diaminopropionic acids or aspartylamide scaffolds and large lipophilic groups seemed to

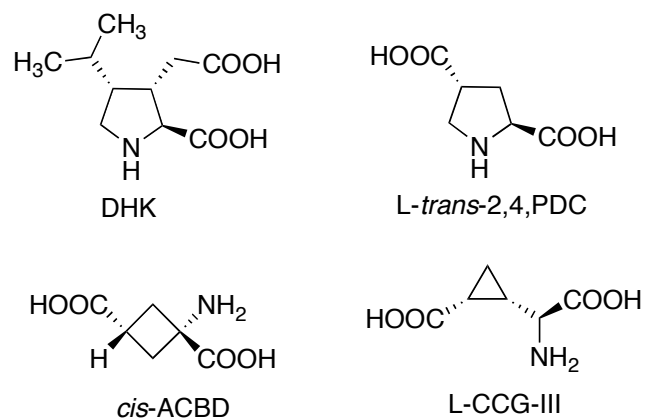


Figure 1.4. Conformationally-constrained glutamate or aspartate analogues are inhibitors that can be used to delineate binding pocket structure and create pharmacophores.

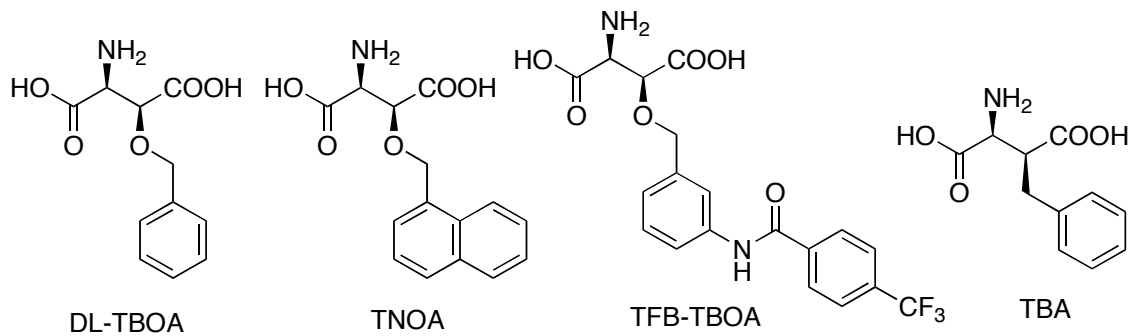


Figure 1.5. Aspartate analogues containing large lipophilic groups can be potent EAAT inhibitors.

validate the conclusions that the lipophilic interactions between the transporters and the ligands are key contributors to the pharmacological activity (Greenfield et al., 2005; Dunlop et al., 2005) (Figure 1.6). Compounds such as (*S*)-2-amino-4-(4-(2-bromo-4,5-difluorophenoxy)phenylamino)-4-oxobutanoic acid (WAY-213613) and (*S*)-4-(9*H*-fluoren-2-ylamino)-2-amino-4-oxobutanoic acid (NBI-59159) have shown low nanomolar range IC₅₀s on EAATs. It is also worth mentioning that this family of non-substrate inhibitors displayed very unusual binding kinetics to the EAATs, with association and dissociation times in the 10-20 minute range. This kinetic feature may also contribute to the high potency by elevating the local concentration in the aqueous bowl of the transporter trimer.

1.7 EAAT Structures

Early predictions of EAAT structures have generally agreed on the first 6 transmembrane domains on the N-termini of the proteins. Extensive site-directed mutagenesis work was performed in the late 1990s and early 2000s to probe the seemingly unstructured C-termini of the EAAT family proteins (Slotboom et al., 2001; Seal et al., 1998; Grunewald et al., 1998). Despite controversies over a few residues, it is now accepted that there are two additional transmembrane regions and two loops, one from the cytoplasmic side and the other from the extracellular side, traverse halfway through the plasma membrane before coming back to the same side of the membrane (Seal et al., 2000; Grunewald et al., 2002). Mutations in these regions often times resulted in the partial or total loss of

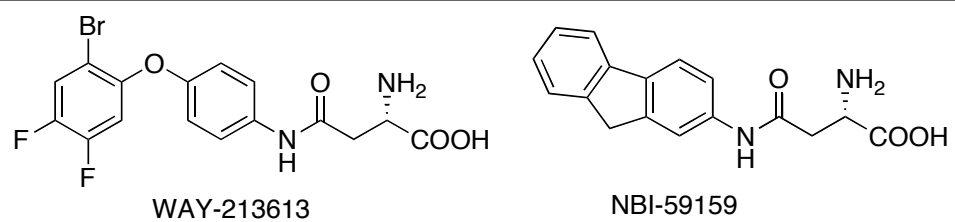
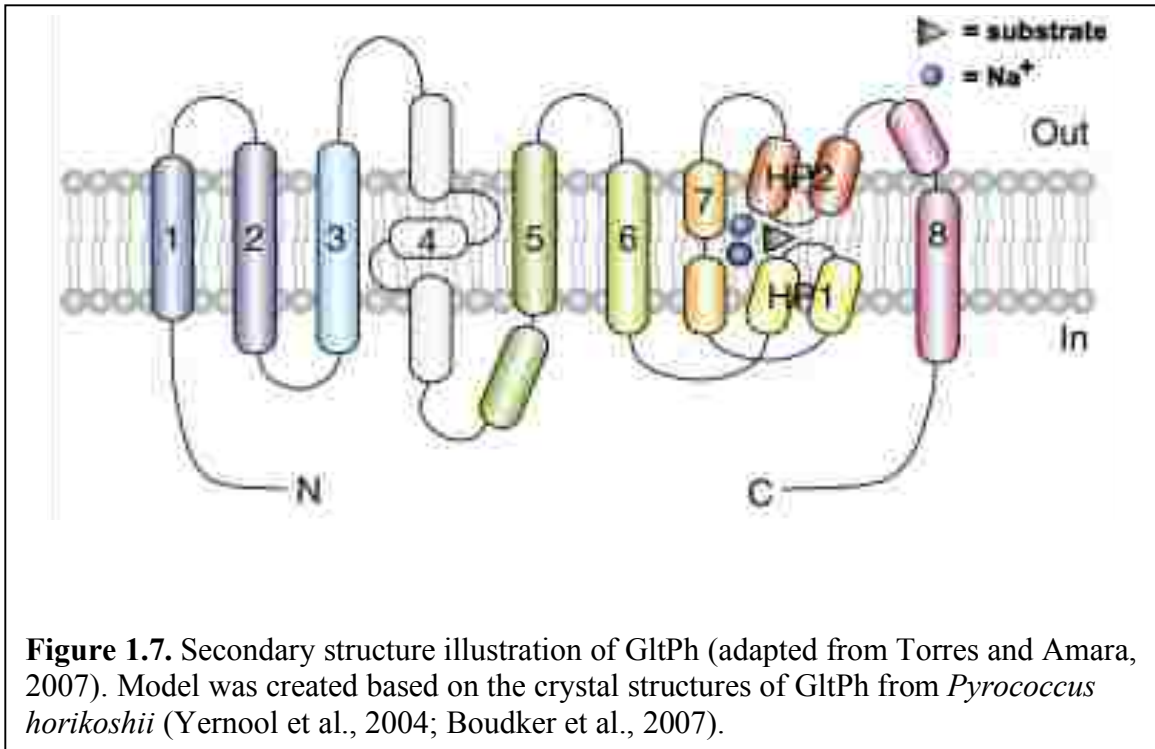


Figure 1.6. Aryl aspartylamides are the most potent group of EAAT inhibitors identified to date with low nanomolar IC_{50} values.

activity of the transporters. These data suggested that C-terminal side of the protein is associated with the binding and translocation of glutamate.

Our understanding of glutamate transporter structures was greatly advanced after the successful crystallization of a bacteria glutamate/aspartate transporter *Glt_{Ph}* (Yernool et al., 2004, PDB accession code: 1XFH). The glutamate transporter homolog from *Pyrococcus horikoshii*, shares about 30-40% primary sequence identity with the human EAATs and preferentially transports aspartate. The solved crystal structure in many aspects agreed well with the predictions made based on biochemical observations. In addition, it also offered a much clearer picture of the structural features of glutamate transporters. The transporters form a trimeric structure with an aqueous bowl in the center. The secondary structure features eight transmembrane domains and two hairpin loops, HP1 and HP2. The authors proposed a model in which HP2 serves as the extracellular gate and HP1, part of TM7 and TM8 form the intracellular gate (Figure 1.7). However, the modest resolution of the structure (3.5 Å) limited the dynamic conformational change information that could be provided by this structure. To follow up this study, high-resolution, inhibitor- and ion-bound glutamate transporters were crystallized and solved by X-ray diffraction (Boudker et al., 2007). In a series of structures (PDB accession codes: 2NWW, 2NWX, 2NWL), the authors were able to demonstrate the transporter conformations in different binding modes. One particularly interesting finding was the non-transportable inhibitor, D,L- *threo*-β-benzyloxyaspartate (TBOA), kept the transporter in an open conformation by placing the bulky benzyl group against the tip of the HP2, therefore prevented the extracellular gate from closing and completing the process of intracellular release. Because of the high sequence homology in



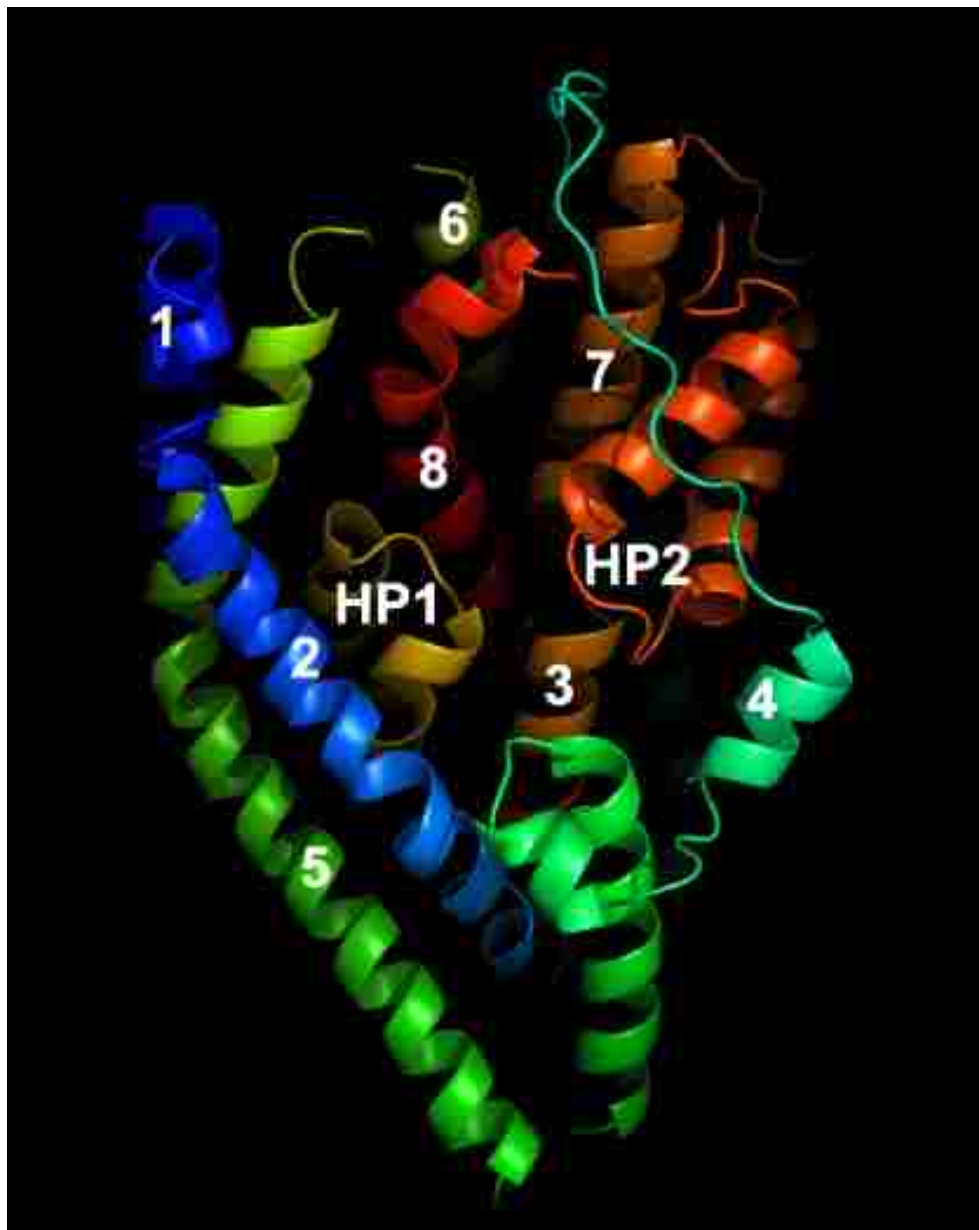


Figure 1.8. Tertiary structure of human EAATs based on the sequence alignment against GltPh. Image was rendered using MacPymol (DeLano Scientific, <http://www.delanoscientific.com/>).

the regions of functional significance between *Glt_{Ph}* and human EAATs, it is quite possible the human glutamate transporters operate by similar mechanisms (Figure 1.8).

1.8 Conclusions

Given their wide distribution in the CNS and important functions in excitatory signaling and excitotoxicity, glutamate transporters represent an interesting target for ligand and drug development. Any subtle change of EAAT activity will likely induce a dramatic alteration to local synaptic environment. The development of subtype-specific inhibitors is a key step towards drug discovery targeting different populations of EAATs. However, such study has been hindered by the incomplete understanding of the transporter structures and the protein-inhibitor interactions.

Although the *Glt_{Ph}* structures shed light on the structures and mechanisms of human EAATs, several key questions still remain to be answered. Protein conformation changes are associated with the movement of the substrate from the external binding site to the internal releasing site. The dynamic nature of this movement is still lacking from the image of TBOA-bound *Glt_{Ph}*. Furthermore, the high potency exhibited by aryl aspartylamides and aryl diaminopropionic acids can not be easily explained by the binding site and orientation of TBOA in *Glt_{Ph}*. Additional efforts need to be focused on delineating the lipophilic pocket of EAATs in general and more importantly, subtype differences.

With an increasing amount of structural, functional and pharmacological data available for the EAATs, the stage is now set for the development and use of

pharmacological probes to investigate structural features of the EAATs that will ultimately provide a better understanding of their structure and function.

CHAPTER 2

EXPRESSION, PURIFICATION, DIGESTION AND MASS SPECTROMETRIC ANALYSIS OF HUMAN EXCITATORY AMINO ACID TRANSPORTER 2 (EAAT2)

2.1 Introduction

Integral membrane proteins (IMPs) are a set of proteins that accounts for about one third of all predicted proteomes (Wallin and von Heijne, 1998; Stevens and Arkin, 2000). IMPs play key roles in essential cell functions, such as receptors signaling, transport and trafficking. Structure-function relationship studies have always been a preferred path to understand the functions and dysfunctions of proteins and their roles in human disease. While X-ray crystallographic and NMR-based approaches represent some of the best methods to reveal protein structural information, solving structures specifically for membrane proteins remains a challenge due to the difficulties in handling such proteins. Indeed, among over 53,000 known protein crystal structures solved (<http://www.rcsb.org>) at atomic resolution, only about 170 of them are for membrane proteins.

The size and complexity of a full proteome easily exceed the dynamic range of any single analytical method (Domon and Aebersold, 2006). Over the last 15 years, mass spectroscopy (MS) techniques have emerged as a powerful tool in analyzing structures and functions of biological macromolecules (Tanaka et al., 2003; Karas and Hillenkamp,

1988; Fenn et al., 1989). The availability of using different instruments and techniques provides a wide range of structural and functional analyses. However, the problems in characterizing integral membrane proteins also poses a challenge to MS techniques (Whitelegge et al., 2003; Wu and Yates III, 2003) because membrane proteins: 1) have poor solubility in aqueous buffers; 2) are typically lower in abundance; 3) are usually unstable and easily form aggregates; 4) often undergo conformational and folding changes; 5) exhibit various forms of post-translational modifications (PTMs). To address the above limitations, modern proteomics studies on membrane proteins employ a number of strategies related to membrane solubilization, including the use of organic solvents (Blonder et al., 2002; Goshe et al., 2003), detergents (Han et al., 2004) and organic acids (Washburn et al., 2001). Protein purification methods such as Immobilized Metal Affinity Chromatography (IMAC) have also been used to enrich and separate membrane proteins (Porath, 1992). The establishments of proteomics data standards, such as the human protein reference database (Peri et al., 2003; <http://www.hprd.org>) and SwissProt (Bairoch et al., 2005; <http://www.pir.uniprot.org>), provide platforms to share PTM information in public databases. Along with the rapid progresses in MS instrumentation and techniques, a large number of integral membrane proteins have been characterized by MS methods, including human tetraspanin membrane protein CD81 (Takayama et al., 2008), human cannabinoid CB2 receptor (Zvonok et al., 2007) and a yeast G-protein coupled receptor Ste2p (Lee et al., 2007).

The selection of detergents in the extraction and purification of membrane proteins is especially important. This choice can greatly effect the purification efficiency and also the downstream MS analysis. Typically, however, the identification of

appropriate detergents in membrane protein purification is determined on a protein-by-protein basis. For example: 3-[(3-cholamidopropyl) dimethylammonio]-propanesulfonate (CHAPS) and *n*-dodecyl- β -D-maltoside (DDM) were used to solubilize the κ opioid receptor (Wannemacher et al., 2008), 1% SDS was chosen in a study of vesicular glutamate transporter 1 (Cox et al., 2008), and DDM was successfully used in the mass spectrometric characterization of human cannabinoid CB2 receptor (Filppula et al., 2004). Generally, in proteomic studies, proteins are resolved on one-dimensional or two-dimensional gels and visualized using various stains. Two-dimensional SDS-PAGE has an exceptionally high separation capacity, e. g. up to 10,000 proteins on one gel. However, in the instance of membrane proteins, solubilized proteins are prone to precipitation during isoelectric focusing in 2D-gel (Santoni et al., 2000). For this reason, many researchers preferred 1D-gel in studying membrane proteins (Ferro et al., 2002; Galeva and Altermann, 2002; Simpson, 2000). The increased protein complexity problem in 1D gel can be overcome by the use of IMAC prior to the gel electrophoresis.

Once the proteins are resolved on gels and protein bands of interest are selected, they are digested into peptides that are then extracted from the gel for the subsequent identification by MS. Trypsin digestion is one of the most widely used methods to cleave proteins. Trypsin specifically hydrolyzes peptide bonds at the carboxyl side of lysine and arginine residues (Keil-Dlouha et al., 1971).

In this study, human excitatory amino acid transporter 2 (EAAT2) was expressed in mammalian cells, extracted, purified and characterized by MS. The MS characterization of this transporter protein provided us a structural template for further protein-ligand interaction studies.

2.2 Materials and Methods

2.2.1 Materials

Laboratory chemical and buffers were from Sigma Chemical Co. (St. Louis, MO) and Fisher Chemical (Pittsburgh, PA). Protease inhibitor cocktail was from Roche Applied Science (Indianapolis, IN). HisTrap chelating columns were from GE Healthcare (Piscataway, NJ). Sequencing-grade modified trypsin was from Promega (Madison, WI). Peptide calibration standards were from Bruker Instruments (Billerica, MA) and Invitrogen (Carlsbad, CA).

2.2.2 Construction of Hexahistidine-tagged hEAAT2

hEAAT2 cDNA was PCR amplified from pBlueScriptEAAT2 (provided by Dr M. Kavanaugh) using primer pairs (forward; 5'-ATTAGGATCCATGGCATCTACGGAAGGTG-3' and reverse 5'-TATTGATATCTTATTTCTCACGTTTCCA-3'). The primer pair introduced BamHI sites at the 5' end and EcoRV sites at the 3' end of the amplified fragment. The PCR fragment was then subcloned into the BamHI and EcoRV sites within the polylinker of the AAV vector pAM-CAG-WPRE (kindly provided by Dr Mathew During, University of Auckland, NZ) to create pAM-CAG-EAAT2-WPRE. Final clones were confirmed by double stranded sequencing. A 96 b.p. HIS-Xpress insert was PCR amplified from pBAD/HIS B (Invitrogen) using primer pairs 5'-TTT GGA TCC ACC ATG GGG GGT TCT CAT-3' and 5'-ATT GGA TCC CTT ATC GTC ATC GTC GTA-3' introducing BAMHI sites to the 5' and 3' ends of the fragment. The PCR fragment was subcloned

into pCR-BLUNT-TOPO (Invitrogen) according to the manufacturer's protocol. Positive clones were mini-prepped and the reading frame and sequence were confirmed by double strand sequencing analysis at the Murdock Lab sequencing facility at the University of Montana. The fragment was isolated by BAMHI digestion, purified and subcloned into pAM/CAG-EAAT2 plasmid at the 5'-end of the gene, generating an N-terminal fusion protein. The correct orientation was confirmed by restriction analysis and PCR amplification.

2.2.3 Cell Culture and Transfection

HEK 293T cells (ATCC, Manassas, VA) between passages 10 and 20 were cultured at 37 °C in a humidified atmosphere containing 5% CO₂ in Dulbecco's modified Eagle's medium (DMEM) supplemented with 10% fetal bovine serum, 1 mM sodium pyruvate, 0.1 mM nonessential amino acids solution, and 0.05% penicillin–streptomycin (5000 units/ml) and gentamicin sulfate (0.05 mg/ml). Cells were seeded at 1 x 10⁵ cells/well in 12-well plates for transporter activity experiments and 1.5 x 10⁶ cells/dish in 100 mm² dishes for membrane preparations. At 48 h after plating, cells were transfected using Lipofectamine 2000 (Invitrogen, Carlsbad, CA) or FuGENE Transfection Reagent (Roche, Indianapolis, IN) in a ratio of 2 ml of Lipofectamine to 2 mg of purified plasmid DNA in accordance with the manufacturer's instructions.

2.2.4 Transporter Activity

Approximately 24 hours after transfection, near-confluent HEK 293T cells were rinsed with a physiological buffer (138 mM NaCl, 11 mM d-glucose, 5.3 mM KCl, 0.4

mM KH₂PO₄, 0.3 mM Na₂HPO₄, 1.1 mM CaCl₂, 0.7 mM MgSO₄, 10 mM HEPES, pH 7.4) and allowed to preincubate at 37 °C for 5 min. Uptake was initiated by replacing the pre-incubation buffer with buffer containing 25 mM D-[³H]-aspartate. Following a 5 min incubation, the media was removed by rapid suction and the cells rinsed three times with ice-cold buffer. The cells were dissolved in 0.4 N NaOH for 24 h and analyzed for radioactivity by liquid scintillation counting and protein by the BCA (Pierce) method. Transport rates were corrected for background, i.e., radiolabel accumulation at 4 °C. Initial studies confirmed that uptake quantified in this manner was linear with time and protein levels and that uptake in untransfected HEK 293T cells was indistinguishable from background.

2.2.5 Membrane Preparation and Immobilized Metal Affinity Chromatography (IMAC)

Approximately 24 hours after transfection, near-confluent HEK 293T cells were rinsed with DPBS (MediaTech, Manassas, VA) after the culture medium was aspirated. Cells were harvested in DPBS with 5mM dithiothreitol (DTT) and EDTA-free complete protease inhibitor (Roche, Indianapolis, IN). The cell suspension was homogenized in 0.2 M sucrose with 5 mM DTT, then centrifuged at 500 g for 5 min. The pellet was discarded and the membrane fraction was centrifuged at 13,000g for 30 min. The membrane pellet was resuspended in 1 ml IMAC suspension buffer containing 0.5 M NaCl, 0.02 M sodium phosphate, 1% *n*-dodecyl- β -D-maltoside (DDM), 30% glycerol, 5 mM DTT and 2 mg/ml aroclor. The membrane suspension was incubated in 4 °C for 8 h, then centrifuged at 14,000 g for 3 min and supernatant was applied to the 1 ml HisTrap High Performance nickel-sepharose column (GE Healthcare, Piscataway, NJ), the flow

through fraction was collected, and the column was washed with 15 ml of buffer containing 0.5 M NaCl, 0.02 M sodium phosphate, 20 mM imidazole, 0.1% DDM, 30% glycerol and 2 mg/ml asolectin. The 6xHIS hEAAT2 was eluted with buffer containing a gradient concentration of imidazole ranging from 50 mM to 300 mM, or a single-step elution of 300 mM imidazole.

2.2.6 Western Blotting

For detection of the hEAAT2 by western immunoblotting, samples were mixed with 2x Laemmli buffer and resolved by SDS-PAGE using 4-15% gradient gels, then transferred to PVDF membranes (Bio-Rad, Hercules, CA). Membranes were blocked for 1 h in 0.1% dried milk, 20 mM Tris base, 130 mM NaCl, 0.1% Tween 20, pH 7.6, followed by overnight incubation at 4 °C with rabbit anti-GLT-1 polyclonal antibody (Affinity Bioreagents, Golden, CO). Membranes were then washed and incubated with anti-rabbit IgG Horseradish Peroxidase (HRP)-linked antibody (Cell Signaling, Danvers, MA) for 1 h at room temperature and developed using ECL western blot chemiluminescence reagent (Cell Signaling, Danvers, MA). Fujifilm LAS 3000 imaging system (Bio-Rad, Hercules, CA) was used to capture chemiluminescence.

2.2.7 SDS-PAGE for In-gel Digestion

Fractions containing the purified hEAAT2 from the HisTrap column were concentrated from 500 ml to 20 ml using Microcon YM50 filters (Millipore, Billerica, MA). The concentrated sample was mixed with 2x Laemmli buffer and loaded onto a 4-

15% SDS-PAGE gel, then stained with Biosafe Coomassie (Bio-Rad). Gel image was taken by a Biorad Molecular Imager ChemiDoc XRS system.

2.2.8 Intact Protein MALDI-TOF Analysis

Intact purified hEAAT2 protein was not reduced or alkylated before being precipitated in 10% trichloroacetic acid (TCA) at 4 °C for 30 min. The protein pellet was collected by centrifugation at 15,000g for 5 min. The protein pellet was then washed with 1 ml of cold 1:1 ethanol:ether (v:v) solution 3 times. The washed pellet was briefly air-dried and resuspended in 50% acetonitrile and 0.1% TFA. An aliquot of the solution was mixed with equal volume of sinapic acid matrix solution in 50% acetonitrile and 0.3% TFA before being spotted onto a MALDI plate. A Bovine Serum Albumin mass spec standard (Sigma-Aldrich, St. Louis, MO) was used for calibration.

2.2.9 Protein Deglycosylation

Purified hEAAT2 protein from HisTrap column was concentrated by Millipore Microcon YM-50 filter to a concentration of 1.1 mg/ml. A denaturant solution containing 2% octyl-*b*-D-glucopyranoside and 100 mM 2-mercaptoethanol was added followed by the addition of 500 units/ml PNGase F (from *Elizabethkingia meningoseptica*, Sigma-Aldrich, St. Louis, MO) at the ratio of 50 units per mg of protein. The solution was mixed and incubated at 37 °C for 1 h. This enzyme recognizes the *N*-glycosylation sites of glycoproteins and cleaves the linkage between Asn and carbohydrate chain (Tarentino and Plummer, 1994). The reaction was stopped by adding appropriate volume of 2x

Laemmli sample buffer and reaction products were analyzed on SDS/PAGE or Western immunoblotting.

2.2.10 In-Solution Digestion

Aliquot of purified hEAAT2 from HisTrap column was precipitated in 10% TCA at 4 °C for 30 min. The protein pellet was collected by centrifugation at 15,000g for 5 min. The protein pellet was then washed with 1 ml of cold 1:1 ethanol:ether (v:v) solution 3 times. The washed pellet was briefly air-dried and resuspended in 50 mM ammonium bicarbonate buffer, pH 8.0 (AMBIC). Sequence grade trypsin (Promega, Madison, WI) was added at a 1:20 ratio, and digestion was allowed to proceed at 37 °C for 20 h. Tryptic peptides were analyzed from the digest solution.

2.2.11 In-Gel Digestion

The SDS-PAGE gel fragment was diced into 1 mm³ pieces and destained twice with 200 ml 50% acetonitrile/25 mM AMBIC, for 1 h to remove the Coomassie blue dye. Gel pieces were then dried in a SpeedVac (Savant) at room temperature. Prior to digestion, gel pieces were reduced with 10 mM DTT in 100 mM ammonium bicarbonate at 56 °C for 1 h, then alkylated with 55 mM iodoacetamide in ammonium bicarbonate for 1 h at room temperature in the dark. Gel pieces were washed with 50% acetonitrile/25 mM ammonium bicarbonate and dehydrated in SpeedVac. Tryptic digestion was started with the addition of 50 mg reconstituted trypsin per mg of EAAT2 protein in 25 mM NH₄HCO₃ at pH 8.0. The concentration of the trypsin solution was 12.5 ng/ml. After reswelling, excess trypsin solutions were removed and the gel pieces were covered with

an overlay of ~20 ml of 25 mM ammonium bicarbonate. The protein was digested for 20 h at 37 °C.

2.2.12 MALDI-TOF MS Analysis

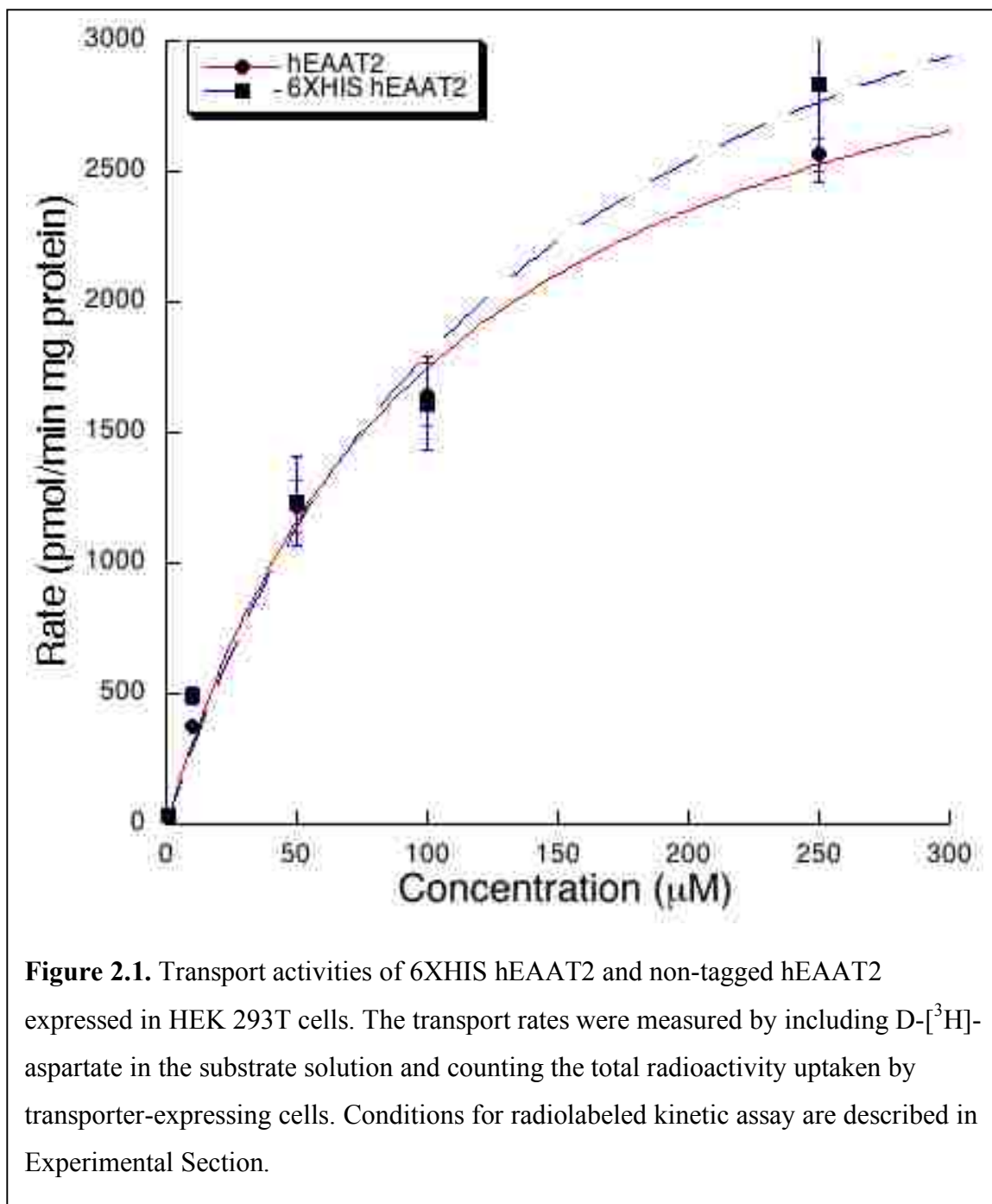
MALDI-TOF analysis was performed on a Voyager DE PRO (Applied Biosystems, Foster City, CA). For whole protein analysis, 0.5 ml of sample was spotted onto the target plate followed by spotting an equal volume of sinapic acid matrix solution in 50% acetonitrile and 0.3% TFA. A bovine serum albumin mass spec standard (Sigma-Aldrich, St. Louis, MO) was used for calibration. For peptide analysis, an aliquot of sample was mixed with an equal volume of CHCA matrix solution in 50% acetonitrile and 0.1% TFA, and 1 ml was spotted onto the target plate. A Bruker peptide standard was used for calibration. For average masses obtained in linear mode, mass accuracy was set at 200 ppm; for monoisotopic masses obtained in reflectron mode, mass accuracy was set at 50 ppm. Masses were searched against the NCBI protein database or a hEAAT database using Mascot (www.matrixscience.com). Modifications for carbamidomethylated cysteines and partial methionine oxidation were included.

2.3 Results and Discussion

2.3.1 Expression and Transporter Activity

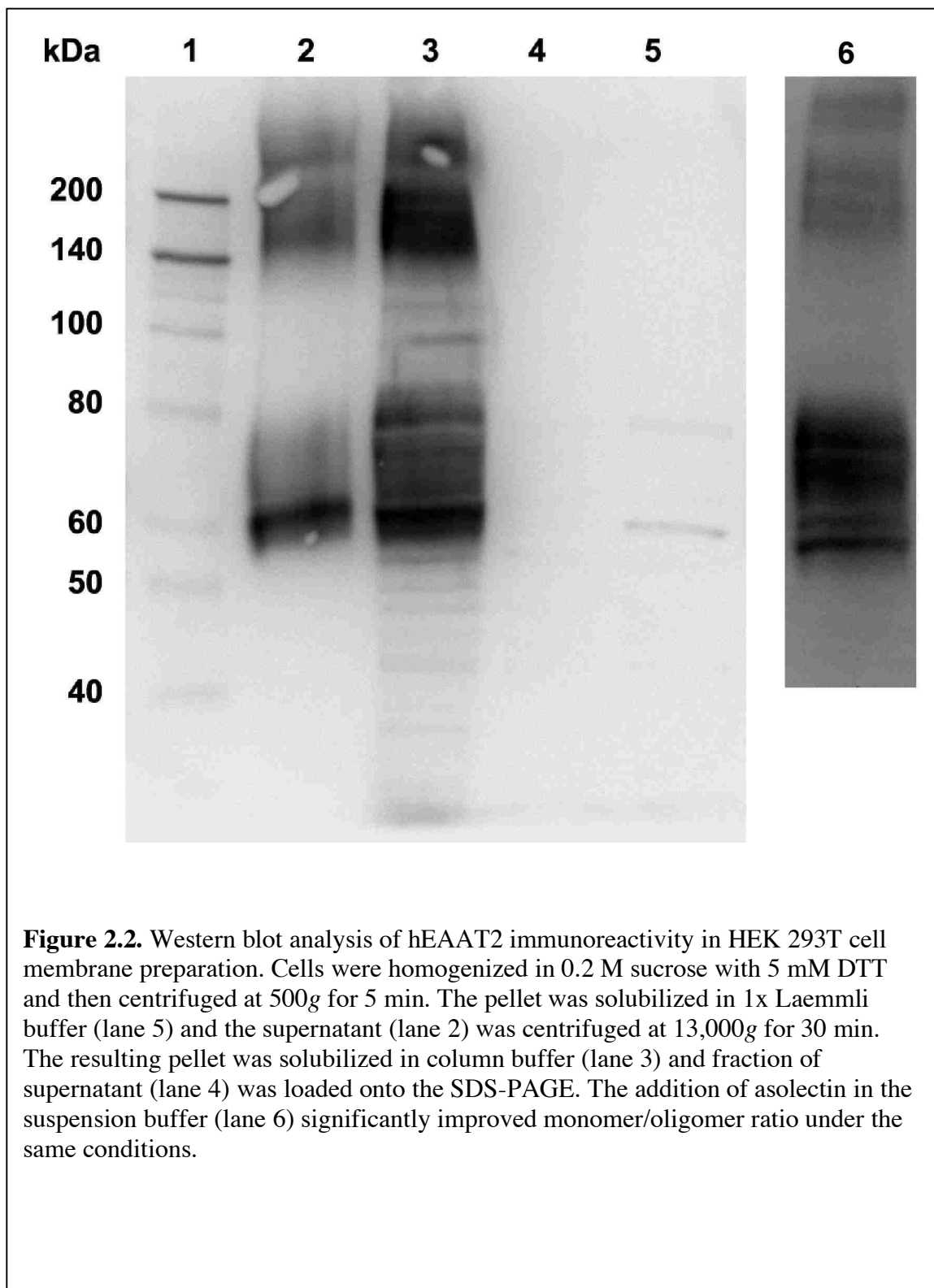
Our intent was to carry out structural studies on human EAAT2 (hEAAT2) that would provide greater mechanistic insight into the how substrates and inhibitors interact with this transporter during the process binding and translocation. hEAAT2 belongs to the solute carrier family 1 (SLC1) proteins that also includes EAATs 1, 3-5, ASCT1 and ASCT2 (Hediger et al., 2004). Owing to the inherent problems associated with the isolation and structural characterization of integral membrane proteins, it is not surprising that few, if any, MS studies have been carried out on members of this family. The challenges readily exemplified by reports that hEAAT2 is a protein without a defined molecular weight (Lehre et al., 1995), is extremely unstable in solution and easy forms SDS-resistant oligomers (Trotti et al., 1998). Previously, efforts have been made to purify the rat homologue of hEAAT2, GLT-1. Danbolt et al. fractionated solubilized brain membranes with lectin affinity chromatography, followed by chromatography on hydroxyapatite and DEAE-cellulose (Danbolt et al., 1990). More recently, Semliki Forest virus particles carrying a HIS-tagged GLT-1 gene were used to infect BHK-21 cells from which the transporter protein was subsequently purified through IMAC (Raunser et al., 2005). In the present work, we chose to employ a routinely-used mammalian cell line (HEK 293T) to express the recombinant protein, as it allowed for more direct comparisons of SAR data, as well as simplified the purification to an one-step process for fast MS characterization.

Based upon numerous biochemical characterizations, and ultimately confirmed in the GltPh crystal structures, both termini of the hEAAT2 are localized to the cytoplasmic side of the plasma membrane. These, as well as site-directed mutagenesis studies, also led to the conclusion that the substrate and ion binding domains are located near the C-terminus of hEAAT2. To minimize any potential effect on ligand binding, a 6XHIS hEAAT2 vector was constructed with the epitope located on the N-terminus of hEAAT2. HEK 293T cells transiently transfected with 6XHIS hEAAT2 cDNA were assayed for transporter activity by quantifying the uptake of D-[³H]-aspartate 24 h after transfection. D-Aspartate is commonly used as a substrate in these assays as it reduces the complications associated with radiolabel metabolism. We found that 6XHIS hEAAT2 expressed in HEK 293T cells is fully functional and closely mimics the activity native hEAAT2 (Figure 2.1). The V_{max} and K_m for D-aspartate uptake were calculated to be $4,318 \pm 734$ pmol/min per mg protein and 140 ± 49 μ M, respectively, for the 6XHIS hEAAT2 and $3,594 \pm 267$ pmol/min per mg protein, *and* 106 ± 18 μ M, respectively, for the native transporter. It is also worth noting that expression of hEAAT2 in HEK 293T cells yield much higher levels of activity and protein than other established mammalian cell expression systems. For example, hEAAT2 expressed in neural progenitor cell line C17.2 exhibited a V_{max} of 501 ± 72 pmol/min per mg protein under the same assay conditions (Esslinger et al., 2005). The pharmacological specificity of the HIS-tagged transporter was also confirmed by characterizing its sensitivity to the well known blockers. Dihydrokainate (DHK) and L-glutamate reduced the levels of hEAAT2-mediated uptake of D-[³H]-aspartate (25 μ M) to 55% and 45% of control, respectively, when included in the assays at 100 μ M.



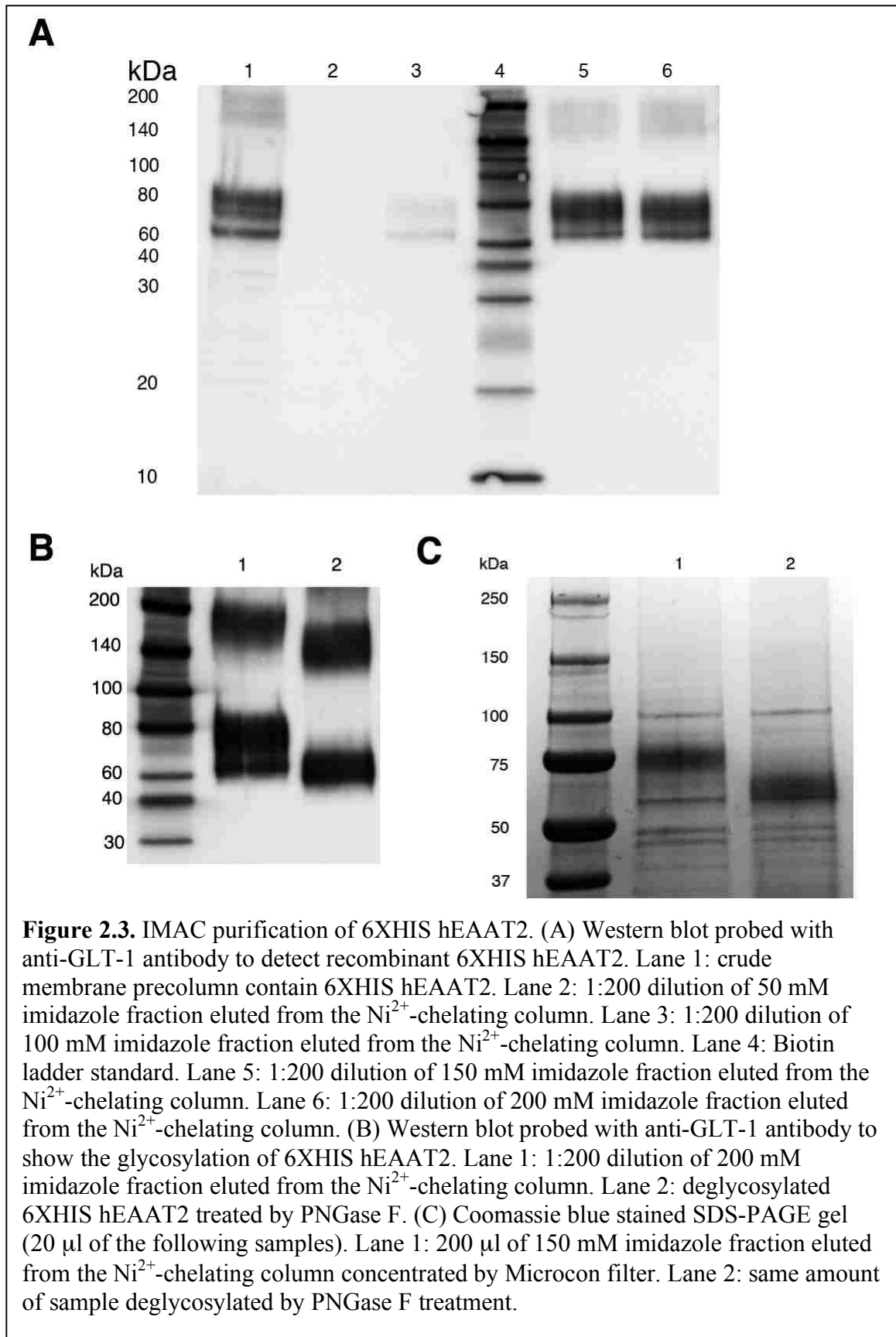
2.3.2 Membrane Solubilization and Protein Purification

Solubilization of membrane protein pellets often requires high salt concentrations, strong detergents, organic solvents (Blonder et al., 2004) and/or organic acids (Washburn et al., 2001). However, these methods are often not compatible with downstream IMAC purification and MS analysis. In light of this, we developed a membrane isolation method that effectively separated and enriched the 6XHIS hEAAT2 proteins as indicated by hEAAT2 immunoreactivity (Figure 2.2, lanes 2-5). To obtain sufficient amounts of membrane protein for the purification of 6xHIS hEAAT2, transfected HEK 293T cells were plated in 100 mm² dishes at a density of 2×10^6 cells/dish. Two dishes were used for each membrane preparation. Dithiothreitol (DTT) was included in the lysis buffer and the suspension buffer at a concentration of 5 mM to prevent cysteine cross-linking. We attempted to solubilize the membrane pellets with several solvent systems and detergents. It was found that at least 0.5 M NaCl was required to effectively solubilize the protein. Among the detergent solutions tested (1% SDS, 2% CHAPS, 2% octyl- β -D-glucoside and 1% DDM), only 1% DDM effectively solubilized the 6XHIS hEAAT2 membrane pellet and was able to prevent the nonspecific binding of other cellular proteins to the IMAC column. DDM is a gentle nonionic detergent that has been shown to enhance protein delipidation and protein mobility in the solubilization and purification of several membrane proteins including glycerol-3-phosphate transporter GlpT (Auer et al., 2001) and the human glucose transporter, Glut1 (Boulter et al., 2001). The improved mobility of the transporter was readily observed in our column purification experiments, as the membrane pellets solubilized with the other detergents had trouble eluting from the columns. Consistent with previous observations of the instability of hEAAT2 in solution



and its tendency to form aggregates (Trotti et al., 1998), a significant amount of oligomeric proteins was observed in our initial membrane preparations (see Western blot in Figure 2.2, lanes 2, 3). The addition of asolectin (2 mg/ml, Raunser et al., 2005) to the suspension buffer greatly increased the monomer/oligomer ratio as illustrated by Western blot analysis (Figure 2.2, lane 6).

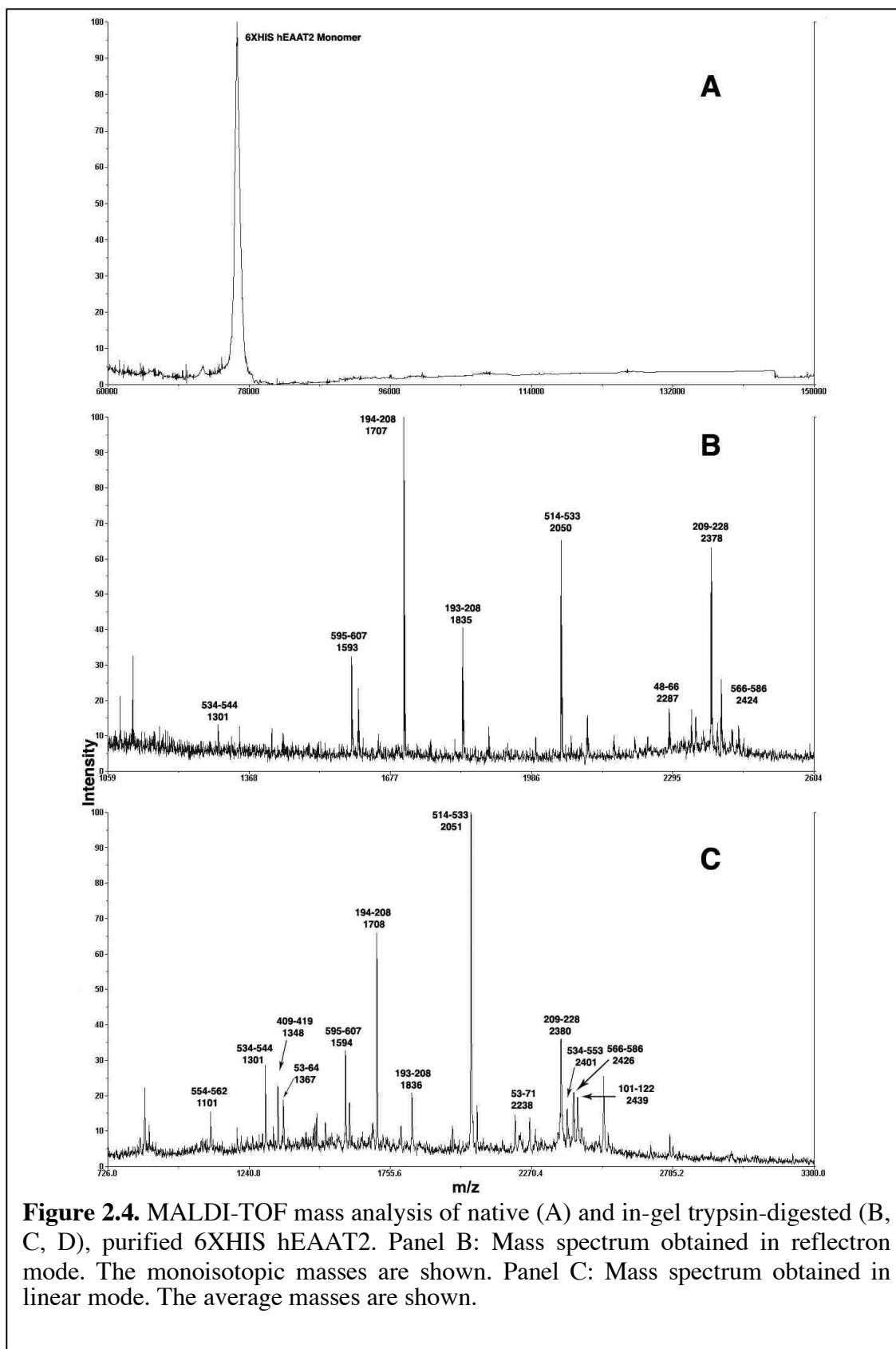
The solubilized membrane fraction containing the 6XHIS hEAAT2 was applied to a HisTrap Ni²⁺ column. Following a 15 ml wash, the column was eluted with sequential applications of 4 ml volumes of elution buffer containing increasing concentrations of imidazole (50-300 mM). The 6XHIS hEAAT2 eluted in the fractions containing 150 mM and 200 mM imidazole (Figure 2.3A, lanes 5, 6). Isolated protein was quantified by Bradford Assay and BCA assay (Pierce). Using this protocol, the average yield of a single preparation from 2 confluent 100mm² dishes of transfect cells was about 300 µg of protein. As has been previously reported for native glutamate transporters²¹, Western blot analysis of the 6XHIS hEAAT2 yielded a wide, fuzzy band that lacked defined edges and had an apparent mass of 70-80 kDa. Given that the calculated molecular weight of 6XHIS hEAAT2 is 66 kD and that hEAAT2 is known to be a glycoprotein with two *N*-glycosylation sites (Danbolt et al., 1992), we treated an aliquot of the suspended protein with peptide-N-glycosidase (PNGase) F. This enzyme cleaves the linkages between Asn and carbohydrate chain at *N*-glycosylation sites. PNGase F treatment resulted in a shift of the monomer 6XHIS hEAAT2 band to around 65 kDa (Figure 2.3B). The observed ~10 kDa change in size is in agreement with the mass of the *N*-linked glycans on GLT-1 (Danbolt et al., 1992) and suggested that the 6XHIS hEAAT2 expressed in HEK 293T cells is fully glycosylated at both sites. In contrast, only partial glycosylation of the



transporter was observed when GLT-1 was expressed in BHK-21 cells (Raunser et al., 2005). Isolated fractions containing 6XHIS hEAAT2 were concentrated by Microcon filters and resolved on SDS-PAGE gels. When gels were stained with Coomassie, a predominant band around 75 kDa was also observed (Figure 2.3C, lane 1), consistent with Western blot analysis, deglycosylation with PNGase F produced a band around 65 kDa (Figure 2.3C, lane 2). Despite the inclusion of DTT and asolectin in the buffer, the isolated 6XHIS hEAAT2 remained relatively unstable in solution as evidenced by either precipitation or aggregate formation on gels. We also observed that freezing precipitated the protein out of solution such that it could not be re-dissolved. Similarly, storage of the protein solution for more than a week at 4 °C resulted in the extensive SDS-resistant aggregation of 6XHIS hEAAT2.

2.3.3 Intact 6XHIS hEAAT2 Protein Analysis by MALDI-TOF

In order to determine an accurate mass for the isolated protein, MALDI-TOF analysis was performed on the intact protein following its elution from IMAC. Protein was precipitated with 10% TCA (final concentration) to desalt and remove detergents and washed with ethanol:ether 1:1 before being dissolved into 50% acetonitrile and 0.1% TFA. Aliquot of the solution was then mixed with equal volume of sinapinic acid matrix and spotted on the target plate. Sonication was used when proteins could not be completely dissolved. The MALDI spectrum of the intact protein displayed a singly charged monomer peak with a molecular mass of $76,451 \pm 20$ Da (Figure 2.4A). No dimer or multimer peaks were observed. The experimental mass determined by MALDI-



TOF matched the apparent mass observed on the Western blot and Coomassie-stained SDS-PAGE.

2.3.4 In-gel Trypsin Digestion and MALDI-MS

An in-gel approach was first used to characterize 6XHIS hEAAT2 protein isolated from IMAC. Briefly, gel pieces were destained in 25 ammonium bicarbonate (AMBIC) solution in 50% acetonitrile, reduced in 10 mM DTT in 100 mM AMBIC and alkylated in 55 mM iodoacetamide in 100 mM AMBIC. Trypsin solution in 25 mM AMBIC (final concentration 12.5 ng/ μ l) was added to speedvac-dried pieces and the reaction was allowed to proceed for 20 h in 37 °C. Tryptic peptides were extracted by 100 μ l of 0.1% TFA in 60% acetonitrile. Peptide solutions were vacuum-dried in speedvac and resuspended in 0.1% TFA in 50% acetonitrile solution for MALDI-TOF. Both linear mode and reflectron mode of the MALDI-TOF produced similar spectra, with more peptides > 2,000 Da observed in linear mode (Figure 2.4B). Experimental masses were searched against the human database of the protein sequences in NCBIInr using MASCOT. Peptides containing cysteines were identified as the carbamidomethylated species, consistent with a complete reduction and alkylation. A few methionine oxidations were also observed, together with a proline to pyro-glutamate modification in the peptide SADCSVEEEPWKR (1592.70 Da, 1606.70 Da modified peptide). The source of the identified peptides from the in-gel digestions were evenly distributed between transmembrane domains and intracellular/extracellular regions. Tryptic fragments NDEVSSLDAFLDLIR (1706.9 Da, GRAVY = 0.073) and

TSVNVVGDSEFGAGIVYHLSK (2050.1 Da, GRAVY = 0.500) generated the strongest ion signals.

As previously mentioned, there are two predicted *N*-glycosylation sites on hEAAT2, both of which were found on the same tryptic peptide:

VLVAPPDDEEANATSAVVSLNETVTEVPEETK (3448.8 Da; GRAVY = -0.073).

This peptide was not observed following the in-gel digestion of the glycosylated protein, but was readily observed in the spectra of deglycosylated 6XHIS hEAAT2. This suggested that *N*-glycosylation did occur at the predicted sites and likely prevented the peptide from being identified. Overall, the in-gel trypsin digestion of 6XHIS hEAAT yielded about 40% sequence coverage of the 66 kDa protein (Table 2.1). Considering the hydrophobic nature of this integral membrane protein (GRAVY = 0.332), the resulting sequence coverage is much higher than that of most in-gel digestions reported. For example, a 18% sequence coverage was achieved following the in-gel digestion of VGLUT1 (Cox et al., 2008).

While the extent of overall sequence coverage was higher than expected, this protocol fell somewhat short with respect to our goal of visualizing the peptides from the proposed drug binding regions. An alignment of the hEAAT2 sequence with the crystal structure of the homologous bacterial glutamate/aspartate transporter GltPh suggests that substrates and inhibitors bind to the region traversing HP1, TMD7, HP2 and TMD8 of hEAAT2 (Figure 2.5). However, our in-gel trypsin digestion protocol yielded only 20% coverage of this 153 amino acid sequence (Figure 2.7). A computationally-based mock

1	GSMGGSHHHH	11	HHGMASMTGG	21	QQMGRDLYDD	31	DDKGSMASTE	41	GANNMPKQVE	51	VRMHDSHLGS
61	EEPKRRHLGL	71	RLCDKLGKNL	81	TMD1 LLTLTVFGVI	91	LGAVCGLLR	101	LASPIHPDVV	111	TMD2 MLIAFPGDIL
121	MRMLKMLILP	131	LISSLITGL	141	SGLDAKASGR	151	LGTRAMVYYM	161	TMD3 STTIIAAVLG	171	VILVLAIHPG
181	NPKLLKQLGP	191	GKKNDEVSSL	201	DAFLDLIRNL	211	FPENLVQACF	221	QQIQTVTKKV	231	LVAPPDDEEA
241	NATSAVVSLL	251	NETVTEVPEE	261	TKMVIKGGLE	271	TMD4 FKDGMNVLGL	281	IGFFIAFGIA	291	MGKMGDQAKL
301	MVDFFNILNE	311	TMD5 IVMKLVIMIM	321	WYSPLGIACL	331	ICGKIIAIKD	341	LEVVARQLGM	351	TMD6 YMTVIIGLI
361	IHGIFLPLI	371	<i>YFVTRKNPF</i>	381	HP1a <i>SFFAGIFQAW</i>	391	<i>ITALGTASSA</i>	401	HP1b <i>GTLPVTFRCL</i>	411	<i>EENLGIDKRV</i>
421	TMD7a TRFVLPVGAT	431	INMDGTALYE	441	TMD7b AVAAIFIAQM	451	NGVVDGGQI	461	HP2a <i>VTVSLTATLA</i>	471	SVGAASIPSA
481	HP2b <i>GLVTMLLILT</i>	491	AVGLPTEDIS	501	LLVAVDWLLD	511	TMD8 RMRTSVNVVG	521	DSFGAGIVYH	531	LKSELDTID
541	SQHRVHEDIE	551	MTKTQSIYDD	561	MKNHRESNSN	571	QCVYAAHNSV	581	IVDECKVTLA	591	ANGKSADCSV
601	EEEPWKREK										

Figure 2.5. Amino acid sequence of the N-terminal 6XHIS-tagged human EAAT2. The transmembrane domains are marked in bold and the hairpin loops are marked in italic. Secondary structure predictions are based on the sequence alignment of hEAAT2 against crystal structure of GltPh (PDB entry: 2NWW).

digestion (ProteinProspector, UCSF) of hEAAT2 predicted an 88 amino acid fragment covering TMD7, HP2 and part of TMD8. The length and hydrophobic nature (GRAVY = 1.147) of this peptide may have precluded its extraction from the gel matrix, even if it had been liberated during the digestion.

2.3.5 In-solution Trypsin Digestion and MALDI-MS

As suggested above, peptide recovery from in-gel digestions can be low because of the difficulties in extracting large, hydrophobic peptides from gel matrices. For this reason, in-solution methods have become a preferred option for membrane protein MS characterizations as exemplified by studies on the human cannabinoid CB2 receptor (Zvonok et al., 2007), bacteriorhodopsin (Blonder et al., 2002), and vesicular glutamate transporter VGLUT1 (Cox et al., 2008). Further, the in-solution digestion performed on lens aquaporin 0 AQP0 suggested that the addition of organic solvents, such as acetonitrile, could improve the digestion efficiency for integral membrane proteins (Han and Schey, 2004). The in-solution trypsin digestion of 6XHis hEAAT2 was carried out following direct precipitation with 10% TCA. The resulting pellet was washed with ethanol:ether to remove detergents and residual TCA. The protein pellet was collected by centrifugation before being dissolved into one of the three digestion buffers: 50 mM AMBIC, 50 mM AMBIC with 10% acetonitrile or 50 mM AMBIC in 60% methanol. Trypsin was added at an enzyme to protein ratio of 1:20. The reaction was allowed to proceed at 37 °C for 20 h, after which the digestion solution was vacuum-dried in a speedvac. The peptides were resuspended in 0.1 TFA, 50% acetonitrile. Trypsin digestion in 50 mM AMBIC with 10% acetonitrile yielded a spectrum with slightly more

peptides than 50 mM AMBIC alone. In contrast, digestion in 60% MeOH produced very few identifiable peptides. This may be attributable to the differential solubility of TCA-precipitated protein pellets in each of the solvent systems. Alternatively, purified proteins were reduced in 5 mM TCEP and alkylated in 100 mM iodoacetamide prior to TCA precipitation. The resulting peptides did not differ in sequence from the peptides identified from native conditions. This suggested reduction and alkylation didn't improve the sequence coverage of in-solution digestion method in our study.

In contrast to peptides identified from in-gel digestion which are mainly short and hydrophilic, the in-solution digestion produced generated many longer, hydrophobic peptides. Searching the human database of the protein sequences in NCBIInr using MASCOT, we were able to identify multiple 6XHIS hEAAT2 tryptic fragments from MALDI-TOF m/z scans ranging from 500 – 3,000 Da, 2,000 – 6,000 Da and 4,000 – 10,000 Da (Figure 2.6). The identified peptides covered 7 out of 8 transmembrane domains with the exception of TMD4. In the region of the presumed binding pocket, we were able to identify HP1 as a single peptide
KNPFSFFAGIFQAWITALGTASSAGTLPVTFR (3,405.9 Da, GRAVY = 0.559).
Moreover, the 88 amino acid fragment predicted from the *in silico* tryptic digestion was identifiable only following in-solution digestion of the 6XHIS hEAAT2. The possible origin of this peptide was examined in greater detail using PNGase F. Comparisons between digestions in the presence and absence of PNGase F confirmed with high confidence that the 9,013 Da peptide was indeed this tryptic fragment in 6XHIS hEAAT2. These finding indicate that glycans are linked to two Asn residues (Asn241 and Asn251 in 6XHIS hEAAT2) in the extracellular space between TMD3 and TMD4

blocked and are consistent with the idea that the entry of trypsin to this specific region of the protein was likely limited. Crystallography studies on GltPh revealed that monomers form a trimeric structure surrounding a ~ 65 Å aqueous bowl. The function of this bowl is unclear, as evidence from kinetic studies suggest each monomer works independently (Yernool et al., 2004; Boudker et al., 2007). More recently, it has been hypothesized that this structural arrangement of trimers may serve to increase the local concentration of substrates and inhibitors and influence their kinetics, as exemplified in studies with the potent hEAAT3 inhibitor, NBI-59159 (Bridges et al., 2008). It was also reported that deglycosylation of GLT-1 does not affect its activity, but could possibly stabilize transporters in solution and membrane (Raunser et al., 2005). The spatial proximity of these glycans to the binding pocket raise interesting questions as to the possible functional influences that glycosylation may have on glutamate transport.

In-solution digestion solutions were vacuum-dried in speedvac and resuspended in several other solvents including: 5% formic acid in 50% acetonitrile, 50% formic acid and FAPH (50% formic acid, 25% acetonitrile, 15% isopropanol, and 10% water) buffer followed by MALDI-MS. No additional peptides were identified using these solutions. Indeed, none of the tested solution produced more peptides than 0.1% TFA in 50% acetonitrile. The sequence coverage of the 6XHIS hEAAT2 by in-solution digestion after deglycosylation was 77% (Table 2.1). It is noteworthy that the coverage of the hypothesized hEAAT2 substrate binding domain markedly increased from 20% via in-gel digestion to 91% via in-solution method. Overall, combining in-gel and in-solution

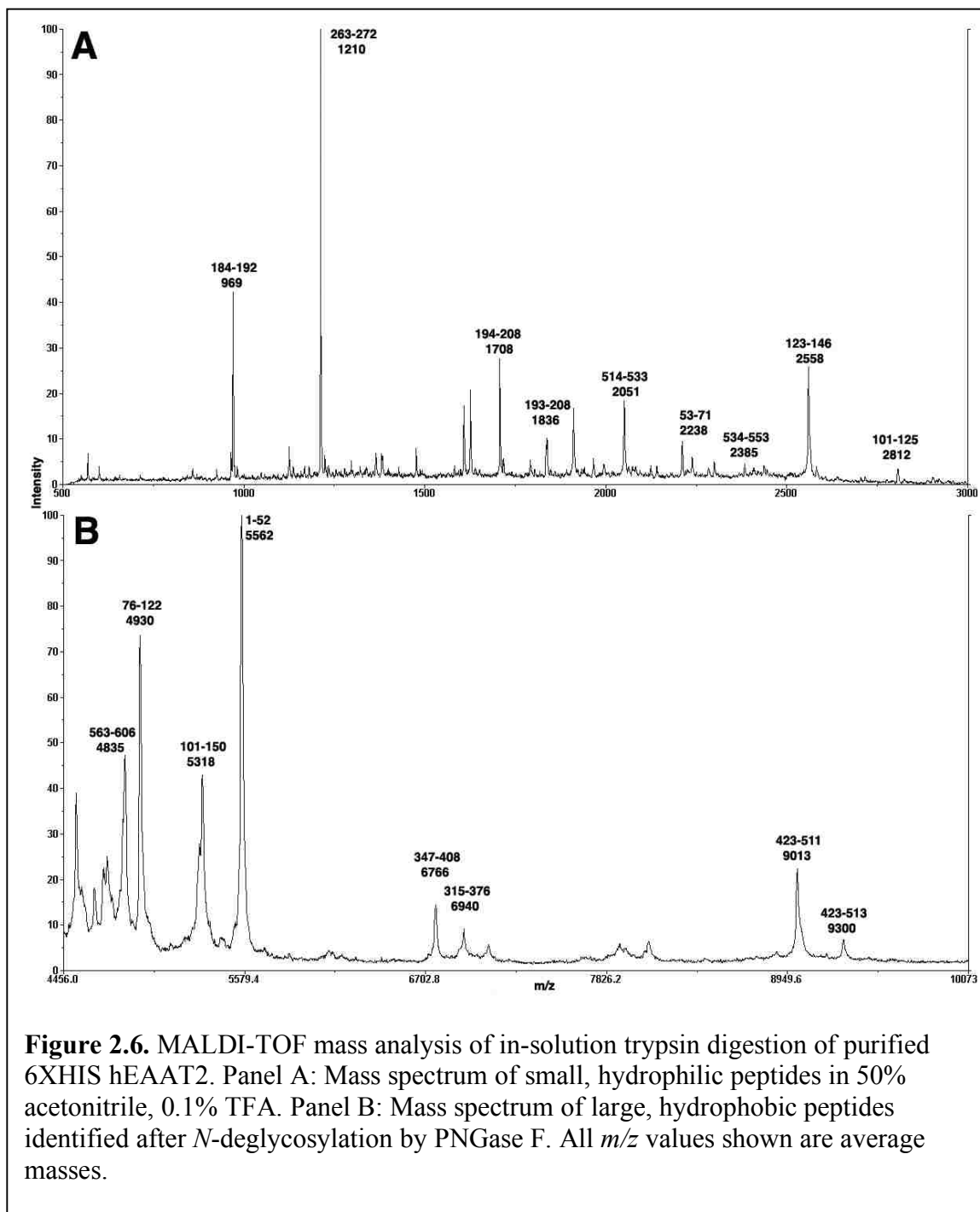


Figure 2.6. MALDI-TOF mass analysis of in-solution trypsin digestion of purified 6XHIS hEAAT2. Panel A: Mass spectrum of small, hydrophilic peptides in 50% acetonitrile, 0.1% TFA. Panel B: Mass spectrum of large, hydrophobic peptides identified after *N*-deglycosylation by PNGase F. All *m/z* values shown are average masses.

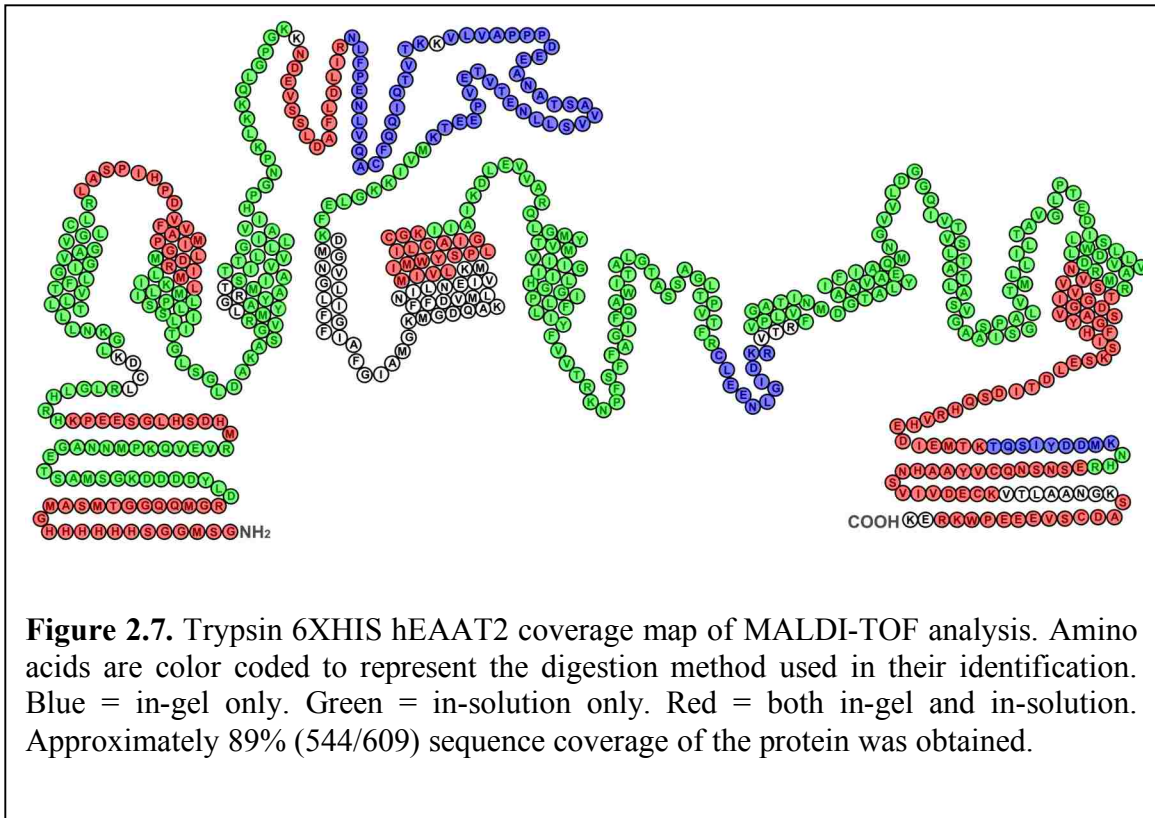


Table 2.1^a. MALDI-TOF Identification of Peptides from 6XHIS hEAAT2 Digested with Trypsin.

peptide position	m/z observed (Da)	in-gel	in-solution	missed cleavages	modification
001-025	2610.48 mi	X			
001-052	5562.39 avg		X	3	
026-047	2405.68 mi		X	1	
053-064	1366.42 mi	X			
053-071	2238.16 avg		X	2	
076-122	4931.46 avg		X	2	
101-122	2438.49 avg	X			2Met-ox
101-125	2811.03 avg		X	1	
101-150	5317.59 avg		X	3	1Met-ox
123-146	2558.32 avg		X	1	
155-183	3056.42 avg		X		
184-192	969.71 avg		X	2	
194-208	1706.88 mi	X	X		
209-228	2378.10 mi	X			1CAM
230-262	3449.10 avg	X			
263-272	1210.68 avg		X	2	
315-334	2372.41 avg	X			2CAM, 2Met-ox
315-376	6940.20 avg		X	3	2Met-ox
347-408	6765.80 avg		X	2	
409-419	1346.85 avg	X			1CAM
423-511	9013.93 avg		X		
423-513	9300.75 avg		X	1	
514-533	2050.03 mi	X	X		
534-544	1300.60 mi	X			
534-553	2400.63 avg	X	X	1	1Met-ox
554-562	1100.18 mi	X			
563-606	4835.07 avg		X	3	
566-586	2424.22 mi	X			2CAM
595-607	1592.73 mi	X		1	1CAM

^ami = observed as a monoisotopic mass. Avg = observed as an average mass, CAM = carbamidomethyl cysteine.

methods produce a 98% coverage of the 155 amino acid region of the hEAAT2 that is particularly relevant to substrate binding (Figure 2.7).

2.4 Conclusions

In order to advance our understandings of the structure of hEAAT2 and facilitate the design of selective inhibitors, functional hEAAT2 was expressed in HEK 293T cells and purified in a single step using IMAC. Kinetic assays indicate the 6XHis epitope engineered into the N-terminus of the transporter did not affect its ability to bind and transport substrates. Recombinant 6XHis hEAAT2 expressed in a much higher level in HEK 293T cells than other tested mammalian cell lines, provided us with sufficient amounts of membrane material to use in the downstream IMAC purification and MS characterization. From our expression system we were able to isolate about 300 µg purified 6XHis hEAAT2 protein in a single purification step. It is noteworthy that the relatively low number of cells we started with (4×10^6) leaves plenty of room for scaling up. Isolated 6XHis hEAAT2 was digested with trypsin by both in-gel and in-solution methods. In-gel digestion resulted in a 40% of sequence coverage of the whole protein but lacked the coverage on the hypothesized substrate and competitive inhibitor binding region. In-solution digestion with the addition of organic solvent greatly increased the number of hydrophobic peptides identified from MALDI-TOF spectra. A 77% sequence coverage was achieved and 91% of the amino acids in the binding site was identified through in-solution method. It was interesting to find that glycosylation of the protein seemed to prevent the identification of a large peptide from the binding pocket.

Combining the in-gel and in-solution methods, 89% of the sequence coverage of the protein was obtained with only TMD4 that remained unidentified in our study. The successful identification of the peptides from the binding site offered us a template for the future study of inhibitor-protein complexes and covalent modifications of the binding pocket. Since the 6XHIS hEAAT2 expressed in HEK 293T cells is fully functional, the relationship between the functional loss of the protein and the structural modifications to the protein can be evaluated by MS analysis. Recently, a modified peptide in the binding site was identified by MALDI-TOF after photo-inactivation of the 6XHIS hEAAT2 in the presence of the 9-fluorenone containing hEAAT2 inhibitors (Chapter 2). In addition, the expression system, protein solubilization, purification and MS methods we developed in this work can easily be adapted to the structural analysis of other glutamate transporter subtypes and other integral membrane proteins with similar topology.

CHAPTER 3

FLUOROPHORE-ASSISTED LIGHT INACTIVATION OF HUMAN EXCITATORY AMINO ACID TRANSPORTER 2 (EAAT2)

3.1 Introduction

3.1.1 Photochemical Tools in Studying Protein Structures

Long before tools such as X-ray crystallography and NMR became useful in protein structure analysis, photochemical techniques represented one of the better methods for studying biological processes at the molecular level. In these experiments, photolysis of a probe containing a photoreactive group generates highly reactive intermediates that can subsequently react with the spatially closest part of the biomolecule. Modifications to the target protein are detectable by such methods as immunoreactions, fluorescence or mass spectrometry. The site of the modification and the functional changes on the modified protein provides us with information about its structural features, as well as the interactions between the target and the small molecule ligands. Depending upon the nature of the reactions involved in the protein modifications, photochemical techniques can be generally divided between photoaffinity labeling and photosensitization. It is also worth mentioning that although interest in photochemical techniques decreased somewhat with the emergence of protein NMR and X-ray crystallography, these approaches have become more popular as they often provide more

information on protein dynamics of ligand binding when compared to the static images of protein structure generated via crystallographic techniques.

3.1.1.1 Photoaffinity labeling

First proposed by Singh and Westheimer in 1962 (Singh et al., 1962), photoaffinity labeling uses analogues bearing photophores that can be photo-activated into reactive intermediates such as carbenes, nitrenes or biradicals. Commonly chosen photophores include arylazides (Henry et al., 2002), diazirines (Smith and Knowles, 1973) and diarylketones (Galardy et al., 1973) (Figure 3.1). The most commonly used diarylketone is benzophenone. A fundamental difference between benzophenone groups and other photophores is that biradicals are generated by 350 nm UV irradiation and the reaction is reversible (Scheme 3.1). The long wavelength where the benzophenone group is activated also makes these probes safer choices for biological systems (for review see Prestwich et al., 1997). More recently, benzophenone-containing photoaffinity labels have been used in probing the structures of the substance P (NK-1) receptor (Kage et al., 1996), p-glycoprotein (Pleban et al., 2005) and the nicotinic acetylcholine receptor (Garcia et al., 2007). In combination with mass spectrometry, a unique inhibitor-binding domain was identified on HIV-1 integrase using benzophenone-linked coumarin IN inhibitors (Al-Mawsawi et al., 2006). In addition to benzophenone itself, several other closely related photophores have been successfully used as photoaffinity labels, including acetophenones (Zor et al., 1995), benzoyl phenothiazines (Golinski et al., 1995) and benzoyl indolines (Sun et al., 1994). The 9-fluorenone group provided another example of benzophenone-like photophores. Fluorenone and benzophenone share similar

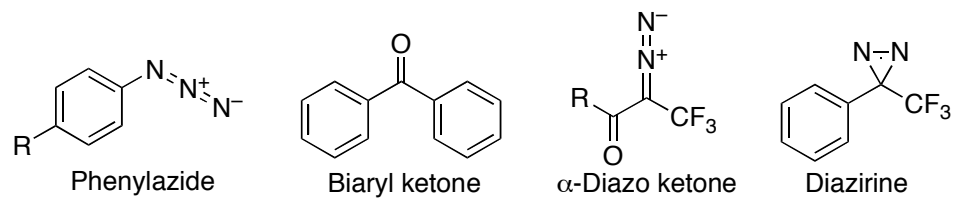
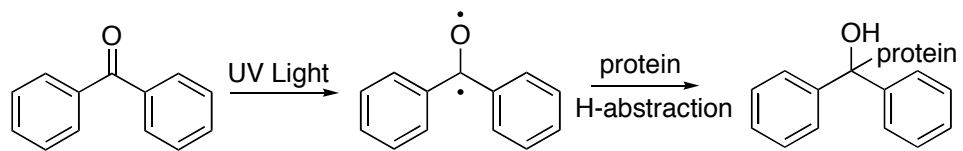


Figure 3.1. Commonly-used photoaffinity labeling groups.

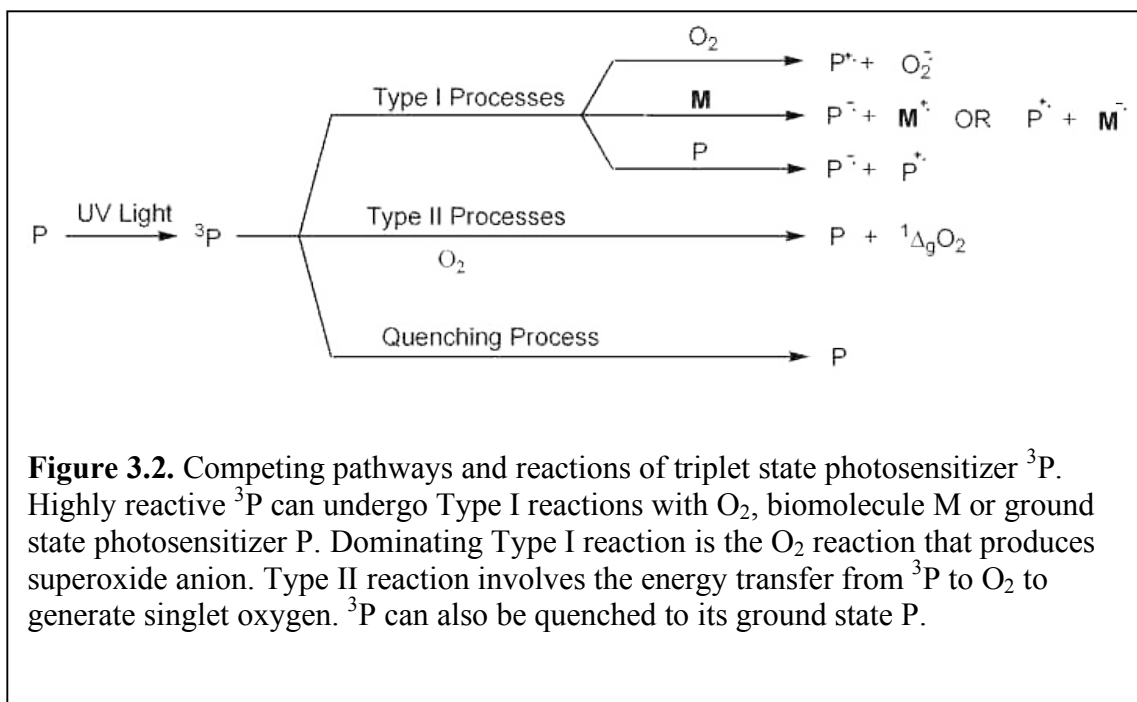


Scheme 3.1. UV photo-activation of benzophenone group. Benzophenone can be activated to its triplet state under 350 nm UV-A irradiation. Resulting biradical can react with reactive carbon-hydrogen bond via hydrogen abstraction mechanism to form benzophenone-protein conjugate.

structural features, differing only by one carbon-carbon bond. The two also have similar photochemical properties. A series of fluorenone-based compounds were shown to be strong β_2 -adrenergic receptor antagonists (Wu and Ruoho, 2000) and used to directly probe the catechol binding domain of the β_2 AR (Wu et al., 2001). Related compounds were later confirmed to be vesicular monoamine transporter-2 (VMAT2) substrates and used to identify the VMAT2 substrate binding pocket (Gopalakrishnan et al., 2007). Coupling Boc-3-(3'-fluorenyl-9'-oxo)-L-alanine or 9-fluorenone-3-carboxylic acid with the parathyroid hormone (PTH) molecule also yields potent agonists of human PTH1 receptor and the photo-crosslinking product generated receptor-ligand photo-conjugates (Han et al., 2000).

3.1.1.2 Photosensitization

Similar to photoaffinity labeling, the reactive intermediates formed during the process of photosensitization also represent the excited states of the photoactive compounds. Following excitation, however, there are multiple pathways that can lead to different reaction products as the group returns to its ground state. In most cases, oxygen molecules are involved and lead to the oxidation of the target protein. In complex biological systems, the photosensitization reactions often consist of competing intermediates and pathways that can further complicate the manner in which the target protein is oxidatively modified. These pathways are summarized in Figure 3.2. Oxygen molecules can participate in one of two processes, referred to as Type I ($O_2^{\cdot-}$) or Type II (1O_2). In most instances the Type II process dominates, because the reaction rate constant is usually two orders of magnitude larger than that of the Type I path. In Type II



processes, $^1\text{O}_2$ is generated from the excitation of ground state oxygen ($^3\Sigma$). Of the two excited states of oxygen, the first singlet state ($^1\Delta_g$) has an energy 22.6 kcal/mol above the ground state, while the second excited state ($^1\Sigma_g$)'s energy is 37.7 kcal/mol above $^3\Sigma$. These energy differences lead to very large differences in the lifetime of the species in aqueous solution (10^{-6} - 10^{-5} for $^1\Delta_g$ and 10^{-11} for $^1\Sigma_g$). When singlet oxygen-mediated Type II photosensitization is the major route of protein photolysis, photooxidation most often occurs at one or more of five amino acid residues: cysteine, histidine, methionine, tryptophan and tyrosine. The reaction mechanisms and photooxidation products have been reviewed in detail by Straight and Spikes (1979) and Davies, (2003). Typically, photosensitization of proteins results in the degradation or oxidation of side chains of the five residues mentioned above, although there have been isolated reports of other amino acid side chains being damaged or producing protein fragmentation. The application of external photosensitization to investigate protein structures is somewhat limited, because the long lifetime of $^1\text{O}_2$ and its diffusion radius (~ 300 Å, compared with 15 Å for triplet biradical) often time results in nonspecific damage to protein side chains. Despite these difficulties, there are numerous examples of successful photosensitization of protein structures (Girotti et al., 1979; Verweij et al., 1981).

3.1.2 Chromophore-Assisted Laser Inactivation (CALI) and Fluorophore-Assisted Light Inactivation (FALI)

A number of approaches have been developed to localize the generation of reactive oxygen species (ROS) by photosensitization and thereby increase selectivity and minimize nonspecific damage to the proteins. First reported in 1988, Jay et al. used 620

nm laser beams to inactivate various enzymes in the presence of malachite green isothiocyanate (MGITC)-coupled antibodies (Jay, 1988). The mechanism of this inactivation, chromophore-assisted light inactivation (CALI), was first proposed to be photothermal denaturation, but was later proven to be hydroxyl radical-mediated (Liao et al., 1994). The maximal radius of damage was estimated to be 15 Å and the specificity was fairly high (Liao et al., 1995). Replacing the malachite green in MGITC with fluorescein resulted in an increase of two orders of magnitude in inactivation efficiency (Buchstaller and Jay, 2000). This marked increase in inactivation efficiency allows diffuse light sources to be used instead of a laser and led to the technique of fluorophore-assisted light inactivation (FALI). The mechanism of FALI was determined to be $^1\text{O}_2$ -mediated and the half-maximal radius of the damage was estimated to be 30~40 Å (Beck et al., 2002). Due to the requirements of using non-blocking antibodies in the original versions of CALI and FALI, the approaches were not widely applicable to different systems. Newer forms of FALI include genetically engineering a tetracysteine motif that binds a fluorescein derivative 4',5'-bis(1,3,2-dithioarsolan-2-yl)fluorescein (FIAsH). The FIAsH-induced FALI has been used in the selective photoinactivation of synaptotagmin I (Marek and Davis, 2002) and calcium regulatory protein calmodulin (CaM) (Yan et al., 2006). In both studies, the photoinactivation was reported to be highly specific. Yan et al. also characterized the resulting oxidation sites in CaM using trypsin digestion and LC-MS. Methionine residues were found to be oxidized to methionine sulfoxides following photolysis. Moreover, based on the peptide peak intensities, it was also concluded that the photolysis modified histidine residues. The development of a fluorescein-conjugated α -bungarotoxin (BTX) polypeptide and its use in the inactivation of metabotropic

glutamate receptor 8a (mGluR8a) on rat sympathetic neurons provided another interesting example of FALI applications (Guo et al., 2006). By engineering a 13 amino acid BTX-binding domain into the N-terminus of mGluR8a, the investigators were able to reduce mGluR8a-mediated inhibition of calcium currents (I_{Ca}) by 50% after photolysis. However, unexpected observations of collateral damage to the GPCR-independent I_{Ca} and natively expressed signaling pathways challenged the specificity of the BTX-FALI system. Instead of developing FALI for individual proteins, Yogo et al. took a general approach and reported a series of environment-sensitive photosensitizers that can be activated by lipophilic environment in the protein's binding pocket while remaining inactivated in aqueous buffer (Yogo et al., 2008). This new strategy of designing protein-selective photoinactivators is likely to become a more general method of developing photochemical probes for lipophilic pocket-containing proteins.

3.1.3 Design of Photochemical Probes for EAATs

Strategies for developing EAAT inhibitors has included both substituted glutamate/aspartate analogues, such as (2*S*,4*R*)-4-methyl glutamate (4-MG), *threo*-3-methylglutamate (T3MG), as well as conformational restricted glutamate/aspartate analogues, such as dihydrokainate (DHK) and *L-trans*-2,4-pyrrolidine dicarboxylate (*L*-2,4-PDC). Using the first approach, aromatic group-containing glutamate/aspartate analogues, such as TBOA series (Shimamoto et al., 2000) and benzyl aspartate series (Esslinger et al., 2005), proved to be potent EAAT inhibitors that also revealed the presence of lipophilic binding domains on the transporter. The presence of such a lipophilic pocket was also supported by actions of another series of very potent EAAT

inhibitors that linked aromatic groups to the distal COOH of aspartate (e.g. aryl aspartylamides and aryl diaminopropionic acids) (Greenfield et al., 2005). Interestingly, the aromatic groups on these aspartate analogues included a number of potential photoactivable moieties. In the present study, aspartate analogues were synthesized in which benzophenone or 9-fluorenone groups were appended to its distal carboxyl group. Our goal was to use the photoactive EAAT inhibitors as probes with which to modify and identify binding domains on the transporter.

3.2 Materials and Methods

3.2.1 *Synthesis of Aryl Diaminopropionic Acids*

General Remarks. Commercially available reagents were purchased from Aldrich Chemical Co., Milwaukee, WI. Analytical thin-layer chromatography (TLC) was conducted on E. Merck aluminum-backed, 0.2 mm silica gel, TLC plates. Flash chromatography was performed with Kieselgel 60, 230-400 mesh (Merck). High-resolution mass spectra (HRMS) were obtained by electrospray ionization (ESI) on a Micromass LCT using caffeine as a mass standard at m/z 195.0882. ^1H and ^{13}C NMR were measured on a Varian VXR 400-NMR instrument (400 MHz and 100MHz respectively).

Synthesis.

(1) General procedures for aryl diaminopropionic acids (**1**).

The target aryl diaminopropionic acids (**1a** and **1b**) were prepared from N-Boc-3-amino-L-alanine and the corresponding aromatic carboxylic acid, as illustrated in Figure 1.

The free carboxylic acid group on N-Boc-3-amino-L-alanine was first protected by diphenyldiazomethane ($\text{Ph}_2\text{C}=\text{N}_2$, prepared from Miller, 1959) with one equivalent of p-toluenesulfonic acid in a mixture of acetonitrile and water. The reaction changed color from purple to colorless in 1 h and the mixture was extracted with ethyl acetate and dried over magnesium sulfate (MgSO_4) to afford the benzyhydril ester **3** (quantitative yield, Baldwin, 1994): ^1H NMR (CDCl_3) δ 1.45 (9 H, s), 2.25 (2 H, br), 3.05-3.15 (2 H, m), 4.42 (1 H, m), 5.82 (1 H, br), 6.92 (1 H, s), 7.30-7.48 (10 H, m); ^{13}C (CDCl_3) 28.3 (3x C),

43.9, 56.0, 76.2, 78.0, 126.5 (2x C), 127.5 (4x C), 128.4 (4x C), 143.8 (2x C), 156.2, 171.5; MS (ESI) m/z 371.1970 (M+H⁺).

9-Fluorenone-2-carboxylic acid or 3-benzophenonecarboxylic acid was activated by BOP reagent ((benzotriazol-1-yloxy)tris(dimethylamino)phosphonium hexafluorophosphate) with one equivalent of triethylamine (Et₃N) in N,N-dimethylformamide (DMF). This activation process was monitored by TLC, which showed the completion of the reaction after 4 h. Benzhydryl ester **3** was added afterwards and the resulting coupling reaction was monitored by TLC. After overnight stirring, the reaction was complete. Water was poured into the reaction and the product was extracted with diethyl ether. The organic layer was collected, dried, and the resulting compound was further purified by flash chromatography to offer the coupling product **4**.

α -N-*tert*-Butoxycarbonyl- β -fluorenonyl-2-carboxylic acid coupled amino-L-alanine benzhydryl ester (**4a**): ¹H NMR (CDCl₃) δ 1.45 (9 H, s), 2.25 (1 H, br), 3.85-3.97 (2 H, m), 4.62 (1 H, m), 5.85 (1 H, br), 6.88 (1 H, s), 7.20-7.38 (10 H, m), 7.40-7.94 (7 H, m); ¹³C (CDCl₃) 28.2 (3x C), 39.9, 58.3, 76.1, 78.6, 126.5 (2x C), 126.9, 127.1 (4x C), 127.4, 128.2, 128.5, 128.6 (4x C), 129.9, 131.2, 134.3, 134.9, 139.3 (2x C), 140.2 (2x C), 143.3 (2x C), 158.4, 166.8, 169.5, 190.3; MS (ESI) m/z 577.14 (M+H⁺), 599.14 (M+Na⁺).

α -N-*tert*-Butoxycarbonyl- β -benzophenonecarboxylic acid coupled amino-L-alanine benzhydryl ester (**4b**): ¹H NMR (CDCl₃) δ 1.35 (9 H, s), 3.24 (1 H, br), 3.75-3.91 (2 H, m), 4.60 (1 H, m), 5.96 (1 H, br), 6.86 (1 H, s), 7.22-7.29 (10 H, m), 7.45 (3 H, m), 7.56 (1 H, t, J = 7.9 Hz), 7.74 (2 H, d, J = 6.7 Hz), 7.86 (2 H, d, J = 7.7 Hz), 8.10 (1 H, s); ¹³C (CDCl₃) 28.1 (3x C), 42.2, 54.3, 78.2, 79.9, 126.8 (2x C), 126.9, 127.8 (4x C), 127.9,

128.3, 128.4, 128.5 (4x C), 130.1, 130.5, 130.8, 132.5, 139.3 (2x C), 137.7 (2x C), 139.4 (2x C), 155.9, 167.1, 169.7, 195.7; MS (ESI) m/z 579.22 (M+H⁺), 601.24 (M+Na⁺).

Compound **4** was deprotected by two equivalent of trifluoroacetic acid (TFA) in dichloromethane (CH₂Cl₂). After overnight stirring, the mixture was dried on a rotatory evaporator and the desired product (**1**) was precipitated under pH 4-5 aqueous solutions.

9-Fluorenyl-2-diaminopropionic acid (1a): ¹H NMR (D₂O) δ 2.85 (2 H, br), 3.31-3.59 (2 H, m), 4.19 (1 H, m), 2.25 (2 H, br), 6.84 (1 H, d, J = 7.7 Hz), 6.93 (3 H, m), 6.99 (1 H, s), 7.12 (1 H, t, J = 7.1 Hz), 7.31 (1 H, d, J = 8.1 Hz); MS (ESI) m/z 311.12 (M+H⁺), 333.11 (M+Na⁺).

benzophenonyl-3-diaminopropionic acid (1b): ¹H NMR (CDCl₃) δ 3.13 (2 H, br), 3.71-3.97 (2 H, m), 4.24 (1 H, m), 7.04 (2 H, br), 7.48 (1 H, m), 7.57 (3 H, m), 7.77 (2 H, d, J = 6.6 Hz), 8.00 (1 H, d, J = 7.8 Hz), 8.24 (1 H, d, J = 8.0 Hz), 8.43 (1 H, s); MS (ESI) m/z 313.15 (M+H⁺), 335.16 (M+Na⁺).

3.2.2 Cell Culture and Transfection

C17.2 or HEK 293T cells (ATCC, Manassas, VA) between passages 10 and 20 were cultured at 37 °C in a humidified atmosphere containing 5% CO₂ in Dulbecco's modified Eagle's medium (DMEM) supplemented with 10% fetal bovine serum, 1 mM sodium pyruvate, 0.1 mM nonessential amino acids solution, and 0.05% penicillin–streptomycin (5000 units/ml) and gentamicin sulfate (0.05 mg/ml). Cells were seeded at 1 X 10⁵ cells/well in 12-well plates for transporter activity experiments and 1.5 X 10⁶ cells/dish in 100 mm² dishes for membrane preparations. At 48 h after plating, cells were transfected using Lipofectamine 2000 (Invitrogen, Carlsbad, CA) or FuGENE

Transfection Reagent (Roche, Indianapolis, IN) in a ratio of 2 μ l of Lipofectamine to 2 μ g of purified plasmid DNA in accordance with the manufacturer's instructions.

3.2.3 Transporter Activity

Twenty four hours after transfection, near-confluent C17.2 or HEK 293T cells were rinsed with a physiological buffer (138 mM NaCl, 11 mM d-glucose, 5.3 mM KCl, 0.4 mM KH₂PO₄, 0.3 mM Na₂HPO₄, 1.1 mM CaCl₂, 0.7 mM MgSO₄, 10 mM HEPES, pH 7.4) and allowed to preincubate at 37 °C for 5 min. Uptake was initiated by replacing the pre-incubation buffer with buffer containing 25 μ M ³H-D-aspartate. Following a 5-min incubation, the media was removed by rapid suction and the cells rinsed three times with ice-cold buffer. The cells were dissolved in 0.4 N NaOH for 24 h and analyzed for radioactivity by LSC and protein by the BCA (Pierce) method. Transport rates were corrected for background, i.e., radiolabel accumulation at 4 °C. Initial studies confirmed that uptake quantified in this manner was linear with time and protein levels and that uptake in untransfected C17.2 or HEK 293T cells was indistinguishable from background.

3.2.4 Light Sources and Illumination

Near-confluent C17.2 or HEK293T cells transfected with hEAAT DNA plasmids were washed with assay buffer and replaced by assay buffer with photosensitizers and/or inhibitors/substrates. Cells in dishes or 12-well plates were placed on ice and irradiated by 350 nm light in a RPR-100 photolysis reactor (Southern New England Ultra Violet Company, Branford, CT) equipped with 8 LZC-UVA lamps (Luzchem, Ottawa, ON) for

1 h. Transporter activities were determined by radiolabeled assay immediately after UV irradiation.

3.2.5 RNO Bleaching Assay

The generation of singlet oxygen by photosensitizers was determined by the bleaching of *N,N*-dimethyl-4-nitrosoaniline (RNO) resulting from the reaction between singlet oxygen and histidine (Kraljic and Mohsni, 1978). The RNO (50 μ M) and L-histidine (100 mM) were mixed with each photosensitizers in assay buffer followed by UV irradiation under 350 nm lamps. The reaction was carried out in 96-well format and the absorbance of the sample at 440 nm was measured in a Versamax microplate reader (Molecular Devices, Sunnyvale, CA). Background absorbance was measured in the absence of histidine and/or photosensitizers. Quantum yields of each photosensitizer were calculated by comparing the bleaching rates of RNO with methylene blue.

3.2.6 In-Solution Trypsin Digestion

Aliquot of purified EAAT2 from His column was precipitated in 10% TCA at 4 °C for 30 min. The protein pellet was collected by centrifugation at 15,000g for 5 min. The protein pellet was then washed with 1 ml of cold 1:1 ethanol:ether (v:v) solution 3 times. The washed pellet was briefly air-dried and resuspended in 20 mM ammonium bicarbonate buffer, pH 8.0 (AMBIC). PNGase F (from *Elizabethkingia meningoseptica*, Sigma-Aldrich, St. Louis, MO) was added at the ratio of 50 units per mg of protein. The solution was mixed and incubated at 37 °C for 1 h. This enzyme recognizes the *N*-glycosylation sites of glycoproteins and cleaves the linkage between Asn and

carbohydrate chain (Tarentino and Plummer, 1994). Sequence grade trypsin (Promega, Madison, WI) was added at a 1:20 ratio, and digestion was allowed to proceed at 37 °C for 20 h. Tryptic peptides were analyzed from the digest solution.

3.2.7 Matrix-Assisted Laser Desorption/Ionization (MALDI) Mass Spectroscopy

MALDI-TOF analysis was performed on a Voyager DE PRO (Applied Biosystems, Foster City, CA). An aliquot of sample was mixed with an equal volume of CHCA matrix solution in 50% acetonitrile and 0.1% TFA, and 1 µl was spotted onto the target plate. A Bruker peptide standard was used for calibration. For average masses obtained in linear mode, mass accuracy was set at 200 ppm; for monoisotopic masses obtained in reflectron mode, mass accuracy was set at 50 ppm. Masses were searched against the NCBI protein database or an EAAT database using Mascot (www.matrixscience.com). Modifications for partial methionine oxidation were included.

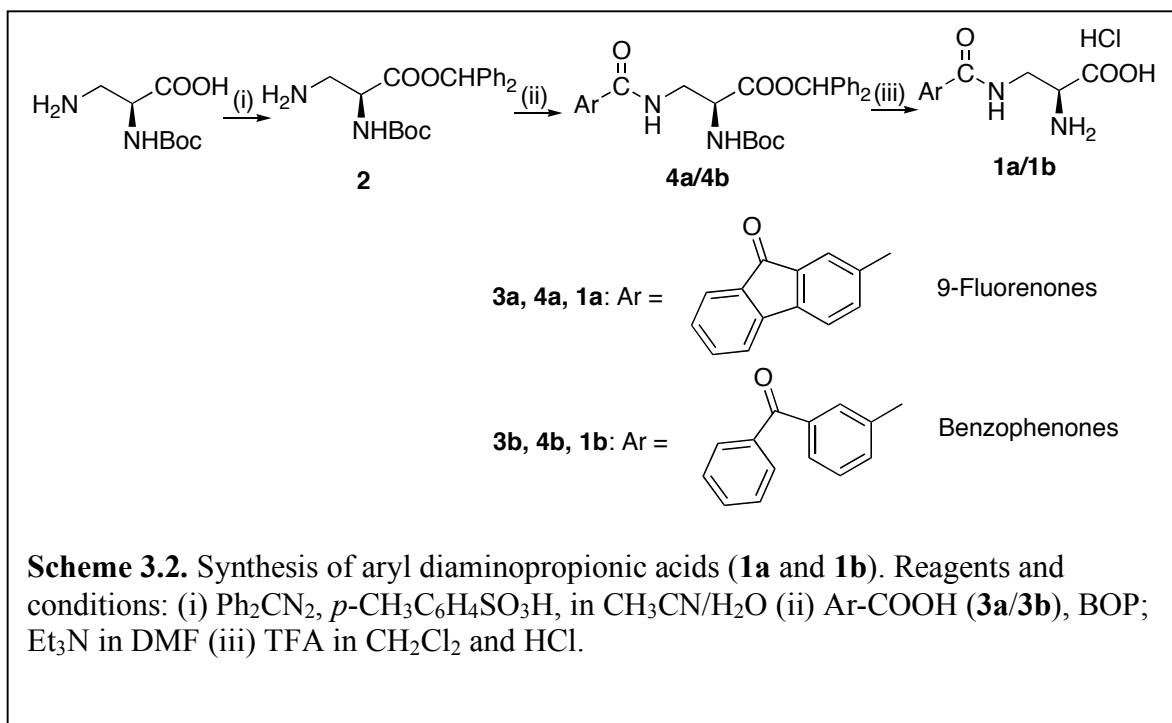
3.3 Results

3.3.1 *Synthesis of Aryl Diaminopropionic Acids*

The steps involved in the synthesis of β -2-Carboxy-fluorenyl-diaminopropionic acid (β -2-CFoDA) and β -2-Carboxy-benzophenonyl-diaminopropionic acid (β -2-CBoDA) are outlined in Scheme 3.2. Our initial attempts to follow the procedures previously reported by Greenfield et al. did not produce an acceptable yield of the desired products. Therefore, a new strategy using benzotriazole-1-yl-oxy-tris-(dimethylamino)-phosphonium hexafluorophosphate (BOP) as the coupling reagent was employed. The protection of the free carboxylic group on *N*-Boc-3-amino-L-alanine was optimized using diphenyldiazomethane ($\text{Ph}_2\text{C}=\text{N}_2$, prepared from Miller et al., 1959). The coupling product was purified by flash chromatography followed by TFA treatment to remove protection groups. Final product was precipitated from aqueous solution by adjusting pH to 4-5. Compared with the coupling reagents reported by Greenfield et al. (*N*-hydroxysuccinimide and DIC (*N,N'*-diisopropylcarbodiimide)), our method had a higher yield (~27%), purity and offered more flexibility in synthesizing other analogues bearing similar scaffolds. The aryl aspartylamides characterized in this chapter were synthesized by Brent Lyda in a collaborative project between the Bridges and Esslinger labs (Bridges et al., 2008).

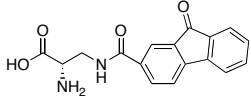
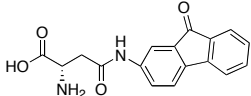
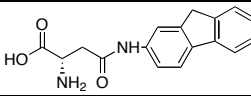
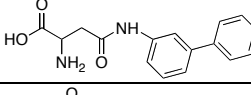
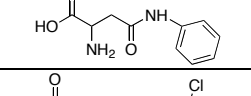
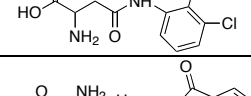
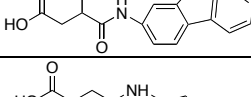
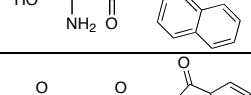
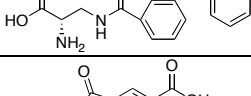
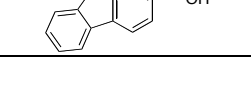
3.3.2 *Pharmacological Characterization of β -2-CFoDA at EAATs*

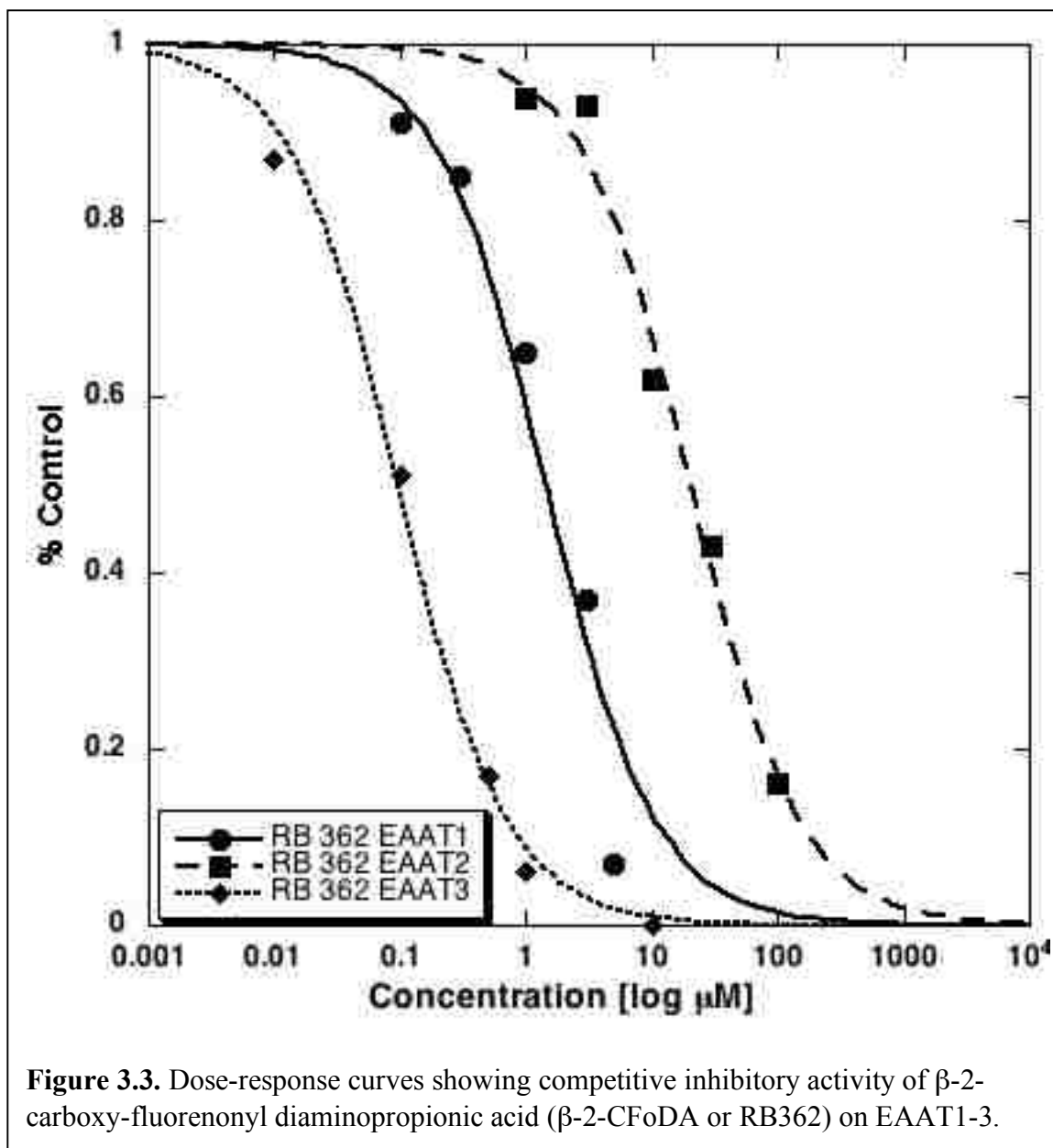
A series of aryl aspartylamides and diaminopropionic acids, that included β -2-CFoDA, were initially screened at 10 μM and 100 μM for the ability to inhibit the uptake



of [³H]-D-aspartate (25 μM) into C17.2 cells expressing EAAT1, EAAT2 or EAAT3. Transporter assays were carried out as described in Methods, with rates appropriately corrected for nonspecific background (4 °C) and normalized for protein content. The data are reported in Table 3.1 as the mean % of control (±SEM) measured in the absence of inhibitors. Thus, the lower the values the greater the level of inhibition. Among the analogues examined, β-2-CFoDA, β-2-FoAA and β-2-FAA proved to be the most potent inhibitors at all EAAT subtypes. Essentially all three compounds were able to inhibit almost 100% of D-aspartate uptake when incubated in the assay at 100 μM. In contrast, β-2-PAA, β-2-BPAA, β-2-DCPAA, β-2-NAA, and β-2-CBoDA showed only low levels of inhibitory activity at EAAT1 and EAAT2. These analogues did exhibit modest actions against EAAT3 at 100 μM, with little inhibition observed when the concentration was decreased to 10 μM. More detailed, dose-response experiments were conducted on β-2-CFoDA, β-2-FoAA and β-2-FAA to examine the concentration-dependence with which they inhibited the EAATs. Results of these assays were reported in Table 3.1 as the concentrations at which D-aspartate uptake was inhibited by 50% (IC₅₀). Representative plots for β-2-CFoDA IC₅₀ plots are shown in Figure 3.3. The data showed that all three compounds are very potent inhibitors of each of the three EAAT subtypes, with IC₅₀ values in the low micromolar to nanomolar range. It is also noteworthy that although there is more than an order of magnitude in the differences in inhibitory potencies of analogues, the rank of potencies at each EAAT subtypes is well preserved (i.e. EAAT3 > EAAT1 > EAAT2).

Table 3.1. Pharmacological screening of aryl diaminopropionic acids and aryl aspartylamides on EAAT1-3. All screening was performed at two inhibitor concentrations: 100 μ M and 10 μ M. Additional concentrations were used to calculate the IC_{50} values for selective compounds.

Abbrevia- tion	Structure	EAAT1		EAAT2		EAAT3	
		100 μ M	10 μ M	100 μ M	10 μ M	100 μ M	10 μ M
β -2-CFoDA		$IC_{50} = 1.44 \pm 0.31$ μ M (3)		$IC_{50} = 20.3 \pm 2.2$ μ M (3)		$IC_{50} = 0.09 \pm 0.01$ μ M (3)	
β -2-FoAA		$IC_{50} = 0.26 \pm 0.01$ μ M (3)		$IC_{50} = 6.2 \pm 0.5$ μ M (3)		$IC_{50} = 0.25 \pm 0.03$ μ M (3)	
β -2-FAA		$IC_{50} = 0.44 \pm 0.001$ μ M (2)		$IC_{50} = 0.61 \pm 0.17$ μ M (5)		$IC_{50} = 0.03 \pm 0.02$ μ M (4)	
β -2-BPAA		89 ± 6 (3)	80 ± 9 (3)	82 ± 7 (3)	82 ± 2 (3)	65 ± 3 (3)	83 ± 4 (3)
β -2-PAA		74 ± 12 (3)	94 ± 9 (3)	72 ± 4 (2)	102 ± 4 (2)	41 ± 6 (3)	80 ± 10 (3)
β -2-DCPAA		80 ± 5 (3)	92 ± 11 (3)	79 ± 5 (3)	83 ± 3 (3)	43 ± 1 (3)	73 ± 9 (3)
-		50 ± 11 (3)	75 ± 8 (3)	78 ± 5 (3)	88 ± 5 (3)	7 ± 1 (3)	45 ± 3 (3)
β -2-NAA		68 ± 10 (3)	91 ± 9 (3)	63 ± 13 (3)	93 ± 3 (3)	35 ± 8 (4)	84 ± 3 (4)
β -2-CBoDA		51 ± 7 (3)	93 ± 4 (3)	52 ± 7 (3)	87 ± 4 (3)	25 ± 5 (2)	77 ± 9 (3)
9F2C		102 ± 2 (3)	-	94 ± 5 (3)	-	109 ± 4 (3)	-



Our results indicated that coupling fluorene or 9-fluorenone groups with an aspartyl amide or a diaminopropionic acids produced very potent EAAT inhibitors with IC_{50} values comparable to some of the most potent EAAT inhibitors identified to date (TFB-TBOA, $IC_{50} = 2-20$ nM, Shimamoto et al., 2002). Compared with the IC_{50} values of the same compounds reported in Greenfield et al. (2005), our assays yielded slightly higher inhibition potencies probably due to differences in cell line and assay conditions. Replacing the fluorene or 9-fluorenone groups with phenyl, biphenyl, naphthyl or dichlorophenyl groups resulted in an almost complete loss of inhibitory activity. More surprisingly, coupling diaminopropionic acids with benzophenone, a group that only differs by one carbon-carbon bond from the 9-fluorenone group, markedly decreased inhibitory activity. Considering that both groups are highly conjugated aromatic systems, the orientation and electron densities should be similar. The dramatic differences in activity thus suggested high specificity interactions between the binding pocket of the proteins and the fluorene/9-fluorenone groups. We did notice the slight drop in potency from β -2-FAA to β -2-FoAA to β -2-CFoDA, which may be attributed to the addition of an extra carbonyl group on 9-fluorenes. Based on the above observations, we believe there is a lipophilic pocket in the EAAT proteins that can accommodate large aromatic ring systems (fluorene, 9-fluorenone) and the molecular recognition mechanism is highly specific. Among all the aromatic groups, fluorene seems to have the highest affinity to the lipophilic pocket.

3.3.3 Photo-Inactivation of EAATs by β -2-CFoDA

It has been known for a long time that 9-fluorenone groups can be activated by UV light to produce triplet state biradicals. The highly reactive fluorenone biradicals are involved in numerous photosensitizing processes and are also capable of generating additional secondary reactive oxygen species (ROS). If proteins are present in the system while these reactive intermediates are being generated, they tend to serve as quenchers or energy acceptors to the intermediates by means of photoreactions. The study of photoreactions between proteins and photosensitizer-induced reactive intermediates provides a good strategy to probe protein structure. More importantly, if the reactions occur in specific regions of proteins, such as at an enzyme-substrate interface, investigating the photochemical interactions could provide greater insights into substrate and inhibitor binding at the molecular level. Among the EAAT inhibitors we synthesized and characterized, β -2-CFoDA and β -2-FoAA possess 9-fluorenone groups that have the potential to be photo-activated and consequently used as photoaffinity probes for the EAATs.

C17.2 Cells expressing EAAT1, EAAT2 or EAAT3 were incubated in physiological buffer with compounds bearing 9-fluorenone groups while being illuminated by 350 nm UV lights in a UV-photolysis reactor. Immediately following UV exposure, the cells were rinsed to remove the inhibitors and then assessed for uptake activity using the standard radiolabeled flux assay. In initial experiments we found that incubation with either β -2-CFoDA or β -2-FoAA in presence of UV illumination led to a decreased level of uptake. To establish control levels of activity, cells incubated with the inhibitors were placed in the UV reactor covered by aluminum foil. Additional

experiments also determined that 350 nm UV illumination did not cause any apparent cell death nor significant nonspecific transporter activity losses in the absence of the photosensitizers. In contrast, neither 300 nm nor diffuse light source (desk lamp) could induce a significant activity loss, while 250 nm illumination greatly reduced cell viability and almost all transporter activity after 15 min.

To further investigate the nature of the 350 nm UV-dependent, 9-fluorenone-mediated inactivation of the EAATs, we performed a series of control experiments. We observed that loss in the EAAT activity was irreversible and did not recover up to 30 min after the cells were removed from the photolysis reactor. Hence we deemed this inhibition to be photo-inactivation. The photo-inactivation was found to be positively correlated to both the times of illumination and concentrations of the inhibitor. The concentration dependence with which β -2-CFoDA and β -2-FoAA inactivated EAAT2 is illustrated in Figure 3.4. Of the two inhibitors, β -2-CFoDA produced a significantly greater levels of inactivation (1 h UV exposure) at all concentrations tested. Interestingly, β -2-FoAA did not induce significant EAAT2 photo-inactivation until its concentration reached 250 μ M. The time dependence of EAAT2 inactivation by β -2-CFoDA (100 μ M) is illustrated in Figure 3.5. We observed the photo-inactivation became significant after 45 min of illumination. After 120 min, EAAT2 activity dropped down to a level that was indistinguishable from background nonspecific activity (Figure 3.5). A 350 nm light sources and 60 min illumination time was used in the remainder studies unless mentioned otherwise.

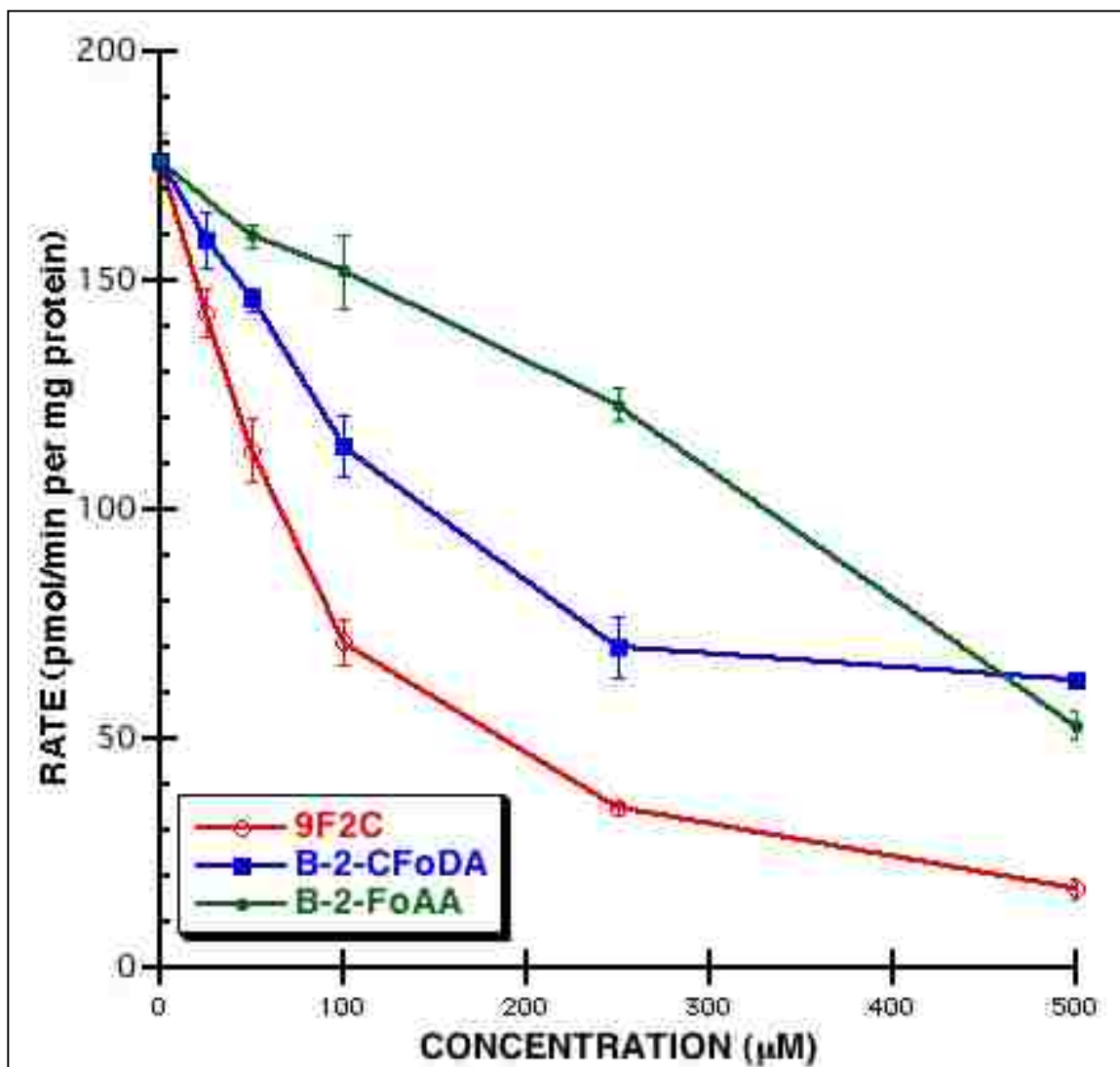
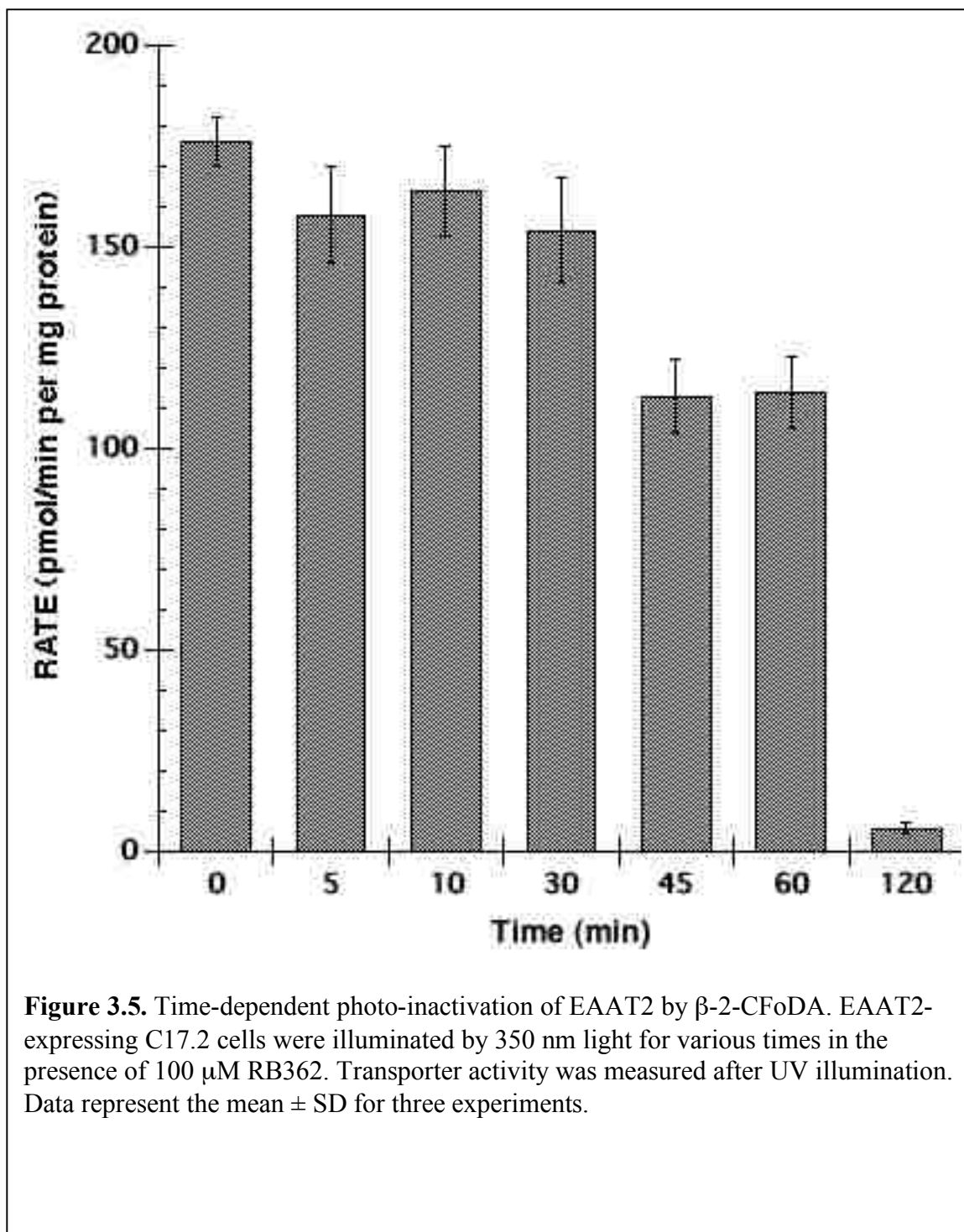


Figure 3.4. EAAT2 activity is irreversibly inhibited by UV-A illumination in the presence of 9-fluorenone-containing compounds. C17.2 cells expression human EAAT2 were illuminated by 350 nm light in the presence of 9F2C, β -2-CFoDA (RB362) or β -2-FoAA (RB363) for 1 h before their activity being measured using radiolabeled uptake assay. Data represents the mean \pm SD for three experiments.



As an additional control we carried out a parallel series of experiments, using the free photophore-9F2C. Uptake studies confirmed that 9F2C is not a competitive inhibitor of any of the EAATs (Table 3.1). To our surprise, 9F2C also led to the inactivation of EAAT2 in the presence of 350 nm UV illumination. As shown in Figure 3.4, 9F2C proved to be the most potent inactivator of the three compounds. The fact that 9F2C does not bind to the EAAT substrate site (i.e., it is not a competitive inhibitor), suggested that it, as well as the other 9-fluorenone-containing ligands, were not acting as direct photoaffinity labels, but inactivating the transporters through an indirect mechanism.

3.3.4 Photosensitizer-Induced EAAT Photo-Inactivation is via Singlet Oxygen Mechanism

As previously discussed, the action of 9F2C suggested that the 9-fluorenone groups were likely inactivating the EAATs indirectly via reactive intermediates. In the presence of photosensitizers and oxygen, UV illumination produces a variety of reactive intermediate species that can participate in different types of photoreactions. When proteins are also introduced into the system, the reaction mechanism becomes even more complicated, with the possible reaction pathway differs on a case-by-case basis. It has been known for a long time that the 9-fluorenone groups are readily excited to its triplet biradical state by 350 nm UV light (Galardy et al., 1973). The photo-inactivation of the EAATs we observed was also most effective at 350 nm UV illumination. A series of experiments was carried out to elucidate the mechanism of inactivation. First, we found that EAAT1, EAAT2, and EAAT3, were all effectively photo-inactivated by all three of the 9-fluorenone-bearing compounds (Figure 3.6). Although each subtype exhibited a different rate of transport in our expression system, the relative decrease in uptake

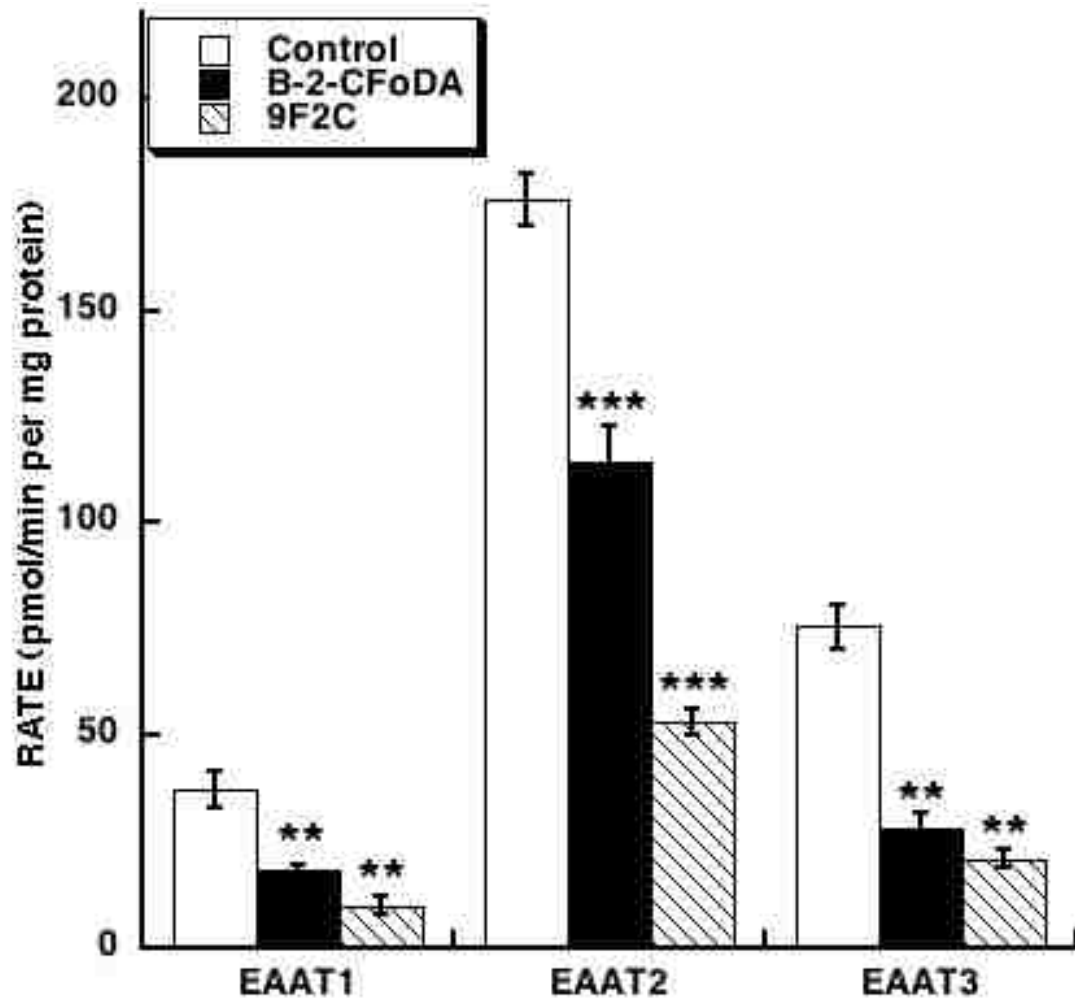
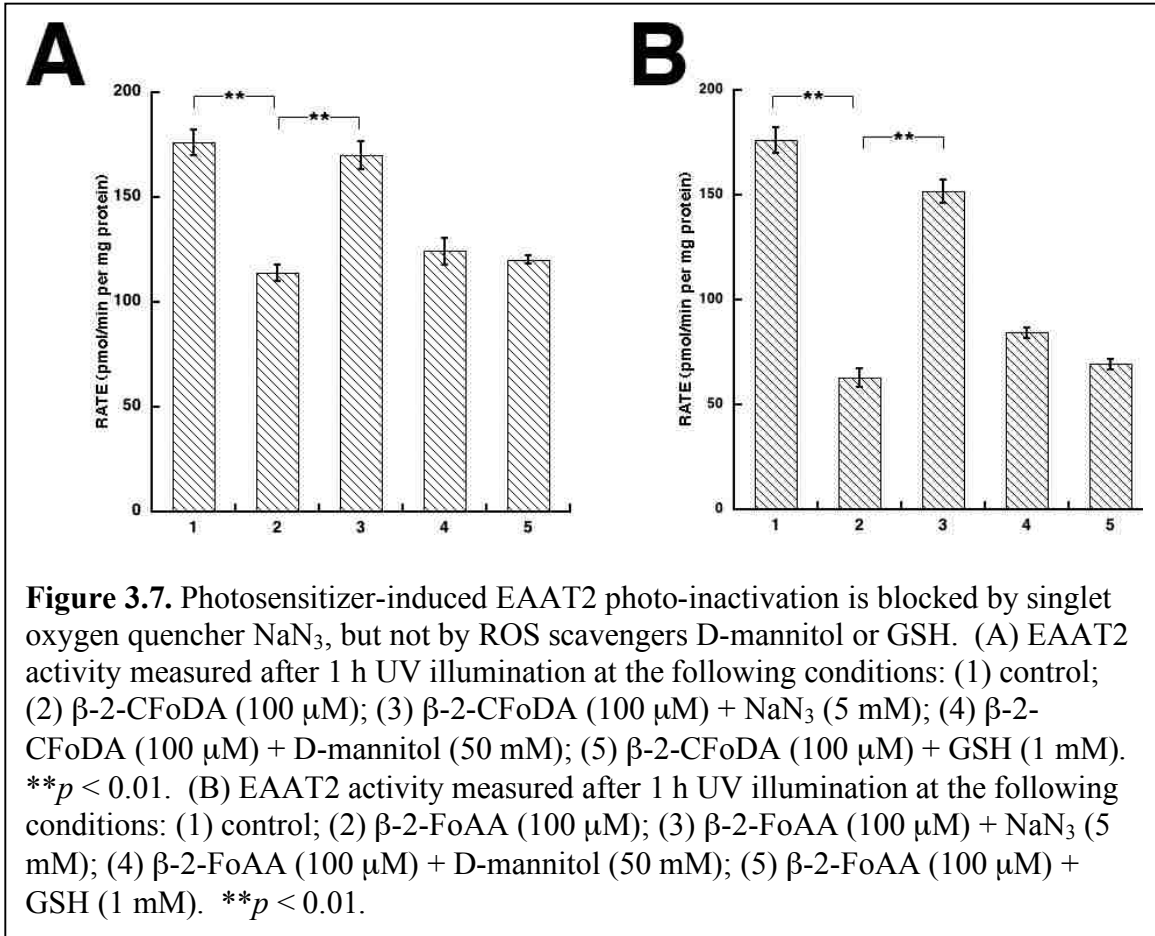


Figure 3.6. Compounds containing 9-fluorenone groups inactivate EAAT activity under 350 nm UV illumination. β -2-CFoDA- and 9F2C- induced photo-inactivation effects were observed in three EAAT subtypes (EAAT1, EAAT2 and EAAT3). UV illumination time was 1 h. Concentrations of β -2-CFoDA and 9F2C are both 100 μ M. ** $p < 0.01$; *** $p < 0.001$.

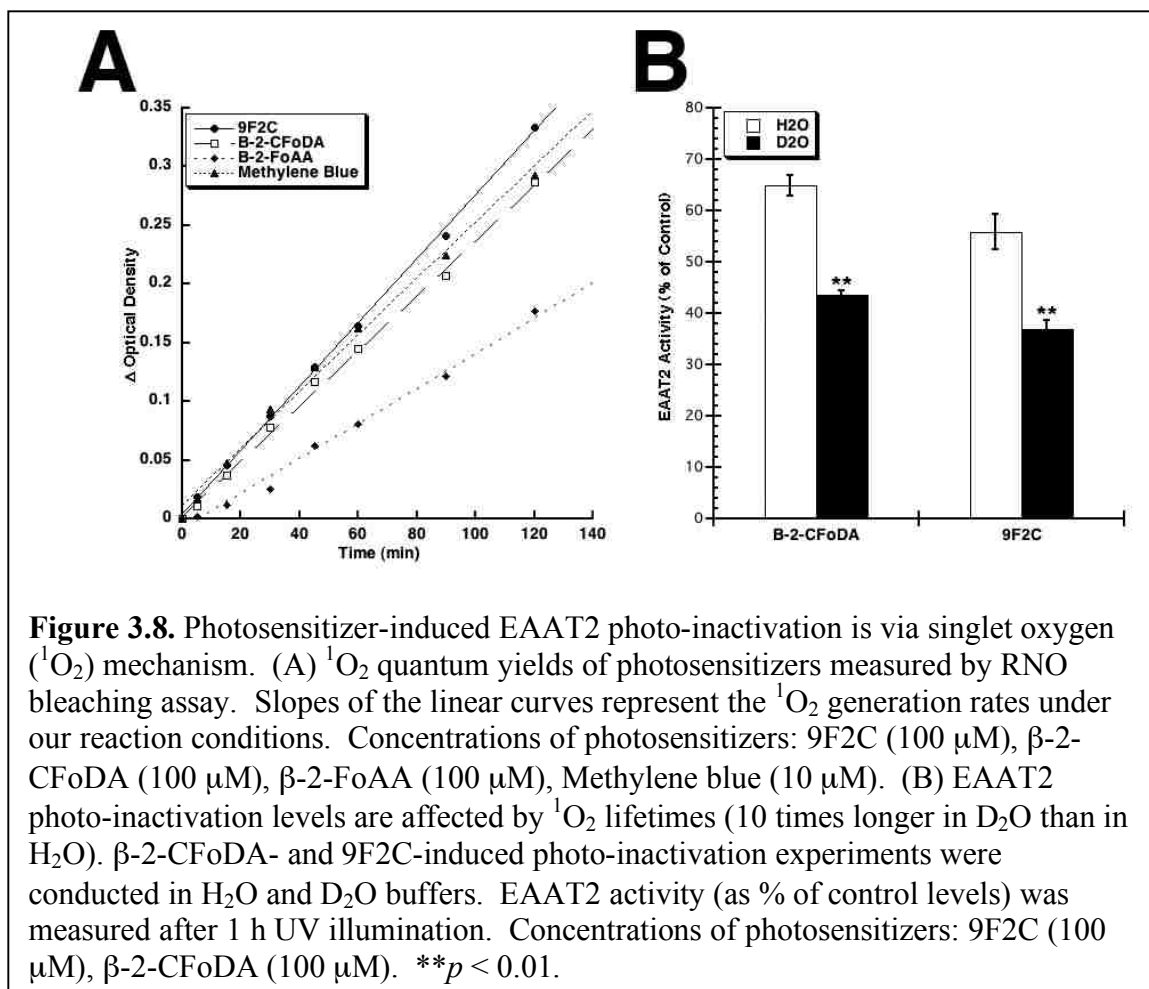
activity caused a photo-inactivation remained roughly the same. In this respect the ability of the analogues to inactivate the EAATs did not correlate with their respective pharmacological profiles. Thus, β -2-FoAA was more potent as a competitive inhibitor than as an inactivator when compared to β -2-CFoDA. This suggested that inactivation was not dependent solely upon the ability of the analogues to bind to the substrate site on the transporters. Once bound, variables such as the orientation and proximity of the photophore to target residues probably have a significant influence on the efficiency of inactivation. This was even more the case for 9F2C which, based on competitive studies, does not even bind to the substrate site on the transporter.

Greater insight into the mechanism came with the demonstration that the inclusion of 5 mM NaN₃ in the reaction buffer effectively prevented the photo-inactivation in all EAAT subtypes induced by both β -2-CFoDA (Figure 3.7A) and 9F2C (Figure 3.7B). Azide ion is a well known singlet oxygen (¹O₂) physical quencher and the protective effects offered by NaN₃ strongly indicate the involvement of ¹O₂ in the photo-inactivation processes. To determine if ¹O₂ is indeed the major intermediate species that caused the photo-inactivation, we carried out a series of studies to explore the possibilities of the involvement of ¹O₂ and other ROS. To compare with the protective effects of NaN₃, we selected two ROS scavengers to test the potential contribution of hydroxyl free radical, superoxide anion and H₂O₂. Concentrations of 50 mM D-mannitol (Melinn and McLaughlin, 1986) and 1 mM glutathione (GSH, Devasagayam et al., 1991) were included in the reaction buffer during the photo-inactivation. Our results show that neither mannitol nor GSH provided significant protection against the photo-inactivation of EAAT2 by either β -2-CFoDA or 9F2C (Figure 3.7). Similar results were also



observed in EAAT1 and EAAT3 photo-inactivation experiments (data not shown). These findings are consistent with the conclusions that $^1\text{O}_2$ played a much more important role than hydroxyl radicals, superoxide anions and H_2O_2 . As a second strategy to confirm that the inactivation was $^1\text{O}_2$ -mediated, assays were designed to exploit the lifetime variations of $^1\text{O}_2$ in different solvents. In D_2O , the lifetime of $^1\text{O}_2$ is about 20 μs , which is about 10 times longer than that in H_2O . Measurements of reaction rate differences in these two solvents are often used to support the direct involvement of $^1\text{O}_2$ in photochemical processes. In our EAAT2 photo-inactivation studies, we replaced H_2O with D_2O in the reaction buffer and noticed an increased level of inactivation level compared to H_2O (Figure 3.8B). The percentages of decrease in EAAT2 activity resulted from both β -2-CFoDA- and 9F2C-mediated photo-inactivation in the D_2O groups were determined to be statistically significant from those in the H_2O groups. We also noticed that the control EAAT2 activity is slightly lower in the D_2O group, indicating that nonspecific (non-photosensitizer-induced) $^1\text{O}_2$ species inhibited EAAT2 activity in D_2O buffer while they normally would be depleted in the H_2O buffer. These observations prompted us to propose a photosensitizer-induced EAAT photo-inactivation pathway in which $^1\text{O}_2$ is the key intermediate directly reacts with the proteins.

Having established a $^1\text{O}_2$ -mediated mechanism for the EAAT photo-inactivation, we sought to determine if this effect is specific to the 9-fluorenone groups. As part of this effort we quantified the rates of $^1\text{O}_2$ production by all three 9-fluorenone-bearing photosensitizers in our reaction solvent system and compared it with known $^1\text{O}_2$ -generator using histidine and *p*-nitrosodimethylaniline (RNO) (Kraljic and Mohsni, 1978). In this RNO bleaching assay analysis, the loss of RNO absorption at 440 nm



produced by the reaction product of histidine and $^1\text{O}_2$ is plotted against time. The resulting slope represents the rate of $^1\text{O}_2$ generation, or quantum yield (Φ_Δ). Under our illumination conditions we found both 9F2C and β -2-CFoDA are efficient $^1\text{O}_2$ producers in our aqueous reaction buffer, while β -2-FoAA is a weaker $^1\text{O}_2$ generator (Figure 3.8A). By comparing Φ_Δ of each photosensitizer with that of a known water-soluble photosensitizer, methylene blue (MB, 0.52, Kochevar and Redmond, 2000), the Φ_Δ s for 9F2C, β -2-CFoDA, β -2-FoAA at 100 μM were determined to be 0.598 ± 0.0095 , 0.519 ± 0.012 and 0.34 ± 0.014 , respectively. The $^1\text{O}_2$ quantum yields agreed quite well with the levels of photo-inactivation we observed with each photosensitizers. The differences in the ability of these photosensitizers to generate $^1\text{O}_2$ can be attributed to the electron donating/withdrawing groups attached to the 9-fluorenone groups. The secondary amine group in β -2-FoAA likely destabilizes the triplet intermediate, while carbonyl groups (in 9F2C and β -2-CFoDA) stabilize the biradical. The difference in $^1\text{O}_2$ quantum yield provide an explanation as to why higher concentrations of β -2-FoAA were required to induce similar levels of EAAT inhibition as 9F2C and β -2-CFoDA. The results are also consistent with 9-fluorenone triplet biradical being the initial intermediate species and that the production of the biradical may be the rate-limiting step of this complex reaction system. Because the Φ_Δ of β -2-CFoDA (0.519) is very close to that of MB in our experimental conditions, we were curious as to what level of photo-inactivation MB would induce in the EAAT proteins. In contrast to 9F2C, co-incubation of MB failed to induce the photo-inactivation of any EAAT subtypes (Figure 3.9). These results suggested that although β -2-CFoDA and MB produced $^1\text{O}_2$ at approximately the same rates, $^1\text{O}_2$ species generated by MB were unable to reach and react with the residues on

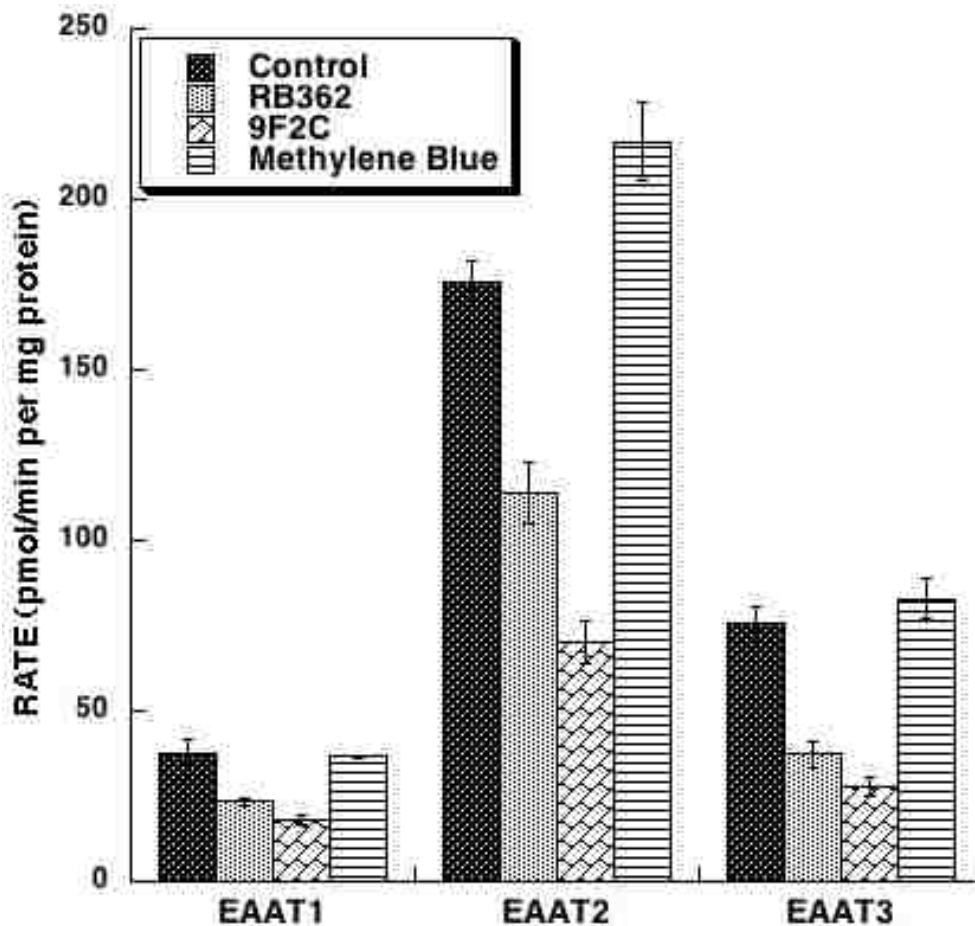
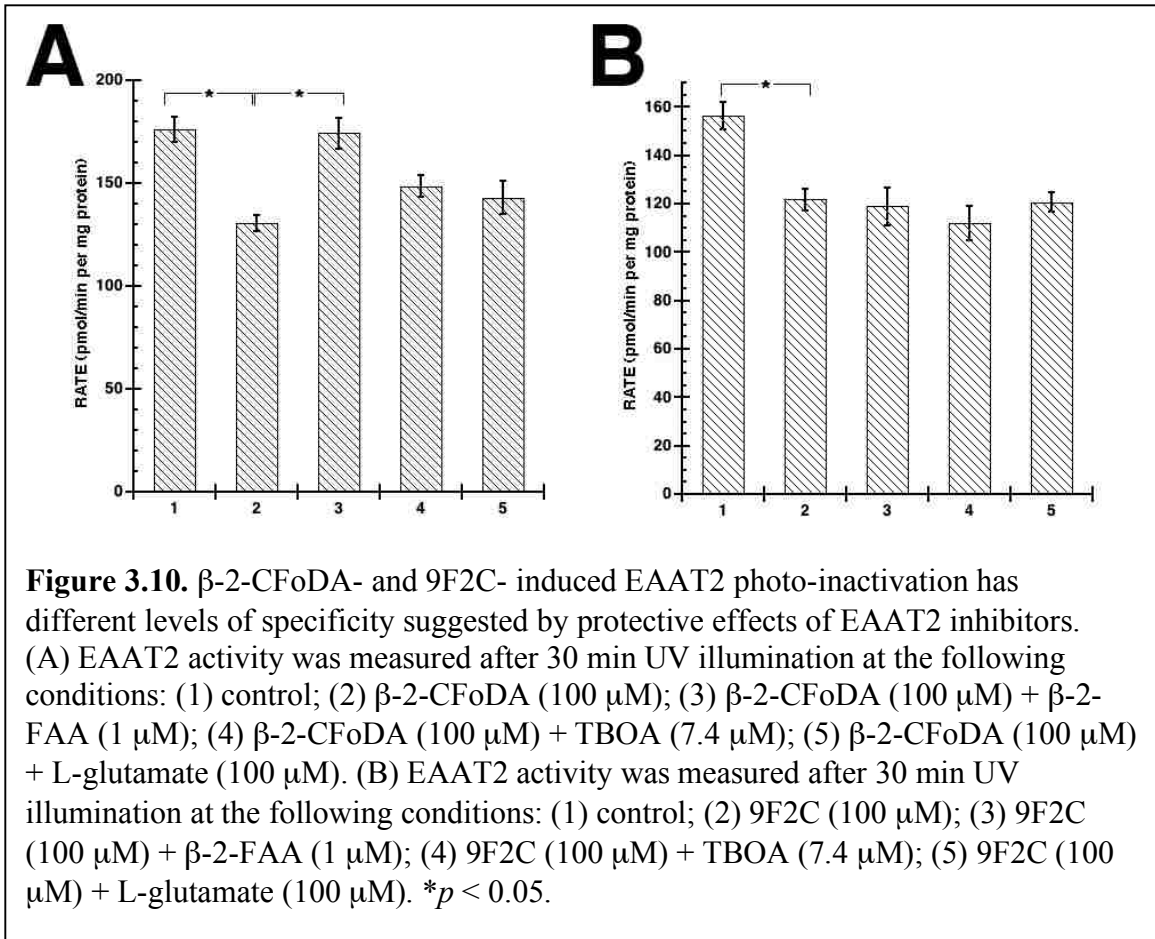


Figure 3.9. Methylene blue (MB) does not photo-inactivate either EAAT subtypes. The singlet oxygen quantum yield of MB is similar to that of 9F2C/ β -2-CFoDA (RB362). However, UV illumination of transporter-expression cells in the presence of MB did not cause a significant decrease of transporter activities. Data represent the mean \pm SD for three experiments.

EAAT2 that would lead to inactivation. In turn this suggests that both β -2-CFoDA and 9F2C were able to interact with the EAATs, in such a manner as to be positioned close enough and long enough for the resulting $^1\text{O}_2$ to inactivate the transporter.

3.3.5 EAAT2 Inhibitors Protect Against β -2-CFoDA-Induced Photo-Inactivation

Our results indicate that the interactions between EAATs and 9-fluorenone groups are highly specific and the sites where $^1\text{O}_2$ being generated are very close to the protein domains on the EAATs. To address this, we introduced various EAAT2 inhibitors and substrates into our photo-inactivation assays to see if any of these ligands could protect against inactivation. The inhibitors and substrates chosen were: L-glutamate, TBOA, and β -2-FAA. L-Glutamate is the endogenous substrate of EAATs and is efficiently transported into the cells. In contrast, TBOA and β -2-FAA are both non-transportable EAAT2 inhibitors. It is thought that the lipophilic groups present on these analogues serve to increase potency when they bind, as well as render their non-substrate properties. In particular, β -2-FAA is a very potent inhibitor that is structurally quite similar to β -2-CFoDA. These compounds were incubated with either 9F2C or β -2-CFoDA during the photo-inactivation reactions. All drug solutions were then washed off before transporter activity was evaluated. The concentrations of the compounds (L-glutamate: 100 μM , TBOA: 7.4 μM , β -2-FAA: 1 μM) were calculated to give approximately the same percentage of occupancy to the proteins based on their IC_{50} or K_i values. We observed very different results from 9F2C- and β -2-CFoDA- induced photo-inactivation experiments. The β -2-CFoDA-induced photo-inactivation was effectively prevented by the co-incubation of β -2-FAA, but not by TBOA or L-glutamate (Figure 3.10A). In

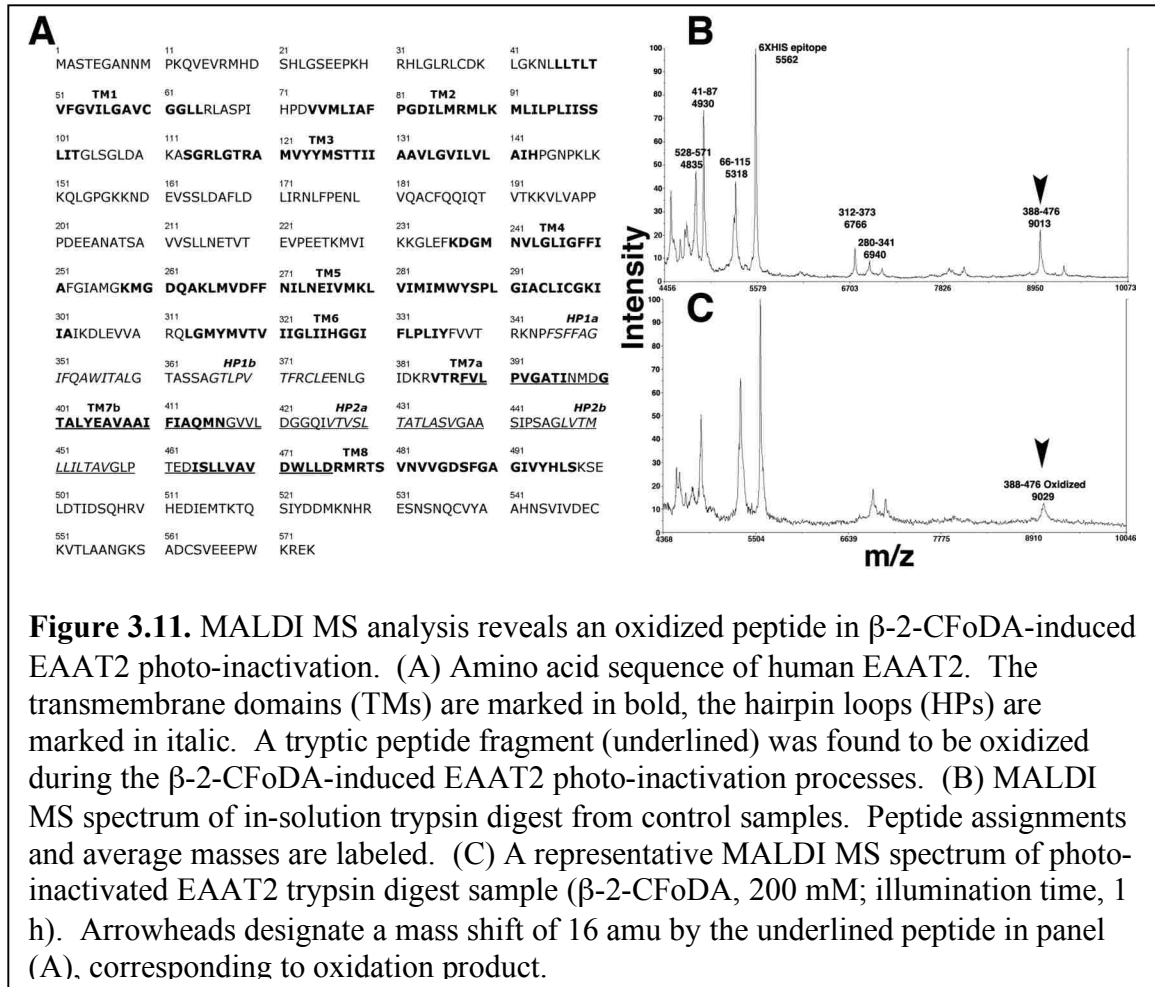


contrast, none of the inhibitors or substrates was able to protect the transporters from being photo-inactivated by 9F2C (Figure 3.10B). The protective actions of β -2-FAA is consistent with the conclusion that β -2-CFoDA was bound in the substrate site when it inactivated the transporter. The inability of either L-glutamate or TBOA to protect may reflect the fact that their association and dissociation rates were not slow enough to prevent β -2-CFoDA to bind and inactivate the transporter during the 60 min incubation. β -2-FAA, on the other hand, has been found to exhibit very long dissociation rates (Bridges et al., 2008; Kavanaugh et al., 2008). However, the binding and unbinding of β -2-FAA with EAAT2 did not seem to affect the photo-inactivation efficiency induced by 9F2C. This would suggest a possible second inactivation site or a different binding orientation by 9F2C from the binding of β -2-CFoDA. From these observations we hypothesize: *i*) EAAT2 proteins were photo-inactivated by 9F2C and β -2-CFoDA both via a $^1\text{O}_2$ -mediated mechanism but the inactivation site(s) may be different; *ii*) The EAAT2 lipophilic interaction site(s) with β -2-CFoDA and β -2-FAA is different from the domains that interact with TBOA, which is HP2 as illustrated by the *Gltp_h* crystal structure (Yernool et al., 2004; Boudker et al., 2007).

3.3.6 β -2-CFoDA-Induced Photo-Inactivation is Caused by Oxidation of a Binding Domain Peptide

In the final set of experiments we used mass spectrometric (MS) tools to locate the site(s) at which the $^1\text{O}_2$ reacted with and inactivated EAAT2. As discussed in Chapter 2 we previously developed a high-yield, functional expression and purification protocol for his-tagged EAAT2 (Ye et al., 2009). Our trypsin digestion method and MALDI MS

characterization offered 89% sequence coverage of the EAAT2. In particular, this protocol resulted in near-complete coverage of the regions of EAAT2 postulated to participate in substrate binding. In this study we took advantage of the EAAT2 MS peptide fingerprint we generated and attempted to identify peptides that were modified through photo-inactivation. In-solution trypsin digestion was performed on both the control samples and the EAAT2 proteins that had been photo-inactivated by either β -2-CFoDA or 9F2C. MS characterization was conducted on peptide fragments from the digestions by MALDI-TOF. Comparison between the MS peptide fingerprint generated from 9F2C-inactivated EAAT2 samples were indistinguishable from control samples in the range of our mass scans. It is also noteworthy that protein cross-linking is often associated with photosensitization and MS detection and analysis of resulting high molecular weight peptides are difficult. However, in the case of β -2-CFoDA-induced EAAT2 photo-inactivation, a large peptide fragment was consistently found to have a higher m/z value from the photo-inactivated sample than from the control sample. The centroid m/z values for this peptide from control samples were 9013 ± 2 in 10 independent experiments. In the EAAT2 samples photo-inactivated by β -2-CFoDA, the same peptide had centroid m/z values of 9040 ± 3 (6 independent experiments). The primary sequence of the human EAAT2 and representative MS spectra are shown in Figure 3.11. In this particular example, a mass shift of 16 amu was observed for the peptide indicating a single oxygen atom addition. In our peptide assignment, this peptide corresponds to amino acid residues 388-476 in EAAT2, covering TM7, HP2 and part of TM8 regions of the protein based on the homology model of EAAT2 generated from



Glt_{Ph} structures. The increased peptide mass suggested possible oxidations of this peptide at one or more residues via ¹O₂. Inspection of this peptide revealed the presence of a tyrosine, a tryptophan and three methionine groups that are considered primary targets for ¹O₂-mediated oxidation.

3.4 Discussion

High-affinity, Na⁺-dependent glutamate transporters play an essential role in fast synaptic neurotransmission, regulating extracellular glutamate concentrations, synaptic plasticity, learning and memory (Tzingounis and Wadiche, 2007). Our current understanding of the tertiary and quaternary structures of this family of integral membrane is based upon cumulative data from a number of approaches, including cysteine surface scanning (Slotboom et al., 2001; Seal and Amara, 1998; Grunewald et al., 1998), the crystallizations of prokaryotic EAAT homolog (Yernool et al., 2004; Boudker et al., 2007), mass spectrometric characterization (Chapter 2), fluorescent labeling (Larsson et al., 2004; Koch et al., 2007), inter-subunit interactions and oligomeric structures (Raunser et al., 2006). With the exception of the crystallographic studies of *Glt_{Ph}*, experiments directly examine the interaction of EAAT domains with different substrates and inhibitors has been limited. The identification of ligand-protein interactions is a key step towards a full understanding of the transporting mechanism. In this study, we took advantage of the established MS peptide fingerprint (Chapter 2), the reports of aryl aspartylamides and aryl diaminopropionic acids as potent EAAT inhibitors (Greenfield et al., 2005), and the photoreactivity of 9-fluorenone groups, and used a

combination of pharmacological, photochemical and mass spectrometric tools to provide evidence of the inhibitor-EAAT interactions.

We synthesized the 9-fluorenyl derivatives of both the aspartylamide and diaminopropionic acids templates and demonstrated that both led to an irreversible loss of activity by all 3 EAATs. This inactivation was dependent upon 350 nm UV illumination and the needed exposure times were consistent with other studies using biaryl ketone groups (Han et al., 2000; Garcia et al., 2007). The photoactive ligand also inactivated the EAATs in a concentration dependent manner. Understanding both the mechanism and specificity of the photoreactive ligand was critical to evaluate their utility as probes of the EAAT binding domains.

3.4.1 9-Fluorenone-Mediated EAAT Inactivation is via Singlet Oxygen Mechanism

Given the functional significance of the EAATs, it is not surprising that considerable efforts have been focused on the development of potent and selective inhibitors of these transporters. Recent studies have identified a series of aryl aspartylamides and aryl diaminopropionic acids as being among the most potent EAAT blockers yet identified, exhibiting IC_{50} values in the nanomolar range (Dunlop and Butera, 2006). An examination of these analogues revealed that the aryl ketones including 9-fluorenone groups are well-known for their photoreactivity. For example, benzophenone-bearing inhibitors have been synthesized and tested their photoaffinity in various studies (Pleban et al., 2005; Garcia et al., 2007). In combination with MS, a unique HIV-1 integrase inhibitor-binding domain was identified by using benzophenone-linked coumarin integrase inhibitor (Al-Mawsawi et al., 2006). The long excitation

wavelength (~350 nm) induces minimal damage to the cells and has made biaryl ketones the photophore of choice for *in vitro* studies (Prestwich et al., 1997). Sharing common structural features with benzophenone, 9-fluorenone exhibits similar photochemical properties and has been used in several studies, such as the human parathyroid hormone 1 receptor ligand binding domain (Han et al., 2000), the catechol binding domain of the β_2 -adrenergic receptor (Wu et al., 2001), and the substrate binding pocket of the vesicular monoamine transporter 2 (Gopalakrishnan et al., 2007).

The combination of photoreactive properties of the 9-fluorenone and the high affinity of the inhibitors suggested the compounds could be used as ligand probes to identify domains on the EAATs that participate in substrate binding. UV illumination of biaryl ketone groups can potentially inactivate proteins through a number of mechanisms, including both direct and indirect pathways. In our studies, the possibility of direct cross-linking between 9-fluorenone biradical was ruled out by the inactivation caused by 9F2C, a non-inhibitor on the EAATs because the short lifetime of the biradical hence the short reaction radius ($< 5 \text{ \AA}$). The possible involvement of ROS radicals was also excluded by the minimal protection effects displayed by GSH (against superoxide anion and H_2O_2) and D-mannitol (against hydroxyl radical). It is interesting in this regard that Volterra et al. reported, in cortical glial cultures, glutamate uptake is inhibited by reactive oxygen species such as superoxide anion, hydroxyl radical and H_2O_2 (Volterra et al., 1994). They also found that the presence of scavengers such as GSH blocked almost all the inhibition. We found that the best protection from the UV-dependent, 9-fluorenone-mediated inactivation was NaN_3 . The azide ion is a strong physical quencher of $^1\text{O}_2$ and is often used to show the involvement of the $^1\text{O}_2$ in the photoreactions (Li et al., 2001). A

$^1\text{O}_2$ -mediated inactivation pathway is also consistent with our demonstration that even greater losses of activity were observed in the D_2O reaction buffer. In the original mechanistic studies of FALI, D_2O experiments provided direct evidence of $^1\text{O}_2$'s role as predominant intermediate (Beck et al., 2002). By using RNO bleaching assay we were able to quantify the $^1\text{O}_2$ quantum yield for each of the photoactive ligand. We found that the rates of $^1\text{O}_2$ generation positively correlated with the level of photo-inactivation. In addition to supporting our conclusion that the inactivation was $^1\text{O}_2$ -mediated, these results also suggested that the rate-limiting step in the photo-inactivation is the excitation of photosensitizers into 9-fluorenone triplet state biradical. However, the inability of MB, which also had a quantum yield comparable to the other ligands, to inactivate EAAT2 also indicated that the loss of activity could not be attributed simply to the presence of $^1\text{O}_2$, and was most likely dependent upon a specific interaction between protein and ligand.

3.4.2 Photosensitizer-Induced EAAT2 Inactivation Exhibited Different Specificity

A central challenge in all studies employing photoactivable ligands is to establish that the compounds are indeed modifying the target protein at the desired site. Our demonstration that the mechanism of inactivation is $^1\text{O}_2$ -mediated suggested that the compounds needed to be in close proximity to critical domains needed for transporter function. It is known that $^1\text{O}_2$ species are quenched quickly in aqueous solvents despite having a longer lifetime than the 9-fluorenone biradicals. Although a $^1\text{O}_2$'s diffusion distance can be as long as 50 nm during its lifetime in aqueous solvents (2 μs), very few $^1\text{O}_2$ generated from photosensitization can reach cells when the photosensitizers are

included in the cell culture medium (Kochevar and Redmond, 2000; Kanofsky, 1991). In a report of fluorophore-assisted light inactivation (FALI) using fluorescein-labeled probes to inactivate $\beta 1$ integrin, the half-maximal radius of $^1\text{O}_2$ damage is estimated to be 40 Å (Beck et al., 2002).

While the $^1\text{O}_2$ -based mechanism suggests a close interaction between the ligands and EAAT2, earlier competition studies pointed out the fact that 9F2C, the most potent inactivator, does not directly interact with domains responsible for binding the substrate L-glutamate. The best approach to resolve the issue of specificity is to determine if the protein can be protected from inactivation by other well known competitive inhibitors. In the instance of β -2-CFoDA we demonstrated that co-incubation with the potent inhibitor β -2-FAA effectively protected EAAT2 from inactivation. Interestingly, other inhibitors, such as TBOA and L-glutamate, showed slight protective effects against β -2-CFoDA-induced photo-inactivation, but the effect did not reach statistical significance level. These results likely reflect the kinetic difference between the inhibitors within the context of 60 min incubation time. The dissociation rate for β -2-FAA is markedly longer than either L-glutamate or TBOA. Thus, even if inhibitor is present at comparable concentrations (based on the K_i 's), the rapid dissociation of TBOA or L-glutamate would still allow multiple bindings and unbindings of β -2-CFoDA, and eventually lead to its inactivation.

In contrast to β -2-CFoDA, β -2-FAA did not protect EAAT2 from inactivation by 9F2C. This result suggests that 9F2C is likely acting at a different site than β -2-CFoDA to photo-inactivate EAAT2. Such a conclusion is also consistent with the inability of 9F2C to act as a competitive inhibitor of EAAT2. Even though 9F2C does not appear to

be acting at the substrate binding domain, it nonetheless must still be in close proximity to important EAAT2 domains, or it would be inactive as was MB.

3.4.3 Trp472 is the Site of Photo-Oxidation in β -2-CFoDA-Induced EAAT2 Inactivation

The demonstration that β -2-CFoDA was likely binding to the substrate site on EAAT2 during the processes of photo-inactivation prompted us to look for evidence of $^1\text{O}_2$ -mediated modification to the EAAT2 protein. Our previous development of an expression, isolation and MS characterization protocol for EAAT2 provided an good starting point for these studies (See Chapter 2). When MALDI-MS analyses were compared between control and β -2-CFoDA-inactivated proteins, one peptide was consistently observed at a 16 m/z value greater than the respective control peptide. Significantly, this peptide spanned residues 388-476 in EAAT2, a portion of sequence that contributes residues to key component of the presumed substrate domain, including TM7, HP2 and TM8. Five amino acid residues are particularly susceptible to oxidative damage induced by $^1\text{O}_2$: cysteine, tyrosine, methionine, tryptophan and histidine (Davies, 2003). Within the oxidized peptide 388-476 five such residues are present: M398, Y404, M415, M450 and W472. Thus, we would suggest that the oxidative modification of one or more of these residues led to the inactivation of the protein.

The probability or likelihood of the reaction between $^1\text{O}_2$ and the side-chains of amino acids are dependent upon several factors, primarily among which are the distances from the $^1\text{O}_2$ generation site to the amino acid and the rate constants for each reaction. In aqueous solvents at physiological pH, the rate constants of $^1\text{O}_2$ -mediated oxidation reactions on His, Trp, Met, Cys and Tyr are estimated to be $3.2 \times 10^7 \text{ dm}^3 \text{ mol}^{-1} \text{ s}^{-1}$, $3.0 \times$

$10^7 \text{ dm}^3 \text{ mol}^{-1} \text{ s}^{-1}$, $1.6 \times 10^7 \text{ dm}^3 \text{ mol}^{-1} \text{ s}^{-1}$, $0.9 \times 10^7 \text{ dm}^3 \text{ mol}^{-1} \text{ s}^{-1}$, and $0.8 \times 10^7 \text{ dm}^3 \text{ mol}^{-1} \text{ s}^{-1}$, respectively (Wilkinson et al., 1995; Monroe, 1985; Matheson et al., 1975; Rougee et al., 1988). Other amino acids react with $^1\text{O}_2$ much more slowly with rate constants of $< 0.7 \times 10^7 \text{ dm}^3 \text{ mol}^{-1} \text{ s}^{-1}$ (Wilkinson et al., 1995).

In order to estimate the distances from the $^1\text{O}_2$ generation site to the potential protein modification site(s), molecular docking studies were performed in the Molecular Computation Core Facility (University of Montana) in collaboration with David Holley (Ph.D. candidate; BMED). Using Gold (<http://www.ccdc.cam.ac.uk/>), β -2-CFoDA was docked into an EAAT2 homology model derived from *Gltp_h* crystal structures. A ChemScore (<http://www.ccdc.cam.ac.uk/>) algorithm was used to determine the top-ranked structures. Molecular docking resulted in a parallel alignment of the 9-fluorenone group with EAAT2 TM8 (Figure 3.12). In three representative docking solutions, the distances from β -2-CFoDA C9 carbonyls to EAAT2 W472 C3 were 6.22 Å, 6.44 Å and 3.68 Å, respectively. In comparison, the average distances from the same carbonyls to each of the other 4 candidate residues were 10.49 Å (Y404), 10.75 Å (M450), 14.29 Å (M398) and 19.32 Å (M415), respectively. It should be noticed that these values only reflect the “static distances” from the photophore to the residues and did not take dynamic motions into consideration. However, based on our knowledge of the nature of the non-substrate EAAT inhibitors, the movements of these inhibitors in the substrate binding domain are thought to be minimal.

Based on the combination of the relatively higher reaction rate and the spatial proximity of the β -2-CFoDA 9-fluorenone group to W472 suggested that this residue was most likely subject to the $^1\text{O}_2$ -mediated photo-inactivation processes. Mechanistic

studies of $^1\text{O}_2$ -mediated tryptophan oxidation revealed multiple pathways and products including tryptophan alcohol (+16 amu), tryptophan hydroperoxide (+32 amu) and *N*-formylkynurenine (FMK, +32 amu) (Ronsein et al., 2008; Rosein et al., 2009). Several tryptophan oxidation products were detected in model peptide samples oxidized by $^1\text{O}_2$ (Kim et al., 2008). However, in a protein oxidation study using cytochrome c, only the Trp+16 adduct was found, indicating that $^1\text{O}_2$ -mediated tryptophan oxidation reactions were affected by protein environment (Kim et al., 2008).

The fact that the photo-inactivation was observed in the EAAT1-3 subtypes suggested the site of oxidation is conserved. Among the five residues, M415 is not conserved in EAAT1 (V416) or EAAT3 (L384). Mutations of M398 to a cysteine in GLT-1 (Zarbiv et al., 1998) and EAAT1 (Seal et al., 2000) both abolished the transporter activity. Y404 was believed to be important in K^+ binding of GLT-1 and mutations of this residue to a Phe, Trp, or Cys led to different levels of activity losses (Zhang et al., 1998). It was also reported that a W473C mutation in GLAST (W472 in EAAT2) caused a near-complete loss of transporter activity ($V_{max} = 14\%$ of control, Seal et al., 2000). We are not aware of any previous mutagenesis studies on M450 in any of the EAATs.

Attempts to validate and experimentally confirm W472 oxidation at the target of $^1\text{O}_2$ -mediated photo-inactivation is limited by the following: 1) point mutations within this peptide often result in an inactive transporter which would preclude functional assays; 2) reports that directly identify tryptophan oxidation products using MS-based approaches are rare (Vanhooren et al., 2002) and most are conducted on model peptides (Kim et al., 2008); 3) tryptic digestion affords only a scant amount of this peptide, and 4) the length and hydrophobicity of the peptide that contains W472 poses technical

challenges in obtaining MS/MS data. Therefore, at this stage we can only speculate that the W472 residue is the likely hEAAT2 photo-oxidation site. Future studies employing an alternative digestion method (such as CNBr) or biophysical technique (i.e. Trp fluorescence) will likely be needed to provide direct evidence for W472 oxidation and to identify oxidation product(s).

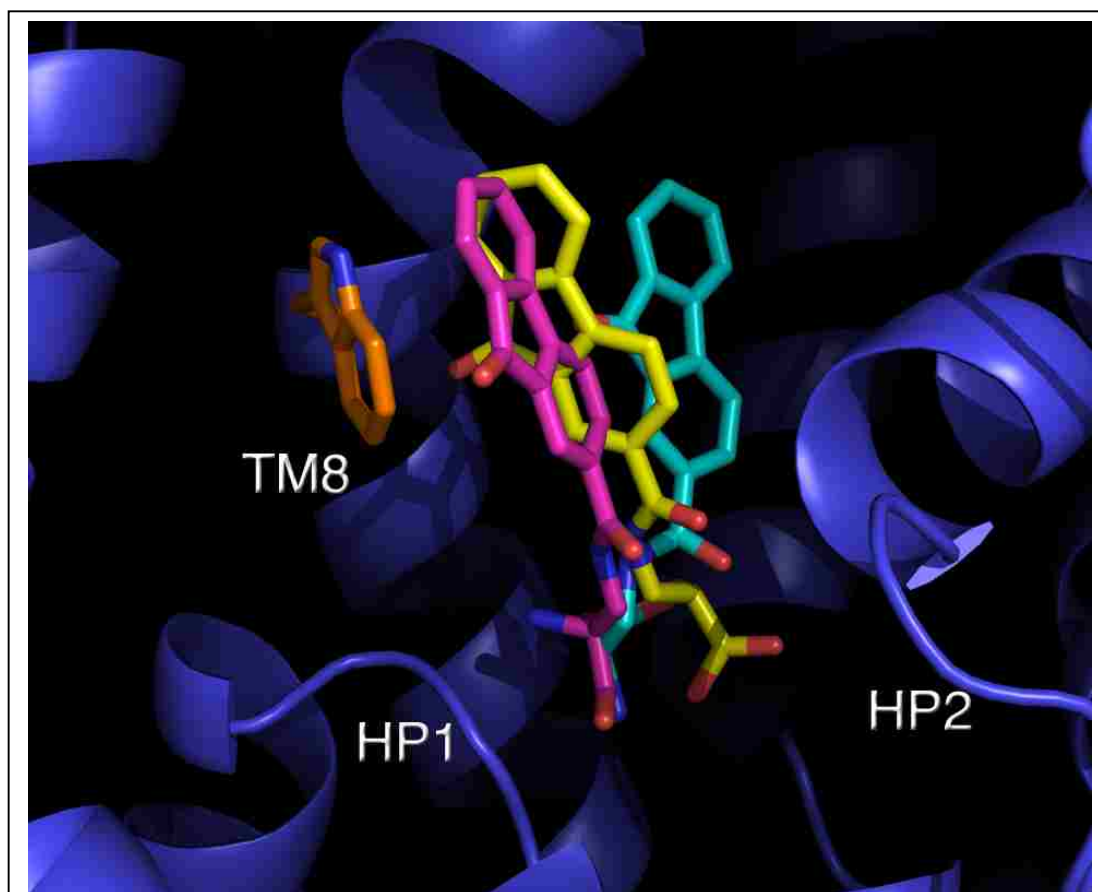


Figure 3.12. Molecular docking of β -2-CFoDA into the binding domain of an EAAT2 model showed the proximity from β -2-CFoDA to W472. Three representative docking solutions are shown. W472 is in orange. The EAAT2 homology model was derived from the *Glt_{ph}* crystal structures (PDB ID: 2NWW). Image was rendered using MacPymol (DeLano Scientific, <http://www.delanoscientific.com/>).

3.5 Conclusions

In summary, we used a combination of pharmacological, photochemical, mass spectrometric and molecular modeling approach to probe the interactions between EAAT2 and inhibitors. We synthesized and pharmacologically characterized a series of aryl diaminopropionic acids and aryl aspartylamide as EAAT inhibitors. We found the specific lipophilic interaction between the 9-fluorenone or fluorene groups with EAAT binding domains dictated the inhibitory potencies of such compounds. A 9-fluorenone-bearing EAAT2 inhibitor, β -2-CFoDA, was able to bind and produce $^1\text{O}_2$ within the binding domain of protein under UV illumination. The spatial proximity from the $^1\text{O}_2$ -generation site to the susceptible residues allowed the oxidation of residues by $^1\text{O}_2$ and inactivation of EAAT functions. Importantly, we noticed the high specificity of the β -2-CFoDA-induced EAAT2 photo-inactivation reactions and the significant protective effects offered by β -2-FAA, a β -2-CFoDA analogue. These results suggested that $^1\text{O}_2$ -mediated, specific binding pocket modification was the mechanism underlying the photo-inactivation. We validated the hypothesis by using MALDI-TOF MS tools to inspect the peptide fingerprint of photo-inactivated EAAT2. We were able to identify a modified peptide fragment spanning the postulated EAAT2 binding domains and attributed the mass shift to the oxidation by $^1\text{O}_2$ and the addition of either one or two oxygen atoms. Molecular docking results revealed the proximity from β -2-CFoDA to W472 located on the TM8 of EAAT2, suggesting W472 was likely to be the oxidation site. These findings demonstrated the involvement and importance of TM8 in the binding of inhibitors with 9-fluorenone and fluorene groups. TM8 is very likely the essential structural component of

the postulated lipophilic pocket in the EAATs. The lipophilic pocket structural differences among different EAAT subtypes may directly contribute to the subtype selectivity and/or transportability in EAAT inhibitors. However, we did not see a subtype difference suggesting other factors related to inactivation predominate inhibitor binding. The elucidation of the lipophilic interaction will greatly benefit the development of subtype-selective EAAT targeting drugs. In addition to the structural-functional aspect, the results of this study also provided an alternative method to selectively inactivate the transporter proteins. Recently, a general photo-inactivation method was reported to selectively inactivate lipophilic pocket-containing proteins (Yogo et al., 2008). Our method utilizes long wavelength UV light sources and requires relatively long time to effectively inactivate the proteins. It would be very interesting to modify our system so visible light source from conventional microscope could be used in direct tissue slice inactivation.

REFERENCES

- Al-Mawsawi LQ, Fikkert V, Dayam R, Witvrouw M, Burke TR, Jr., Borchers CH and Neamati N (2006) Discovery of a small-molecule HIV-1 integrase inhibitor-binding site. *Proc Natl Acad Sci U S A* 103:10080-5.
- Aoyama K, Suh SW, Hamby AM, Liu J, Chan WY, Chen Y and Swanson RA (2006) Neuronal glutathione deficiency and age-dependent neurodegeneration in the EAAC1 deficient mouse. *Nat Neurosci* 9:119-26.
- Aprico K, Beart PM, Crawford D and O'Shea RD (2004) Binding and transport of [3H](2S,4R)-4-methylglutamate, a new ligand for glutamate transporters, demonstrate labeling of EAAT1 in cultured murine astrocytes. *J Neurosci Res* 75:751-9.
- Aprico K, Beart PM, Lawrence AJ, Crawford D and O'Shea RD (2001) [(3)H](2S,4R)-4-Methylglutamate: a novel ligand for the characterization of glutamate transporters. *J Neurochem* 77:1218-25.
- Arriza JL, Eliasof S, Kavanaugh MP and Amara SG (1997) Excitatory amino acid transporter 5, a retinal glutamate transporter coupled to a chloride conductance. *Proc Natl Acad Sci U S A* 94:4155-60.
- Arriza JL, Fairman WA, Wadiche JI, Murdoch GH, Kavanaugh MP and Amara SG (1994) Functional comparisons of three glutamate transporter subtypes cloned from human motor cortex. *J Neurosci* 14:5559-69.
- Auer M, Kim MJ, Lemieux MJ, Villa A, Song J, Li XD and Wang DN (2001) High-yield expression and functional analysis of *Escherichia coli* glycerol-3-phosphate

- transporter. *Biochemistry* 40:6628-35.
- Bairoch A, Apweiler R, Wu CH, Barker WC, Boeckmann B, Ferro S, Gasteiger E, Huang H, Lopez R, Magrane M, Martin MJ, Natale DA, O'Donovan C, Redaschi N and Yeh LS (2005) The Universal Protein Resource (UniProt). *Nucleic Acids Res* 33:D154-9.
- Barbour B and Hausser M (1997) Intersynaptic diffusion of neurotransmitter. *Trends Neurosci* 20:377-84.
- Beck S, Sakurai T, Eustace BK, Beste G, Schier R, Rudert F and Jay DG (2002) Fluorophore-assisted light inactivation: a high-throughput tool for direct target validation of proteins. *Proteomics* 2:247-55.
- Bergles DE and Jahr CE (1997) Synaptic activation of glutamate transporters in hippocampal astrocytes. *Neuron* 19:1297-308.
- Bliss TV and Collingridge GL (1993) A synaptic model of memory: long-term potentiation in the hippocampus. *Nature* 361:31-9.
- Blonder J, Goshe MB, Moore RJ, Pasa-Tolic L, Masselon CD, Lipton MS and Smith RD (2002) Enrichment of integral membrane proteins for proteomic analysis using liquid chromatography-tandem mass spectrometry. *J Proteome Res* 1:351-60.
- Bonde C, Norberg J, Noer H and Zimmer J (2005) Ionotropic glutamate receptors and glutamate transporters are involved in necrotic neuronal cell death induced by oxygen-glucose deprivation of hippocampal slice cultures. *Neuroscience* 136:779-94.
- Boston-Howes W, Gibb SL, Williams EO, Pasinelli P, Brown RH, Jr. and Trotti D (2006) Caspase-3 cleaves and inactivates the glutamate transporter EAAT2. *J Biol Chem*

281:14076-84.

- Boudker O, Ryan RM, Yernool D, Shimamoto K and Gouaux E (2007) Coupling substrate and ion binding to extracellular gate of a sodium-dependent aspartate transporter. *Nature* 445:387-93.
- Boulter JM and Wang DN (2001) Purification and characterization of human erythrocyte glucose transporter in decylmaltoside detergent solution. *Protein Expr Purif* 22:337-48.
- Bridges RJ and Esslinger CS (2005) The excitatory amino acid transporters: pharmacological insights on substrate and inhibitor specificity of the EAAT subtypes. *Pharmacol Ther* 107:271-85.
- Bridges RJ, Kavanaugh MP and Chamberlin AR (1999) A pharmacological review of competitive inhibitors and substrates of high-affinity, sodium-dependent glutamate transport in the central nervous system. *Curr Pharm Des* 5:363-79.
- Bridges RJ, Rhoderick J, Barany A, Lyda B, Ye R, Esslinger CS and Gerdes J (2008) Selective inhibition of the excitatory amino acid transporter EAAT3 by 7-halo-fluorenyl-aspartylamides., in Society for Neuroscience's 38th annual meeting, Washington D. C.
- Brustovetsky T, Purl K, Young A, Shimizu K and Dubinsky JM (2004) Dearth of glutamate transporters contributes to striatal excitotoxicity. *Exp Neurol* 189:222-30.
- Buchstaller A and Jay DG (2000) Micro-scale chromophore-assisted laser inactivation of nerve growth cone proteins. *Microsc Res Tech* 48:97-106.
- Butchbach ME, Tian G, Guo H and Lin CL (2004) Association of excitatory amino acid

transporters, especially EAAT2, with cholesterol-rich lipid raft microdomains: importance for excitatory amino acid transporter localization and function. *J Biol Chem* 279:34388-96.

Clements JD, Lester RA, Tong G, Jahr CE and Westbrook GL (1992) The time course of glutamate in the synaptic cleft. *Science* 258:1498-501.

Cox HD, Chao CK, Patel SA and Thompson CM (2008) Efficient digestion and mass spectral analysis of vesicular glutamate transporter 1: a recombinant membrane protein expressed in yeast. *J Proteome Res* 7:570-8.

Coyle JT (2004) The GABA-glutamate connection in schizophrenia: which is the proximate cause? *Biochem Pharmacol* 68:1507-14.

Curtis DR, Phillis JW and Watkins JC (1960) The chemical excitation of spinal neurones by certain acidic amino acids. *J Physiol* 150:656-82.

Curtis DR, Phillis JW and Watkins JC (1961) Actions of aminoacids on the isolated hemisected spinal cord of the toad. *Br J Pharmacol Chemother* 16:262-83.

Danbolt NC (2001) Glutamate uptake. *Prog Neurobiol* 65:1-105.

Danbolt NC, Storm-Mathisen J and Kanner BI (1992) An [Na⁺ + K⁺]coupled L-glutamate transporter purified from rat brain is located in glial cell processes. *Neuroscience* 51:295-310.

Davies MJ (2003) Singlet oxygen-mediated damage to proteins and its consequences. *Biochem Biophys Res Commun* 305:761-70.

Devasagayam TP, Di Mascio P, Kaiser S and Sies H (1991) Singlet oxygen induced single-strand breaks in plasmid pBR322 DNA: the enhancing effect of thiols. *Biochim Biophys Acta* 1088:409-12.

- Diamond JS and Jahr CE (1997) Transporters buffer synaptically released glutamate on a submillisecond time scale. *J Neurosci* 17:4672-87.
- Domon B and Aebersold R (2006) Challenges and opportunities in proteomics data analysis. *Mol Cell Proteomics* 5:1921-6.
- Dugan LL, Bruno VM, Amagasa SM and Giffard RG (1995) Glia modulate the response of murine cortical neurons to excitotoxicity: glia exacerbate AMPA neurotoxicity. *J Neurosci* 15:4545-55.
- Dunlop J and Butera JA (2006) Ligands targeting the excitatory amino acid transporters (EAATs). *Curr Top Med Chem* 6:1897-906.
- Dunlop J, McIlvain HB, Carrick TA, Jow B, Lu Q, Kowal D, Lin S, Greenfield A, Grosanu C, Fan K, Petroski R, Williams J, Foster A and Butera J (2005) Characterization of novel aryl-ether, biaryl, and fluorene aspartic acid and diamino propionic acid analogs as potent inhibitors of the high-affinity glutamate transporter EAAT2. *Mol Pharmacol* 68:974-82.
- Eliasof S, McIlvain HB, Petroski RE, Foster AC and Dunlop J (2001) Pharmacological characterization of threo-3-methylglutamic acid with excitatory amino acid transporters in native and recombinant systems. *J Neurochem* 77:550-7.
- Esslinger CS, Agarwal S, Gerdes J, Wilson PA, Davis ES, Awes AN, O'Brien E, Mavencamp T, Koch HP, Poulsen DJ, Rhoderick JF, Chamberlin AR, Kavanaugh MP and Bridges RJ (2005) The substituted aspartate analogue L-beta-threo-benzyl-aspartate preferentially inhibits the neuronal excitatory amino acid transporter EAAT3. *Neuropharmacology* 49:850-61.
- Fairman WA, Vandenberg RJ, Arriza JL, Kavanaugh MP and Amara SG (1995) An

- excitatory amino-acid transporter with properties of a ligand-gated chloride channel. *Nature* 375:599-603.
- Fenn JB, Mann M, Meng CK, Wong SF and Whitehouse CM (1989) Electrospray ionization for mass spectrometry of large biomolecules. *Science* 246:64-71.
- Ferro M, Salvi D, Riviere-Rolland H, Vermat T, Seigneurin-Berny D, Grunwald D, Garin J, Joyard J and Rolland N (2002) Integral membrane proteins of the chloroplast envelope: identification and subcellular localization of new transporters. *Proc Natl Acad Sci U S A* 99:11487-92.
- Filppula S, Yaddanapudi S, Mercier R, Xu W, Pavlopoulos S and Makriyannis A (2004) Purification and mass spectroscopic analysis of human CB2 cannabinoid receptor expressed in the baculovirus system. *J Pept Res* 64:225-36.
- Foster AC and Kemp JA (2006) Glutamate- and GABA-based CNS therapeutics. *Curr Opin Pharmacol* 6:7-17.
- Galardy RE, Craig LC and Printz MP (1973) Benzophenone triplet: a new photochemical probe of biological ligand-receptor interactions. *Nat New Biol* 242:127-8.
- Galeva N and Altermann M (2002) Comparison of one-dimensional and two-dimensional gel electrophoresis as a separation tool for proteomic analysis of rat liver microsomes: cytochromes P450 and other membrane proteins. *Proteomics* 2:713-22.
- Garcia G, 3rd, Chiara DC, Nirthanan S, Hamouda AK, Stewart DS and Cohen JB (2007) [³H]Benzophenone photolabeling identifies state-dependent changes in nicotinic acetylcholine receptor structure. *Biochemistry* 46:10296-307.
- Girotti AW (1979) Protoporphyrin-sensitized photodamage in isolated membranes of

- human erythrocytes. *Biochemistry* 18:4403-11.
- Golinski M, DeLaLuz PJ, Floresca R, Delcamp TJ, Vanaman TC and Watt DS (1995) Synthesis, binding affinity, and cross-linking of monodentate photoactive phenothiazines to calmodulin. *Bioconjug Chem* 6:549-57.
- Gonzalez MI, Bannerman PG and Robinson MB (2003) Phorbol myristate acetate-dependent interaction of protein kinase C α and the neuronal glutamate transporter EAAC1. *J Neurosci* 23:5589-93.
- Gonzalez MI, Kazanietz MG and Robinson MB (2002) Regulation of the neuronal glutamate transporter excitatory amino acid carrier-1 (EAAC1) by different protein kinase C subtypes. *Mol Pharmacol* 62:901-10.
- Gonzalez MI and Robinson MB (2004) Protein kinase C-dependent remodeling of glutamate transporter function. *Mol Interv* 4:48-58.
- Gopalakrishnan A, Sievert M and Ruoho AE (2007) Identification of the substrate binding region of vesicular monoamine transporter-2 (VMAT-2) using iodoaminoflisopolol as a novel photoprobe. *Mol Pharmacol* 72:1567-75.
- Goshe MB, Blonder J and Smith RD (2003) Affinity labeling of highly hydrophobic integral membrane proteins for proteome-wide analysis. *J Proteome Res* 2:153-61.
- Gouaux E (2009) Review. The molecular logic of sodium-coupled neurotransmitter transporters. *Philos Trans R Soc Lond B Biol Sci* 364:149-54.
- Greenfield A, Grosanu C, Dunlop J, McIlvain B, Carrick T, Jow B, Lu Q, Kowal D, Williams J and Butera J (2005) Synthesis and biological activities of aryl-ether-, biaryl-, and fluorene-aspartic acid and diamino propionic acid analogs as potent

- inhibitors of the high-affinity glutamate transporter EAAT-2. *Bioorg Med Chem Lett* 15:4985-8.
- Grunewald M, Bendahan A and Kanner BI (1998) Biotinylation of single cysteine mutants of the glutamate transporter GLT-1 from rat brain reveals its unusual topology. *Neuron* 21:623-32.
- Grunewald M, Menaker D and Kanner BI (2002) Cysteine-scanning mutagenesis reveals a conformationally sensitive reentrant pore-loop in the glutamate transporter GLT-1. *J Biol Chem* 277:26074-80.
- Guiramand J, Martin A, de Jesus Ferreira MC, Cohen-Solal C, Vignes M and Recasens M (2005) Gliotoxicity in hippocampal cultures is induced by transportable, but not by nontransportable, glutamate uptake inhibitors. *J Neurosci Res* 81:199-207.
- Guo J, Chen H, Puhl HL, 3rd and Ikeda SR (2006) Fluorophore-assisted light inactivation produces both targeted and collateral effects on N-type calcium channel modulation in rat sympathetic neurons. *J Physiol* 576:477-92.
- Han J and Schey KL (2004) Proteolysis and mass spectrometric analysis of an integral membrane: aquaporin 0. *J Proteome Res* 3:807-12.
- Han Y, Bisello A, Nakamoto C, Rosenblatt M and Chorev M (2000) 3-(3'-fluorenyl-9'-oxo)-L-alanine: a novel photoreactive conformationally constrained amino acid. *J Pept Res* 55:230-9.
- Haugeto O, Ullensvang K, Levy LM, Chaudhry FA, Honore T, Nielsen M, Lehre KP and Danbolt NC (1996) Brain glutamate transporter proteins form homomultimers. *J Biol Chem* 271:27715-22.
- Henry LK, Khare S, Son C, Babu VV, Naider F and Becker JM (2002) Identification of a

- contact region between the tridecapeptide alpha-factor mating pheromone of *Saccharomyces cerevisiae* and its G protein-coupled receptor by photoaffinity labeling. *Biochemistry* 41:6128-39.
- Hynd MR, Scott HL and Dodd PR (2004) Glutamate-mediated excitotoxicity and neurodegeneration in Alzheimer's disease. *Neurochem Int* 45:583-95.
- Jackson M, Song W, Liu MY, Jin L, Dykes-Hoberg M, Lin CI, Bowers WJ, Federoff HJ, Sternweis PC and Rothstein JD (2001) Modulation of the neuronal glutamate transporter EAAT4 by two interacting proteins. *Nature* 410:89-93.
- Jay DG (1988) Selective destruction of protein function by chromophore-assisted laser inactivation. *Proc Natl Acad Sci U S A* 85:5454-8.
- Johnston RB, Jr., Keele BB, Jr., Misra HP, Lehmeyer JE, Webb LS, Baehner RL and RaJagopalan KV (1975) The role of superoxide anion generation in phagocytic bactericidal activity. Studies with normal and chronic granulomatous disease leukocytes. *J Clin Invest* 55:1357-72.
- Kage R, Leeman SE, Krause JE, Costello CE and Boyd ND (1996) Identification of methionine as the site of covalent attachment of a p-benzoyl-phenylalanine-containing analogue of substance P on the substance P (NK-1) receptor. *J Biol Chem* 271:25797-800.
- Kanai Y and Hediger MA (1992) Primary structure and functional characterization of a high-affinity glutamate transporter. *Nature* 360:467-71.
- Kanofsky JR (1991) Quenching of singlet oxygen by human red cell ghosts. *Photochem Photobiol* 53:93-9.
- Karas M and Hillenkamp F (1988) Laser desorption ionization of proteins with molecular

- masses exceeding 10,000 daltons. *Anal Chem* 60:2299-301.
- Keil-Dlouha VV, Zylber N, Imhoff J, Tong N and Keil B (1971) Proteolytic activity of pseudotrypsin. *FEBS Lett* 16:291-295.
- Kim J, Rodriguez ME, Guo M, Kenney ME, Oleinick NL and Anderson VE (2008) Oxidative modification of cytochrome c by singlet oxygen. *Free Radic Biol Med* 44:1700-11.
- Klockgether T and Turski L (1990) NMDA antagonists potentiate antiparkinsonian actions of L-dopa in monoamine-depleted rats. *Ann Neurol* 28:539-46.
- Klotz LO, Pellieux C, Briviba K, Pierlot C, Aubry JM and Sies H (1999) Mitogen-activated protein kinase (p38-, JNK-, ERK-) activation pattern induced by extracellular and intracellular singlet oxygen and UVA. *Eur J Biochem* 260:917-22.
- Koch HP, Brown RL and Larsson HP (2007) The glutamate-activated anion conductance in excitatory amino acid transporters is gated independently by the individual subunits. *J Neurosci* 27:2943-7.
- Kochevar IE and Redmond RW (2000) Photosensitized production of singlet oxygen. *Methods Enzymol* 319:20-8.
- Kraljic I and Mohsni SE (1978) A new method for the detection of singlet oxygen in aqueous solutions. *Photochem Photobiol* 28:577-581.
- Langlois R, Ali H, Brasseur N, Wagner JR and van Lier JE (1986) Biological activities of phthalocyanines--IV. Type II sensitized photooxidation of L-tryptophan and cholesterol by sulfonated metallo phthalocyanines. *Photochem Photobiol* 44:117-123.

- Larsson HP, Tzingounis AV, Koch HP and Kavanaugh MP (2004) Fluorometric measurements of conformational changes in glutamate transporters. *Proc Natl Acad Sci U S A* 101:3951-6.
- Lee BK, Jung KS, Son C, Kim H, VerBerkmoes NC, Arshava B, Naider F and Becker JM (2007) Affinity purification and characterization of a G-protein coupled receptor, *Saccharomyces cerevisiae* Ste2p. *Protein Expr Purif* 56:62-71.
- Lehre KP, Levy LM, Ottersen OP, Storm-Mathisen J and Danbolt NC (1995) Differential expression of two glial glutamate transporters in the rat brain: quantitative and immunocytochemical observations. *J Neurosci* 15:1835-53.
- Li MY, Cline CS, Koker EB, Carmichael HH, Chignell CF and Bilski P (2001) Quenching of singlet molecular oxygen (1O_2) by azide anion in solvent mixtures. *Photochem Photobiol* 74:760-4.
- Li S, Mallory M, Alford M, Tanaka S and Masliah E (1997) Glutamate transporter alterations in Alzheimer disease are possibly associated with abnormal APP expression. *J Neuropathol Exp Neurol* 56:901-11.
- Liao JC, Berg LJ and Jay DG (1995) Chromophore-assisted laser inactivation of subunits of the T-cell receptor in living cells is spatially restricted. *Photochem Photobiol* 62:923-9.
- Liao JC, Roeder J and Jay DG (1994) Chromophore-assisted laser inactivation of proteins is mediated by the photogeneration of free radicals. *Proc Natl Acad Sci U S A* 91:2659-63.
- Lin CI, Orlov I, Ruggiero AM, Dykes-Hoberg M, Lee A, Jackson M and Rothstein JD (2001) Modulation of the neuronal glutamate transporter EAAC1 by the

- interacting protein GTRAP3-18. *Nature* 410:84-8.
- Liu Y, Vidensky S, Ruggiero AM, Maier S, Sitte HH and Rothstein JD (2008) Reticulon RTN2B regulates trafficking and function of neuronal glutamate transporter EAAC1. *J Biol Chem* 283:6561-71.
- Mallolas J, Hurtado O, Castellanos M, Blanco M, Sobrino T, Serena J, Vivancos J, Castillo J, Lizasoain I, Moro MA and Davalos A (2006) A polymorphism in the EAAT2 promoter is associated with higher glutamate concentrations and higher frequency of progressing stroke. *J Exp Med* 203:711-7.
- Marek KW and Davis GW (2002) Transgenically encoded protein photoinactivation (FLAsH-FALI): acute inactivation of synaptotagmin I. *Neuron* 36:805-13.
- Marie H, Billups D, Bedford FK, Dumoulin A, Goyal RK, Longmore GD, Moss SJ and Attwell D (2002) The amino terminus of the glial glutamate transporter GLT-1 interacts with the LIM protein Ajuba. *Mol Cell Neurosci* 19:152-64.
- Masliah E, Alford M, Mallory M, Rockenstein E, Moechars D and Van Leuven F (2000) Abnormal glutamate transport function in mutant amyloid precursor protein transgenic mice. *Exp Neurol* 163:381-7.
- Matheson IB, Etheridge RD, Kratowich NR and Lee J (1975) The quenching of singlet oxygen by amino acids and proteins. *Photochem Photobiol* 21:165-71.
- Mathews GC and Diamond JS (2003) Neuronal glutamate uptake contributes to GABA synthesis and inhibitory synaptic strength. *J Neurosci* 23:2040-8.
- Mavencamp TL, Rhoderick JF, Bridges RJ and Esslinger CS (2008) Synthesis and preliminary pharmacological evaluation of novel derivatives of L-beta-threo-benzylaspartate as inhibitors of the neuronal glutamate transporter EAAT3.

- Bioorg Med Chem 16:7740-8.
- Melinn M and McLaughlin H (1986) Hydroxyl radical scavengers inhibit human lectin-dependent cellular cytotoxicity. *Immunology* 58:197-202.
- Monroe B (1985) Singlet oxygen in solution: lifetimes and reaction rate constants, in *Singlet oxygen* (Frimer AA ed) pp 177-224, CRC Press, Boca Raton.
- Nakagawa M, Watanabe H, Kodato S, Okajima H, Hino T, Flippen JL and Witkop B (1977) A valid model for the mechanism of oxidation of tryptophan to formylkynurenine-25 years later. *Proc Natl Acad Sci U S A* 74:4730-4733.
- Natale NR, Magnusson KR and Nelson JK (2006) Can selective ligands for glutamate binding proteins be rationally designed? *Curr Top Med Chem* 6:823-47.
- Nieoullon A, Canolle B, Masméjean F, Guillet B, Pisano P and Lortet S (2006) The neuronal excitatory amino acid transporter EAAC1/EAAT3: does it represent a major actor at the brain excitatory synapse? *J Neurochem* 98:1007-18.
- Olney JW (2003) Excitotoxicity, apoptosis and neuropsychiatric disorders. *Curr Opin Pharmacol* 3:101-9.
- Peri S, Navarro JD, Amanchy R, Kristiansen TZ, Jonnalagadda CK, Surendranath V, Niranjana V, Muthusamy B, Gandhi TK, Gronborg M, Ibarrola N, Deshpande N, Shanker K, Shivashankar HN, Rashmi BP, Ramya MA, Zhao Z, Chandrika KN, Padma N, Harsha HC, Yatish AJ, Kavitha MP, Menezes M, Choudhury DR, Suresh S, Ghosh N, Saravana R, Chandran S, Krishna S, Joy M, Anand SK, Madavan V, Joseph A, Wong GW, Schiemann WP, Constantinescu SN, Huang L, Khosravi-Far R, Steen H, Tewari M, Ghaffari S, Blobe GC, Dang CV, Garcia JG, Pevsner J, Jensen ON, Roepstorff P, Deshpande KS, Chinnaiyan AM, Hamosh A,

- Chakravarti A and Pandey A (2003) Development of human protein reference database as an initial platform for approaching systems biology in humans. *Genome Res* 13:2363-71.
- Pileni MP, Santus R and Land EJ (1978) On the photosensitizing properties of N-formylkynurenine and related compounds. *Photochem Photobiol* 28:525.
- Pines G, Danbolt NC, Bjoras M, Zhang Y, Bendahan A, Eide L, Koepsell H, Storm-Mathisen J, Seeberg E and Kanner BI (1992) Cloning and expression of a rat brain L-glutamate transporter. *Nature* 360:464-7.
- Pleban K, Kopp S, Csaszar E, Peer M, Hrebicek T, Rizzi A, Ecker GF and Chiba P (2005) P-glycoprotein substrate binding domains are located at the transmembrane domain/transmembrane domain interfaces: a combined photoaffinity labeling-protein homology modeling approach. *Mol Pharmacol* 67:365-74.
- Porath J (1992) Immobilized metal ion affinity chromatography. *Protein Expr Purif* 3:263-81.
- Prestwich GD, Dorman G, Elliott JT, Marecak DM and Chaudhary A (1997) Benzophenone photoprobes for phosphoinositides, peptides and drugs. *Photochem Photobiol* 65:222-34.
- Rao RV and Bredesen DE (2004) Misfolded proteins, endoplasmic reticulum stress and neurodegeneration. *Curr Opin Cell Biol* 16:653-62.
- Raunser S, Haase W, Bostina M, Parcej DN and Kuhlbrandt W (2005) High-yield expression, reconstitution and structure of the recombinant, fully functional glutamate transporter GLT-1 from *Rattus norvegicus*. *J Mol Biol* 351:598-613.

- Raunser S, Haase W, Franke C, Eckert GP, Muller WE and Kuhlbrandt W (2006)
Heterologously expressed GLT-1 associates in approximately 200-nm protein-lipid islands. *Biophys J* 91:3718-26.
- Robinson MB, Djali S and Buchhalter JR (1993) Inhibition of glutamate uptake with L-trans-pyrrolidine-2,4-dicarboxylate potentiates glutamate toxicity in primary hippocampal cultures. *J Neurochem* 61:2099-103.
- Ronsein GE, de Oliveira MC, de Medeiros MH and Di Mascio P (2009) Characterization of O(2) ((1)delta(g))-derived oxidation products of tryptophan: a combination of tandem mass spectrometry analyses and isotopic labeling studies. *J Am Soc Mass Spectrom* 20:188-97.
- Ronsein GE, Oliveira MC, Miyamoto S, Medeiros MH and Di Mascio P (2008)
Tryptophan oxidation by singlet molecular oxygen [O₂(¹Δ_g): mechanistic studies using ¹⁸O-labeled hydroperoxides, mass spectrometry, and light emission measurements. *Chem Res Toxicol* 21:1271-83.
- Rosenberg PA, Amin S and Leitner M (1992) Glutamate uptake disguises neurotoxic potency of glutamate agonists in cerebral cortex in dissociated cell culture. *J Neurosci* 12:56-61.
- Rothstein JD, Van Kammen M, Levey AI, Martin LJ and Kuncl RW (1995) Selective loss of glial glutamate transporter GLT-1 in amyotrophic lateral sclerosis. *Ann Neurol* 38:73-84.
- Rougee M, Bensasson RV, Land EJ and Pariente R (1988) Deactivation of singlet molecular oxygen by thiols and related compounds, possible protectors against skin photosensitivity. *Photochem Photobiol* 47:485-9.

- Santoni V, Kieffer S, Desclaux D, Masson F and Rabilloud T (2000) Membrane proteomics: use of additive main effects with multiplicative interaction model to classify plasma membrane proteins according to their solubility and electrophoretic properties. *Electrophoresis* 21:3329-44.
- Schoepp DD, Jane DE and Monn JA (1999) Pharmacological agents acting at subtypes of metabotropic glutamate receptors. *Neuropharmacology* 38:1431-76.
- Schousboe A (1981) Transport and metabolism of glutamate and GABA in neurons are glial cells. *Int Rev Neurobiol* 22:1-45.
- Seal RP and Amara SG (1998) A reentrant loop domain in the glutamate carrier EAAT1 participates in substrate binding and translocation. *Neuron* 21:1487-98.
- Seal RP, Leighton BH and Amara SG (2000) A model for the topology of excitatory amino acid transporters determined by the extracellular accessibility of substituted cysteines. *Neuron* 25:695-706.
- Sheldon AL and Robinson MB (2007) The role of glutamate transporters in neurodegenerative diseases and potential opportunities for intervention. *Neurochem Int* 51:333-55.
- Shigeri Y, Seal RP and Shimamoto K (2004) Molecular pharmacology of glutamate transporters, EAATs and VGLUTs. *Brain Res Brain Res Rev* 45:250-65.
- Shimamoto K, Lebrun B, Yasuda-Kamatani Y, Sakaitani M, Shigeri Y, Yumoto N and Nakajima T (1998) DL-threo-beta-benzyloxyaspartate, a potent blocker of excitatory amino acid transporters. *Mol Pharmacol* 53:195-201.
- Shimamoto K, Sakai R, Takaoka K, Yumoto N, Nakajima T, Amara SG and Shigeri Y (2004) Characterization of novel L-threo-beta-benzyloxyaspartate derivatives,

- potent blockers of the glutamate transporters. *Mol Pharmacol* 65:1008-15.
- Shimamoto K, Shigeri Y, Yasuda-Kamatani Y, Lebrun B, Yumoto N and Nakajima T (2000) Syntheses of optically pure beta-hydroxyaspartate derivatives as glutamate transporter blockers. *Bioorg Med Chem Lett* 10:2407-10.
- Simpson RJ, Connolly LM, Eddes JS, Pereira JJ, Moritz RL and Reid GE (2000) Proteomic analysis of the human colon carcinoma cell line (LIM 1215): development of a membrane protein database. *Electrophoresis* 21:1707-32.
- Singh A, Thornton ER and Westheimer FH (1962) The photolysis of diazoacetylchymotrypsin. *J Biol Chem* 237:3006-8.
- Slotboom DJ, Konings WN and Lolkema JS (2001) Glutamate transporters combine transporter- and channel-like features. *Trends Biochem Sci* 26:534-9.
- Smith RA and Knowles JR (1973) Letter: Aryldiazirines. Potential reagents for photolabeling of biological receptor sites. *J Am Chem Soc* 95:5072-3.
- Sonnenberg JD, Koch HP, Willis CL, Bradbury F, Dauenhauer D, Bridges RJ and Chamberlin AR (1996) The role of the C-4 side chain of kainate and dihydrokainate in EAA receptor and transporter selectivity. *Bioorg Med Chem Lett* 6:1607-1612.
- Stevens TJ and Arkin IT (2000) Do more complex organisms have a greater proportion of membrane proteins in their genomes? *Proteins* 39:417-20.
- Storck T, Schulte S, Hofmann K and Stoffel W (1992) Structure, expression, and functional analysis of a Na(+)-dependent glutamate/aspartate transporter from rat brain. *Proc Natl Acad Sci U S A* 89:10955-9.
- Straight R and Spikes J (1979) Photosensitized oxidation of biomolecules., in Singlet O₂

(Frimer AA ed) pp 91-146, CRC Press, Boca Raton.

- Takayama H, Chelikani P, Reeves PJ, Zhang S and Khorana HG (2008) High-level expression, single-step immunoaffinity purification and characterization of human tetraspanin membrane protein CD81. *PLoS ONE* 3:e2314.
- Tanaka K (1993) Cloning and expression of a glutamate transporter from mouse brain. *Neurosci Lett* 159:183-6.
- Tanaka K (2003) The origin of macromolecule ionization by laser irradiation (Nobel lecture). *Angew Chem Int Ed Engl* 42:3860-70.
- Tanaka K, Watase K, Manabe T, Yamada K, Watanabe M, Takahashi K, Iwama H, Nishikawa T, Ichihara N, Kikuchi T, Okuyama S, Kawashima N, Hori S, Takimoto M and Wada K (1997) Epilepsy and exacerbation of brain injury in mice lacking the glutamate transporter GLT-1. *Science* 276:1699-702.
- Trotti D, Danbolt NC and Volterra A (1998) Glutamate transporters are oxidant-vulnerable: a molecular link between oxidative and excitotoxic neurodegeneration? *Trends Pharmacol Sci* 19:328-34.
- Tzingounis AV and Wadiche JI (2007) Glutamate transporters: confining runaway excitation by shaping synaptic transmission. *Nat Rev Neurosci* 8:935-47.
- Vandenberg RJ, Mitrovic AD, Chebib M, Balcar VJ and Johnston GA (1997) Contrasting modes of action of methylglutamate derivatives on the excitatory amino acid transporters, EAAT1 and EAAT2. *Mol Pharmacol* 51:809-15.
- Verweij H, Dubbelman TM and Van Steveninck J (1981) Photodynamic protein cross-linking. *Biochim Biophys Acta* 647:87-94.
- Vizi ES and Mike A (2006) Nonsynaptic receptors for GABA and glutamate. *Curr Top*

- Med Chem 6:941-8.
- Volterra A, Trotti D, Floridi S and Racagni G (1994) Reactive oxygen species inhibit high-affinity glutamate uptake: molecular mechanism and neuropathological implications. *Ann N Y Acad Sci* 738:153-62.
- Wadiche JI, Amara SG and Kavanaugh MP (1995) Ion fluxes associated with excitatory amino acid transport. *Neuron* 15:721-8.
- Wallin E and von Heijne G (1998) Genome-wide analysis of integral membrane proteins from eubacterial, archaean, and eukaryotic organisms. *Protein Sci* 7:1029-38.
- Wannemacher KM, Terskiy A, Bian S, Yadav PN, Li H and Howells RD (2008) Purification and mass spectrometric analysis of the kappa opioid receptor. *Brain Res* 1230:13-26.
- Washburn MP, Wolters D and Yates JR, 3rd (2001) Large-scale analysis of the yeast proteome by multidimensional protein identification technology. *Nat Biotechnol* 19:242-7.
- Watkins JC and Jane DE (2006) The glutamate story. *Br J Pharmacol* 147 Suppl 1:S100-8.
- Waxman SG and Dib-Hajj S (2005) Erythralgia: molecular basis for an inherited pain syndrome. *Trends Mol Med* 11:555-62.
- Whitelegge JP, Gomez SM and Faull KF (2003) Proteomics of membrane proteins. *Adv Protein Chem* 65:271-307.
- Wilkinson F, Helman WP and Ross AB (1995) Rate constants for the decay and reactions of the lowest electronically excited state of molecular oxygen in solution. An expanded and revised compilation. *Journal of Physical and Chemical Reference*

Data 24:663-1021.

- Wu CC and Yates JR, 3rd (2003) The application of mass spectrometry to membrane proteomics. *Nat Biotechnol* 21:262-7.
- Wu Z and Ruoho AE (2000) A high-affinity fluorenone-based beta 2-adrenergic receptor antagonist with a photoactivatable pharmacophore. *Biochemistry* 39:13044-52.
- Wu Z, Thiriot DS and Ruoho AE (2001) Tyr199 in transmembrane domain 5 of the beta2-adrenergic receptor interacts directly with the pharmacophore of a unique fluorenone-based antagonist. *Biochem J* 354:485-91.
- Yan P, Xiong Y, Chen B, Negash S, Squier TC and Mayer MU (2006) Fluorophore-assisted light inactivation of calmodulin involves singlet-oxygen mediated cross-linking and methionine oxidation. *Biochemistry* 45:4736-48.
- Ye R, Rhoderick J, Thompson CM and Bridges RJ (2009) Functional expression, purification and mass spectrometric characterization of human excitatory amino acid transporter 2.
- Yernool D, Boudker O, Jin Y and Gouaux E (2004) Structure of a glutamate transporter homologue from *Pyrococcus horikoshii*. *Nature* 431:811-8.
- Yogo T, Urano Y, Mizushima A, Sunahara H, Inoue T, Hirose K, Iino M, Kikuchi K and Nagano T (2008) Selective photoinactivation of protein function through environment-sensitive switching of singlet oxygen generation by photosensitizer. *Proc Natl Acad Sci U S A* 105:28-32.
- Zarbiv R, Grunewald M, Kavanaugh MP and Kanner BI (1998) Cysteine scanning of the surroundings of an alkali-ion binding site of the glutamate transporter GLT-1 reveals a conformationally sensitive residue. *J Biol Chem* 273:14231-7.

- Zerangue N and Kavanaugh MP (1996) Flux coupling in a neuronal glutamate transporter. *Nature* 383:634-7.
- Zhang Y, Bendahan A, Zarbiv R, Kavanaugh MP and Kanner BI (1998) Molecular determinant of ion selectivity of a (Na⁺ + K⁺)-coupled rat brain glutamate transporter. *Proc Natl Acad Sci U S A* 95:751-5.
- Zor T, Halifa I, Kleinhaus S, Chorev M and Selinger Z (1995) m-Acetylanilido-GTP, a novel photoaffinity label for GTP-binding proteins: synthesis and application. *Biochem J* 306 (Pt 1):253-8.
- Zvonok N, Yaddanapudi S, Williams J, Dai S, Dong K, Rejtar T, Karger BL and Makriyannis A (2007) Comprehensive proteomic mass spectrometric characterization of human cannabinoid CB2 receptor. *J Proteome Res* 6:2068-79.